REGIONS INVOLVED IN THE OLIGOMERIZATION AND ACTIVITY OF THE SPIRAL FORMING NITRILASE CYANIDE DIHYDRATASE

A Dissertation

by

JASON MICHAEL PARK

Submitted to the Office of Graduate and Professional Studies of
Texas A&M University
in partial fulfillment of the requirements for the degree of

DOCTOR OF PHILOSOPHY

Chair of Committee,	Michael Benedik
Committee Members,	Michael Manson
	Steve Lockless
	James Hu
Head of Department,	Tom McKnight

August 2014

Major Subject: Microbiology

ABSTRACT

Nitrilases offer an economic and environmentally friendly solution for the production of valuable chemicals, and the degradation of toxic industrial nitrile wastes. A lack of fine structural data has impeded rational engineering of these enzymes to expand their utility. The nitrilases form large spiral shaped oligomers, seen by electron microscopy. These spiral structures are seen in all active nitrilases, and mutations altering this structure influence activity, stability, and substrate specificity. Currently no spiral forming nitrilase has been amenable to crystallization, leaving a significant gap in our understanding of these enzymes. Crystal structures from the larger nitrilase-superfamily reveal a conserved dimer structure and active site.

Three regions in nitrilases are hypothesized to associate these dimer building blocks into the spiral oligomer. Two stand out as insertions relative to the crystallized homologs. These regions are hypothesized to associate the basic nitrilase dimer to form the large spiral structure. I investigate this hypothesis in the nitrilase $CynD_{pum}$ by constructing mutations throughout these insertion regions and ascertaining their effect on enzyme activity as well as on oligomerization.

A third region that stands out from the nitrilase sequences in comparison to the crystallized superfamily members is the extension of the C-terminus. Mutations to the C-terminus in various nitrilases can alter the proteins stability, activation, and substrate specificity, but how it interacts with other regions of the protein is not understood. .

In CynD, exchanging the C-terminus between the *Bacillus pumilus* enzyme and that of *Pseudomonas stutzeri* ($CynD_{stut}$) shows a one-way compatibility. When $CynD_{pum}$ is paired with the *P. stutzeri* C-terminus ($CynD_{pum\text{-}stut}$), the hybrid enzyme is active and more stable than either parent enzyme. Conversely, the reverse hybrid, where the *P. stutzeri* CynD is paired with the *B. pumilus* C-terminus ($CynD_{stut\text{-}pum}$) is not active. In this study I exploit the stabilizing effect of the C-terminus from *B. pumilus* to test whether it participates in spiral formation. Additionally, I identify regions interacting with the C-terminus by looking for suppressing substitutions in $CynD_{stut\text{-}pum}$ that restore activity.

DEDICATION

This dissertation is dedicated to my brilliant and beautiful wife Dr. Dana Shaw. She has been a constant source of support, advice, encouragement, and inspiration.

ACKNOWLEDGEMENTS

I would not have been able to finish this dissertation without the guidance of my committee, contributions from collaborators, help from co-workers, and the support of friends and family.

I first would like to thank my graduate advisor Dr. Michael Benedik for his patience, guidance, advice, and support throughout my graduate career. His instruction has given me a foundation to build from as I move forward in my career. I would also like to thank my graduate committee members, Dr. Michael Manson, Dr. Jim Hu, and Dr. Steve Lockless, for their assessment and guidance of my research. Additionally I would like to thank Dr. Deborah Siegele for providing advice and guidance.

For their advice, collaboration, and contribution to this research I thank Dr. Trevor Sewell and Dr. Mary Abou-Nader Crum. Much of my work built directly off of their findings. I also thank Andani Mulelu and Chris Ponder for their help and contributions to my research. For generously lending their time, expertise, and equipment, I would like to thank Dr. James Smith and his lab members.

For their support and camaraderie I thank my fellow graduate students and friends, who are too numerous to list here.

TABLE OF CONTENTS

Page

Page

Page

Page

LIST OF FIGURES

Page

Page

LIST OF TABLES

Page

CHAPTER I

INTRODUCTION AND LITERATURE REVIEW

NITRILASES

Nitrilase enzymes hydrolyze carbon-nitrogen triple bonds (nitrile groups) into ammonia and the corresponding acid product (Thimann and Mahadevan 1964), although some nitrilases are also able to release amide products in addition to or instead of ammonia and carboxylic acids (Basile et al. 2008; Woodward 2011). The first nitrilases were initially discovered in the 1960's beginning with their isolation and purification from barley leaves (Thimann and Mahadevan 1964). These enzymes were found to catalyze the conversion of a range of nitriles to their corresponding carboxylic acid (Mahadevan and Thimann 1964). Since then, nitrilases have been identified in a several bacteria, fungi, yeast, and plants with activities against a wide range of nitriles (Gong et al. 2012). Also a large number of nitrilase related proteins have been discovered, leading to the categorization of the nitrilase superfamily of enzymes (Pace and Brenner 2001).

Nitrilase superfamily

Nitrilase enzymes make up just the first branch in the thirteen branch nitrilase superfamily of enzymes. Members of this superfamily all perform hydrolysis of carbon-nitrogen bonds, share a conserved cysteine-glutamate-lysine catalytic triad, and have a characteristic αββα monomer fold (Pace and Brenner 2001). Recently an additional

glutamate was implicated in catalysis, which expanded the triad to a cysteine-glutamate-glutamate-lysine tetrad (Kimani et al. 2007).

In spite of the name, only one of the thirteen branches of the nitrilase superfamily carries out hydrolysis of nitrile groups to carboxylic acids and ammonia, or amide products. The other 12 branches of the family have amidase, carbamylase, or amide condensation activity (Pace and Brenner 2001). Branch 1 of the family are the nitrilases and members are capable of hydrolyzing nitrile groups. Aliphatic amidases are in branch 2 and hydrolyze the side chains of glutamine and asparagine. Branch 3 are the amino-terminal amidases involved in regulating protein degradation. Branch 4 are biotinidases, which are involved in releasing biotin, and have can contain multiple nitrilase-like domains per protein. Branch 5 are β-ureidopropionases, which carry out β-alanine synthesis and pyrimidine catabolism. Branch 6 are carbamylases involved that act on D-amino acids. Branch 7 and 8 are prokaryotic and eukaryotic glutamine-dependent NAD synthases. The nitrilase-like domain in these NAD synthases hydrolyses glutamine to supply ammonia to the NAD synthase domain. Branch 9 are apolipoprotein N-acyltransferaces that post-translationally modify lipoproteins. Branch 10 includes the Nit domain of the eukaryotic NitFhit tumor suppressor protein. While Nit is thought to function with Fhit in a cell death pathway, the substrates and enzymatic activities of branch 10 proteins are currently unknown. Further branch 10 proteins have been identified in prokaryotes, although their functions are also not characterized. Branches 11, 12, and 13 contain no functionally characterized members but are all distinct similarity groups based on sequence (Pace and Brenner 2001).

Nitrilases in nature

The exact biological function of most nitrilases is not known. Many nitrilases were identified in screens for hydrolysis of nitriles of industrial interest (Gong et al. 2012). Others were identified by genome mining for similarity to known nitrilases (Basile et al. 2008). Though the exact natural substrates may not be known, natural nitrile compounds found in the environment could provide clues to the role nitrilases are playing. Nitriles have also been found to have antibacterial and antifungal activity (Fleming 1999). Nitrilases could provide resistance mechanisms to these compounds and, correspondingly, transgenic expression of nitrilases in plants provides resistance to nitrile based herbicides (Stalker et al. 1988).

The biological role of nitrilases is most extensively studied in plants. The function of nitrilases in plants was initially proposed upon their discovery. The barley nitrilase was identified as the activity hydrolyzing indoleacetonitrile, produced naturally in plants (Thimann and Mahadevan 1964) to produce indoleacetic acid, a natural plant hormone auxin that plays an important role in plant growth. Plant nitrilases have also been presumed to detoxify cyanide, a byproduct of ethylene synthesis (Jenrich et al. 2007).

Cyanide is commonly found in plants and other organisms as cyanogenic glucosides and lipids, which they use for defense (Fleming 1999). Once metabolized, these nitriles release cyanide, which exerts a toxic effect on pathogens or herbivores. In response, other organisms have evolved nitrilases to detoxify the cyanide. As a result, nitrilase expressing organisms have also been found to survive in environments that are

highly polluted due to industrial cyanide usage (Meyers et al. 1991; Watanabe et al. 1998). These cyanide degrading nitrilases have great potential to deal with the environmental costs of industrial cyanide usage.

NITRILASE: INDUSTRIAL GREEN BIOCATALYSTS

Beyond the role of nitrilases in plants, interest in nitrilases primarily stems from their potential as efficient, selective, and environmentally friendly catalysts (Singh et al. 2006). Use of nitrilases is more environmentally responsible than many chemical strategies and can improve the overall quality of the product. The environmental impact of nitrile wastes can also be addressed using nitrilases to degrade the chemical into non-toxic acids or amides.

Nitrilases in chemical synthesis

Nitrilases offer greener solution for the production of high value chemicals, while avoiding drawbacks normally associated with their conventional chemical synthesis. Discussed here are a few examples of where nitrilases are improving industrial chemical production.

Over four metric tons of acrylic acid is used each year in applications that include textiles, adhesives, dispersants, and paper treatment. The chemical synthesis by gas-phase oxidation of propylene produces large amounts of inorganic byproducts (Gong et al. 2012). Nitrilases on the other hand do not require other cofactors or substrates and therefore avoid the accumulation of unwanted side products. By using a nitrilase from

Rhodococcus rhodochrous J1 (J1 nitrilase) to produce acrylic acid from acrylonitrile, these wasteful byproducts are avoided. The native enzyme does, however, require pre-activation by benzonitrile to induce oligomer formation (Nagasawa et al. 2000).

Environmental concerns can be raised by the substrate used in a process. Nicotinic acid (or vitamin B3) is used in feed additives and as precursors of pharmaceuticals. The standard synthesis from nicotine raises significant environmental concerns. Nitrilases can relieve this problem by allowing the use of an alternate nitrile substrate. Using a nitrilase from *Rhodococcus* sp. NDB 1165 allows the safer cyanopyridine to replace nicotine in the production of nicotinic acid (Prasad et al. 2007). This has prompted the company Lanza to take up this biocatalyst strategy in their production of nicotinic acid (Gong et al. 2012).

Glycolic acid can be found in cleaners, cosmetics, motor oil, electrical elements, and oil well flow enhancers (Gong et al. 2012). It is currently produced by reacting formaldehyde with carbon monoxide under pressure, high heat, and acidic conditions, raising costs and safety concerns. The mild reaction conditions of nitrilases relieve the need for extreme conditions required in some conventional chemical methods. An enzymatic strategy using a re-engineered nitrilase from *Acidovorax facilis* 72W can produce glycolic acid from glycolonitrile under very mild conditions (Wu et al. 2008).

The harsh conditions using in chemical synthesis can damage the product during processing. The polymer polyacrylonitrile is used extensively in textiles. It is often modified to alter properties such as dye uptake. The high heat and harsh chemical conditions normally used can leave the polymers damaged and discolored (Gong et al.

2012). By using nitrilases, dye uptake can be increased two-fold while avoiding damage to the polymer (Matamá et al. 2007).

Conventional chemical synthesis often results in enantiomeric mixtures, of which only one form is usually desired. The chirality of mandelic acid is important in the production of pharmaceuticals such as penicillins, cephalosporins, antitumor agents, and anti-obesity agents. Traditional chemical means of producing mandelic acid yield about 50% of the *R* enantiomer. Enzymatic catalysis can allow only the desired product to be created. Using an enantioselective nitrilase from *Alcaligenes faecalis*, pure (*R*)-(-)-mandelic acid can be produced from (*R*, *S*)-mandelonitrile (Xue et al. 2011).

Waste remediation

The use of nitrile chemicals raises significant safety and environmental concerns, as many are highly toxic, mutagenic, carcinogenic, and corrosive. Their toxicity can stem from the liberation of the cyano group as cyanide, or from actions of the larger nitrile itself (Pollak et al. 2000). As such, nitrilases are being investigated for the degradation of nitrile containing wastes from a variety of industries (Banerjee et al. 2002; Gong et al. 2012).

The popular nitrile herbicide bromoxynil and related compounds are widely used as broad leaf weeds killers. Their popularity raises concerns of soil and water contamination due to repeated applications. The nitrilase from *Klebsiella pneumo*niae subsp. *ozaenae* is able to efficiently degrade many bromoxynil related herbicides (Detzel et al. 2013) and could serve to clean contaminated water and overexposed soils.

Transgenic expression of this nitrilase in plants has already lead to the creation of bromoxynil resistant crops (Stalker et al. 1988).

The most notable environmental risk of nitrilases comes from the use of cyanide. It is used in the production of larger nitriles for use in industry (Pollak et al. 2000), but its widest use stems from its ability to bind and solubilize metals, leading to extensive use in electroplating and leach mining (Muezzinoglu 2003). Its application as such produces large quantities of cyanide-laden wastewater. It is possible for cyanide to be detoxified by chemical methods, but the materials used and the end products of the reaction can pose their own environmental hazards (Akcil 2003). This would suggest that cyanide hydrolyzing nitrilases would be of particular interest. The nitrilase cyanide dihydratase (CynD) from *Pseudomonas stutzeri* ($CynD_{stut}$) and *Bacillus pumilus* ($CynD_{pum}$) can degrade cyanide to ammonia and formate (Meyers et al. 1993; Watanabe et al. 1998). Additionally, nitrilase-related fungal cyanide hydratases (not to be confused with metal containing hydratases) can degrade cyanide and release formamide instead (Basile et al. 2008).

ENGINEERING NITRILASES

While the use of nitrilases can be less wasteful and environmentally hazardous than conventional chemical strategies, many require improvements in order to be adapted for use in industry. Their tolerance to industrial conditions, substrate specificity, specific activity, and overall stability are often less than ideal (Gong et al. 2012). This suggests protein engineering could lead to improved nitrilases properties.

Directed evolution using error-prone-PCR together with high throughput screens has proven a successful strategy for improving nitrilases for various applications. Substrate specificity was successfully altered though a directed evolution study of a nitrilase from *Acidovorax facilis* 72W, this work identified residues affecting specific activity towards 3-hydroxyvaleronitrile, or glycolonitrile. Saturation mutagenesis at these sites revealed mutants with 7.3 fold improved specific activity towards 3-hydroxyvaleronitrile (Wu et al. 2007), and others with 15.3 fold improvements towards glycolonitrile (Wu et al. 2008). In a nitrilase from *Alcaligenes faecalis* (NITAf) mutants were identified that had greater activity towards (R)-2-Cl-mandelonitrile and improved tolerance to lower pH conditions, both important to maintain enantiopurity (Schreiner et al. 2010).

A major obstacle to using nitrilases to degrade cyanide wastes has been pH tolerance. Cyanide is kept under very alkaline conditions to prevent it from forming hydrogen cyanide gas. Directed evolution of the cyanide degrading nitrilase, cyanide dihydratase CynD, from *B. pumilus* C1 has produced mutants with enhanced tolerance of high pH conditions (Wang et al. 2012) improved specific activity towards cyanide (Abou Nader 2012).

Without a crystal structure of any spiral forming nitrilase it is difficult to predict how mutations identified by directed evolution are affecting the protein's activity and stability. An improved knowledge of the nitrilase structure would not only provide context for existing improvements to the enzymes but also direct future studies. Understanding how those regions unique to nitrilases relative to crystallized homologs,

might influence activity and stability could enable some rational engineering of these proteins (Eijsink et al. 2004).

NITRILASE STRUCTURE

The predicted secondary, tertiary, and initial dimer structure of nitrilases are in line with the common core structure of the superfamily, but the oligomerization of the core structure into large spiral structures is unique to the nitrilase branch of the family (Thuku et al. 2009).

αββα-αββα dimer

An understanding of the basic monomer and dimer structure comes from structures from other branches of the larger superfamily. Despite great sequence divergence within the nitrilase superfamily, members have shown significant structural homology (Thuku et al. 2009). The monomer structure was first revealed to be a αββα sandwich from the crystal structure of the Nit domain from the NitFhit protein (branch 10) (Pace et al. 2000). In this and other crystal structures of family members this αββα monomer is paired to form a αββα-αββα dimer, a defining characteristic of the superfamily (Gordon et al. 2013; Kumaran et al. 2003; Nakai et al. 2000b; Pace and Brenner 2001; Pace et al. 2000). The interface pairing the monomer subunits into this αββα-αββα dimer is commonly referred to as the A-surface (Sewell et al. 2003). From the nitrilase branch of the superfamily, the *R. rhodochrous* J1 nitrilase can be purified as inactive dimers, which are the building blocks for their larger active structure(Nagasawa

et al. 2000). Secondary structure predictions, and circular dichroism data from nitrilase proteins indicate that the αββα-αββα dimer structure in conserved in the nitrilase branch (Mueller et al. 2006; Sewell et al. 2003; Thuku et al. 2007). Based on the dimer structures from the larger superfamily, dimer models have been constructed for a few members from the nitrilase branch (Figure 1.1) (Dent et al. 2009; Sewell et al. 2003; Sewell et al. 2005; Thuku et al. 2007; Williamson et al. 2010b).

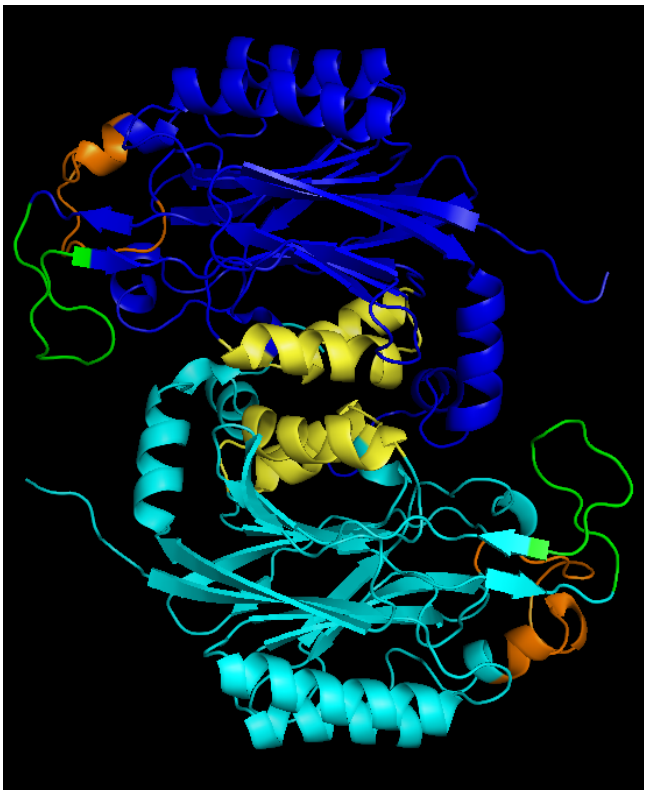

Figure 1.1 Updated dimer model of $CynD_{pum}$ taking into account latest crystallized homolog (B.T. Sewell, personal correspondence). Monomers colored blue and light blue. Predicted A-surface helices highlighted in yellow. Putative C-surface regions 1 and 2 highlighted in orange and green respectively. Figure generated in PyMol.

Spiral oligomer

In some structures of the superfamily members, the basic dimer structure can associate further to form a variety of oligomeric complexes. These include tetramers (Nakai et al. 2000b; Pace et al. 2000), hexamers (Kimani et al. 2007), and C-shaped octamers (Lundgren et al. 2008). While all structures share a common dimer interface, or A-surface, how these dimers associate into larger quaternary structures varies among different superfamily branches.

When the sizes of actual nitrilases were examined, they were found to form large oligomers, ranging from ~400kDa decamers to variable length oligomers >1MDa (Meyers et al. 1993; Nagasawa et al. 2000; Watanabe et al. 1998). Under an electron microscope (EM) these nitrilase oligomers appear as large spiral oligomers (Dent et al. 2009; Jandhyala et al. 2003; Meyers et al. 1993; Sewell et al. 2003; Thuku et al. 2007; Vejvoda et al. 2008; Woodward 2011; Woodward et al. 2008). Three-dimensional reconstructions from EM tomography have revealed these large oligomers to be left handed corkscrew shaped spirals (Dent et al. 2009; Jandhyala et al. 2003; Sewell et al. 2003; Thuku et al. 2007; Woodward et al. 2008) (Figure 1.2). In the nitrilase from *R. rhodochrous* J1 (prior to modification) and *Geobacillus pallidus* RAPc8, the oligomer does not complete a full turn and instead resembles rings or C-shaped oligomers (Williamson et al. 2010b). These partial turns of the spiral beg comparison to the C-shaped octomers of β-alanine synthesis from *Drosophila melanogaster* which, if stacked, could resemble the spiral structure seen in the nitrilase branch (Figure 1.3) (Lundgren et al. 2008).

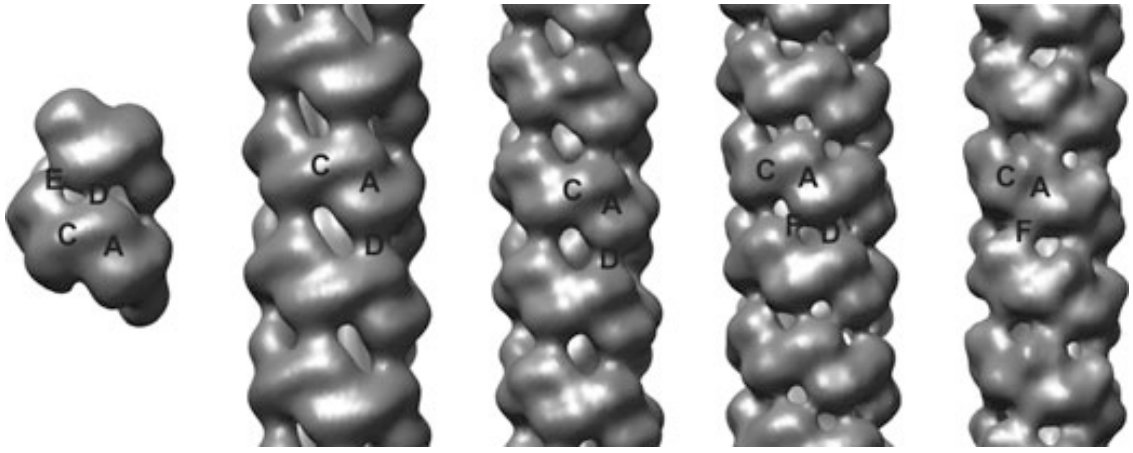

Figure 1.2 3D EM reconstructions of spiral nitrilases. From left to right; self-terminated $CynD_{pum}$, extended $CynD_{pum}$ at pH 5.4, C-terminally truncated J1 nitrilase, cyanide hydratases from *Neurospora crassa* and *Gloecercospora sorghi*. The intersubunit surfaces are labeled A, C, D, E, and F (Thuku et al. 2009).

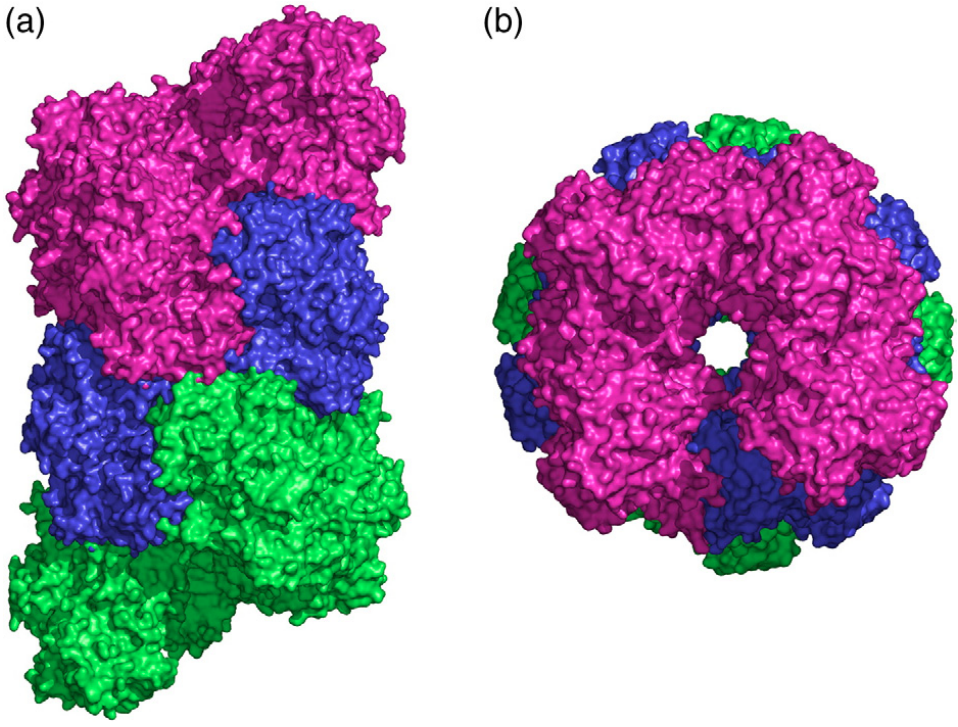

Figure 1.3 C-shape oligomer of octomers of β-alanine synthesis from *Drosophila melanogaster* stacked to resemble the nitrilase spiral oligomer. (a) Side and (b) top view (Lundgren et al. 2008). Octomers are diferentially colored.

Spiral formation and nitrilase function

In all nitrilases that have been examined, the formation of this spiral structure is obligatory for activity. This is thought to be due to the positioning of a catalytic glutamate in the active site upon oligomerization (Williamson et al. 2010b). The nitrilase from *R. rhodochrous* J1, which can be purified as a dimer, only becomes active once triggered to oligomerize further into C-shaped or variable length spirals. This oligomerization is triggered by the addition of the substrate benzonitrile. Following activation by benzonitrile, the nitrilase's specificity includes additional substrates that themselves can not trigger activation (Nagasawa et al. 2000). The C-shaped oligomers of the J1 nitrilase can associate further into spiral structures following a spontaneous auto-cleavage of their C-terminus. Expression of the J1 nitrilase, truncated at the auto-cleavage site, results in active extended oligomers, removing the need for activation by benzonitrile (Thuku et al. 2007).

CynD from *B. pumilus* forms 18 subunit spirals at neutral pH, but when the pH is lowered to 5.4 it extends into long non-terminating spirals. This is also associated with a bump in cyanide degrading activity. It is hypothesized that this bump in activity is due to activation of the terminal subunits of the 18-mers when they associate into the larger spirals (Jandhyala et al. 2003; Jandhyala et al. 2005). Similarly mutations in CynD that were identified for enhanced high pH tolerance were found to cause non-terminating spirals at neutral pH (Wang et al. 2012).

The shape of the spiral also seems to influence the accessibility of the active site cavity. When the spiral shape and the substrate specificity of various spiral nitrilases

were compared, a correlation was found between the twist per subunit of the spiral and the size of substrates accepted. Plant nitrilases with less twist per subunit are able to accept nitriles with much larger R-groups than tightly wound nitrilases, such as CynD, which can only hydrolyze cyanide (Woodward 2011). Understanding the surfaces involved in oligomerization may allow the properties of nitrilases to be manipulated.

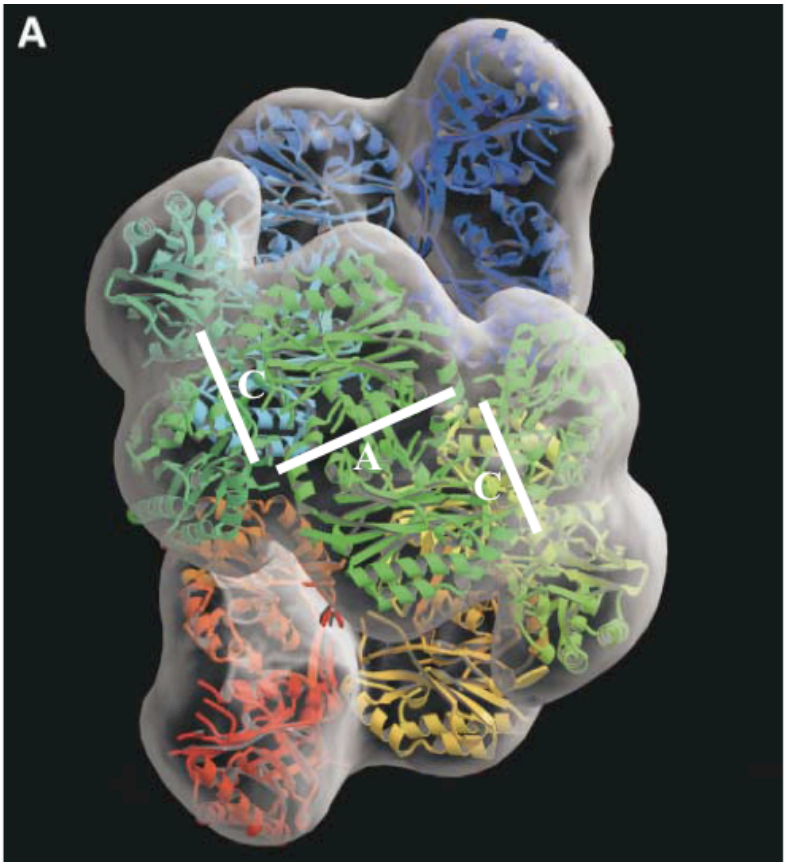

Figure 1.4 Seven dimer models of $CynD_{stut}$ fit to the 3D shell created from EM reconstructions. Dimers are differentially colored. The C-terminal tail, and the two C-surface regions are not included in this model (Sewell et al. 2003). The A-surface forming the center dimer and the C-surface interfaces of adjacent dimers are indicated and labeled over the structure.

OLIGOMERIC SURFACES

To picture how the basic nitrilase dimer interacts to form the larger spiral oligomer, their dimer models were fit to their 3D-reconstructions from EM tomography (Dent et al. 2009; Sewell et al. 2003; Thuku et al. 2007; Williamson et al. 2010b) (Figure 1.4). In these fitted models multiple contacting surfaces are seen between subunits. The A-surface is the interface between monomers that form the dimer building block and is conserved throughout the superfamily. The primary interface between adjacent dimers has been called the C-surface (Sewell et al. 2003) (Figure 1.2 and 1.3). These two surfaces are the basis for spiral formation (Figure 1.4). Other interactions are among the adjacent turns in the spiral and vary between different nitrilases but include the D, E, and F surfaces (Figure 1.2). The D and F surfaces are symmetric interactions seen in various 3D reconstructions and are thought to stabilize the spiral shape (Dent et al. 2009; Sewell et al. 2003; Sewell et al. 2005; Thuku et al. 2007; Woodward et al. 2008). In the self terminating nitrilase CynD from *B. pumilus* and *P. stutzeri* an asymmetric interaction is seen in between the dimer at the terminal end of the spiral and the previous turn. This E-surface interaction is thought to be responsible for terminating the spiral (Sewell et al. 2003; Sewell et al. 2005). Our current understanding of these inter-subunit surfaces is reviewed here.

A-surface

The A-surface is formed by two α-helixes on each monomer, which interact to form the αββα-αββα pair (Figure 1.1). The sequence and pattern of interactions across this interface varies but the A-surface structure is seen in all superfamily crystal structures as the basis for dimer formation (Gordon et al. 2013; Kimani et al. 2007; Kumaran et al. 2003; Wang et al. 2001b). The conservation of dimer formation at the A-surface may stem from a role in positioning the active site cysteine, as seen in the crystal structure of the putative CN hydrolase from yeast (Kumaran et al. 2003). In the nitrilase CynD from *B. pumilus* and *P. stutzeri* mutations in the predicted A-surface helices disrupted activity (Sewell et al. 2005), possibly through this mechanism.

Another region thought to participate in the A-surface is the C-terminus. In some structures from superfamily members the C-termini interact with and strengthens the A-surface, although the sequence and structure is divergent (Kimani et al. 2007; Lundgren et al. 2008). Nitrilases have extended C-termini relative to many other superfamily members, but the sequence and secondary structure characteristics of the C-terminal region vary greatly even among closely related nitrilases (Sewell et al. 2005).

C-surface

The C-surface is the primary interaction between dimers in the formation of the larger spiral structure of nitrilases. This surface can be seen as the interaction between adjacent dimers in the fitted dimer models (Dent et al. 2009; Sewell et al. 2003; Thuku et al. 2007) (Figure 1.4). The C-surface lies perpendicular to the A-surface. Together these

two surfaces establish the shape of the spiral structure. The angle across the C-surface varies among nitrilases and determines the degree of twist in the spiral. There are two regions of sequence in the nitrilases that are thought to participate in this surface (C-surface region 1 and 2) (Figure1.1). When sequences of nitrilases are aligned with those homologs with known structures, C-surface regions 1 and 2 stand out as insertions missing in all known structures (Sewell et al. 2005).

One crystallized homolog, the C-shaped superfamily member β-alanine synthase (βaS) from *D. melanogaster*, resembles the C-shaped oligomers of the J1 and *G. pallidus* nitrilases. This structure has allowed a C-surface interaction to be viewed at atomic resolution for the first time (Lundgren et al. 2008). The βaS structure contains an insertion region relative to the other crystallized homologs, similar to the nitrilase C-surface region 2. This region in βaS participates in oligomerization though two symmetric salt-bridges. Similarly charged residues are present in region 2 of nitrilases and could be participating in the C-surface if they are paired across the it (Thuku et al. 2009). In CynD, deletion of region 2 disrupts nitrilase activity, but this mutant was not examined for quaternary structure (Sewell et al. 2005). This region 2 in βaS also forms the roof of the active site. This could explain the correlation seen between the twist of nitrilase spirals and the size of substrates accepted (Woodward 2011). Folding of this surface may also influence the active site by positioning the second catalytic glutamate, which lies in close proximity to the C-surface, as proposed in the structure of the aliphatic amidase from *G. pallidus* RAPc8 (Kimani et al. 2007).

The βaS structure is less predictive of whether C-surface region 1 contributes to spiral formation. βaS does have residues in this region that do participate in the C-surface, but the nitrilase C-surface region is much larger and stands out as an insertion relative to the βaS and other superfamily members (Thuku et al. 2009). This C-surface region 1 has not been tested for a potential role in activity or oligomerization.

D and F surface

Symmetric cross spiral interactions, D and F, vary depending on the nitrilase but are seen in 3D reconstructions as contacts between consecutive turns of the nitrilase spiral. CynD and the J1 nitrilase only have the D-surface (Sewell et al. 2005; Thuku et al. 2007), whereas cyanide hydratases from *Gloecercospora sorghi* and *Neurospora crassa* have an F-surface contact or both D and F-surfaces (Figure 1.2) (Dent et al. 2009; Woodward et al. 2008). A mixture of charged residues on the D surface in CynD and the J1 nitrilase suggest that salt bridging across this surface could be stabilizing the spiral (Sewell et al. 2005; Thuku et al. 2007). Mutations removing predicted salt bridging did not alter activity in CynD(Sewell et al. 2005), however the mutation Q86R, which is predicted to add a salt bridge at the D-surface, increased CynD's thermal stability and tolerance of higher pH (Wang et al. 2012). Other groups are currently testing these cross-spiral interactions role in oligomerization (personal correspondence).

E-surface

In self-terminating spiral nitrilases, namely CynD from *B. pumilus* and *P. stutzeri*, an asymmetric cross-spiral interaction is seen between the terminal dimer and the previous turn of the spiral. This interface has been named the E-surface and it hypothesized to be responsible to the self-termination of CynD. Variations in E-surface interactions are seen between CynD species, $CynD_{pum}$ terminates at 18 subunits (Jandhyala et al. 2003) and $CynD_{stut}$ at 14 subunits (Sewell et al. 2003).

C-terminus tail

The highly variable nitrilase C-terminus could be interacting with multiple oligomeric surfaces. In all nitrilases the C-terminus of the protein is extended by 40-100 amino acids relative to many of the nitrilases with known structures. Furthermore within the nitrilase branch itself, the sequence of this region is highly variable even between closely related enzymes (Thuku et al. 2009). CynD from *B. pumilus* and *P. stutzeri* share 76% identity overall, but only 30% identity in the C-terminal tail (Abou Nader 2012). The C-terminus has been predicted to participate in oligomerization, but its role likely varies among nitrilases, given the variability of this tail. In the 3D reconstruction of $CynD_{stut}$, the C-terminus is predicted to lie in the center of the spiral where it could potentially make multiple contacts (Sewell et al. 2003).

C-terminal extensions in other superfamily members propose possible roles of this region in nitrilase oligomerization. The crystal structure of the amidase from *G. pallidus* has the C-terminus interlocking and strengthening the A-surface in dimer

formation (Kimani et al. 2007; Lundgren et al. 2008). Modeling of the fungal nitrilase cyanide hydratase from *N. crassa*, based on the amidase structure, places part of the C-terminus at both the A and C-surfaces (Dent et al. 2009). In βaS from *D. melanogaster* the tail folds in the center of the C-shaped spiral where it contributes to both the A and C-surfaces (Lundgren et al. 2008).

In nitrilases modification of the C-terminal tail has been seen to have a variety of effects on spiral length. In the J1 nitrilase from *R. rhodochrous* J1 the extended C-terminus prevents oligomerization. Once triggered by substrate the protein auto-cleaves the C-terminus removing the last 39 amino acids. This allows the protein to then oligomerize into the active spiral structure. Expression of this protein with shorter or longer truncations resulted in short, poorly formed oligomers, leading to the hypothesis that the position of the C-terminus in the center of the spiral allows it to influence the shape of the spiral and the alignment of the cross-spiral D surface (Thuku et al. 2007). Consistent with this is the pH dependant change in spiral size of $CynD_{pum}$. When the pH is lowered to 5.4 $CynD_{pum}$ shifts from 18 subunit spirals terminating at the E-surface, to long variable length spirals. This behavior is thought to be driven by histidines in the C-terminal tail gaining a charge, changing the conformation of this region, and altering the shape of the spiral, preventing the E-surface from aligning (Jandhyala et al. 2005). Another $CynD_{pum}$ variant (8A3) that lacks these histidines in the tail does not show this pH transition (Jandhyala et al. 2003).

Truncations to the C-terminus of other nitrilases are tolerated to a varying degree. In the nitrilase from *Pseudomonas fluorescens* EBC191, truncations of the C-

terminus resulted in reduced activity, increased amide formation, and loss of enantioselectivity. Replacement of the C-terminus with tails from a nitrilase in *R. rhodochrous* NCIMB11216 was able restore the wild-type characteristics to the nitrilase *P. fluorescens* (Kiziak et al. 2007). C-terminal truncations in CynD show different levels of tolerance between the *B. pumilus* and *P. stutzeri* enzymes. $CynD_{pum}$ was able to tolerate large deletions up to 38 residues and remain partially active. $CynD_{stut}$ by comparison was inactive with equivalent or smaller truncations. Swapping the C-terminal tails between $CynD_{pum}$ and $CynD_{stut}$ was tolerated in the $CynD_{pum}$ enzyme ($CynD_{pum\text{-}stut}$), but the reverse hybrid ($CynD_{stut\text{-}pum}$) was inactive (Sewell et al. 2005). Further exaggerating this one sided compatibility, the $CynD_{pum\text{-}stut}$ hybrid was found to be much more thermally stable and have greater tolerance to alkaline conditions than either parent CynD or any mutant identified during directed evolution experiments (Abou Nader 2012).

CYANIDE DIHYDRATASE

Work with cyanide dihydratase (CynD) from *B. pumilus* and *P. stutzeri* has contributed greatly to our understanding of the nitrilase oligomeric structure, and is the focus of this and other current studies (Abou Nader 2012; Wang et al. 2012). *B. pumilus* C1 was first isolated from enriched cultures started with soil from a cyanide waste-water dam in the Transvaal, South Africa (Meyers et al. 1991) and *P. stutzeri* AK61 was isolated from cyanide-laden wastewater from a metal plating plant (Watanabe et al. 1998). Sequence analysis and point mutagenesis of the conserved active site residues

demonstrated CynD's relation to other nitrilase enzymes (Watanabe et al. 1998). Electron microscopy of CynD from *B. pumilus* first revealed the spiral shape of nitrilase oligomers (Jandhyala et al. 2003; Meyers et al. 1993). Further 3D EM reconstruction of $CynD_{pum}$ and $CynD_{stut}$ revealed the nitrilase spirals to be left handed corkscrew shaped fibers (Jandhyala et al. 2003; Sewell et al. 2003). This led to the modeling and fitting of the $CynD_{stut}$ dimer into these 3D reconstruction and the prediction of the inter-dimer surfaces C, D, and E (Sewell et al. 2003). To begin testing the predicted oligomeric regions the effects on activity of mutating the A surface, C surface, D surface, and the C-terminus were investigated in $CynD_{pum}$ and $CynD_{stut}$ though the quaternary structure was not examined (Sewell et al. 2005).

A characteristic of CynD that has enabled investigation of nitrilase oligomerization is its self-termination. The self-termination of CynD at the E-surface limits the size to 18 or 14 subunit spirals respectively (Jandhyala et al. 2003; Sewell et al. 2003). This allows the protein to be purified as a single peak by size exclusion, and any disruption or distortions of the oligomer to be detected as changes to the normal elution pattern. Also the difference in the alignment of the E-surface between the $CynD_{pum}$ 18-mer and $CynD_{stut}$ 14-mer may allow for changes in the spirals shape to be detected through changes in self-termination. While other nitrilases such as the J1 nitrilase and the *G. pallidus* nitrilase can be purified as partial spiral or C-shaped oligomers, they either eventually oligomerize further (Thuku et al. 2007) or vary in size (Williamson et al. 2010b). In this work I examine the participation of the two predicted

C-surface regions by examining how substituting residues in these regions affect activity and oligomerization of $CynD_{pum}$.

Effects of the C-terminal tail on nitrilase activity, substrate and product specificity, stability, and oligomer formation has been observed in multiple nitrilases, but which other regions of the protein this tail interacts with is unclear (Abou Nader 2012; Kiziak et al. 2007; Sewell et al. 2005; Thuku et al. 2007). The phenotypes of the two CynD tail-swap hybrids present an opportunity to investigate where this region interacts elsewhere in the protein. Experiments described herein test if the C-terminus participates in oligomerization between dimers by investigating whether the stabilizing effects of the $CynD_{stut}$ C-terminal tail can suppress disruptive mutants in $CynD_{pum}$'s C-surface. Furthermore, experiments were performed to identify other regions of the protein that the C-terminus may interact with by starting with the inactive $CynD_{stut\text{-}pum}$ hybrid and experimentally determining if swapping other domains for the $CynD_{pum}$ sequence could suppress the disruptive effect of the $CynD_{pum}$ C-terminal tail.

CHAPTER II

PROBING AN INTERFACIAL SURFACE IN THE CYANIDE DIHYDRATASE FROM *BACILLUS PUMILUS,* A SPIRAL FORMING NITRILASE

SYNOPSIS

Nitrilases are of significant interest both due to their potential for industrial production of valuable products as well as degradation of hazardous nitrile-containing wastes. All members of the nitrilase superfamily are found as an αββα-αββα dimer. The nitrilases expand upon this basic dimer and form large spiral shaped homo-oligomers. The formation of this larger structure is linked to both the activity and substrate specificity of these nitrilases. The sequences of the spiral nitrilases differ from the non-spiral forming homologs by the presence of two insertion regions. These regions are hypothesized to be responsible for associating the nitrilase dimers into the oligomer. Here we used cysteine scanning across these two regions, in the spiral forming nitrilase cyanide dihydratase from *Bacillus pumilus* (CynD), to identify residues altering the oligomeric state or activity of the nitrilase. Several mutations were found to cause changes to the size of the oligomer as well as reduction in activity. Additionally one mutation, R67C, caused a partial defect in oligomerization with the accumulation of smaller oligomer variants. These results support the hypothesis that these insertion regions contribute to the unique quaternary structure of the spiral microbial nitrilases.

INTRODUCTION

Nitrilase enzymes from the large nitrilase-superfamily are of significant industrial interest due to their ability to process nitrile compounds into valuable acid products such as nicotinic acid, acrylic acid, and glycolic acid (Gong et al. 2012; Singh et al. 2006). They also offer economic and environmentally friendly alternatives to current hazardous and costly methods of detoxifying nitrilase wastes (Gong et al. 2012; Korte and Coulston 1995). One of the most prevalent and certainly the most toxic nitrile waste is cyanide, which has extensive uses in industry from polymer synthesis to mining and electroplating (Akcil 2003; Korte and Coulston 1995). Nitrilases such as cyanide dihydratase, CynD, provide an attractive option for degrading the high volumes of cyanide wastes produced by these industries (Meyers et al. 1993; Watanabe et al. 1998).

In order to exploit further applications of these nitrilases, enzymes often need to be engineered to tolerate industrial conditions or recognize specific substrates. While random mutagenesis and high throughput screening have revealed useful mutants (Abou Nader 2012; Schreiner et al. 2010; Wang et al. 2012), our ability to make rational changes is impeded by the absence of structural information of these enzymes. Crystal structures have been solved for several proteins within the larger nitrilase superfamily (Kimani et al. 2007; Kumaran et al. 2003; Lundgren et al. 2008; Nakai et al. 2000a; Pace et al. 2000; Wang et al. 2001a), but attempts to crystallize members of the nitrilase branch have not yet been successful. Three dimensional, negative stain electron microscopy (3D EM) has shown that all active nitrilases examined to date form large

spiral shaped oligomers (Dent et al. 2009; Jandhyala et al. 2003; Sewell et al. 2003; Thuku et al. 2007; Williamson et al. 2010a; Woodward et al. 2008).

The spiral structure has also been linked to the activation and substrate specificity of nitrilases. In the nitrilase from *Rhodococcus rhodochrous* J1 the protein purifies as an inactive dimer. These dimers oligomerize into decamers when incubated with the substrate benzonitrile. Once activated by oligomerization, the nitrilase is able to recognize additional substrates that were unable to themselves activate the enzyme (Nagasawa et al. 2000).

The cyanide dihydratase (CynD) from *Bacillus pumilus*, which forms a self-terminating 18-mer at neutral pH, fails to terminate and forms long variable oligomers when the pH is lowered to 5.4 (Jandhyala et al. 2003). The elongation is associated with a slight increase in CynD activity thought to stem from the activation of formerly terminal subunits when they interact across the elongation interface (Jandhyala et al. 2005).

The quaternary structures of most of the crystallized homologs do not resemble the spirals seen in the nitrilases, however they all share a common monomer and dimer structure. The monomers form the αββα fold, which associate across the A-surface to form the αββα-αββα dimer (Kimani et al. 2007; Kumaran et al. 2003; Lundgren et al. 2008; Nakai et al. 2000a; Pace et al. 2000; Wang et al. 2001a). To understand how these dimers may interact to form the spiral structure, the dimers were fitted into the 3D shells obtained from 3D EM (Dent et al. 2009; Sewell et al. 2003; Sewell et al. 2005; Thuku et al. 2007; Williamson et al. 2010a; Woodward et al. 2008). The docked dimers enable

pseudo-atomic models of the elongated fibers to be obtained, and these models in turn enable the identification of those amino acids that may play a role in the interface.

The interface between dimers that plays a primary role in the elongation of the spiral has been referred to as the C-surface (Sewell et al. 2003). This C-surface interaction is one of two classes of interactions of the dimers seen in the fully elongated spirals. Other interactions form once the spiral completes a full turn. The details of these surfaces appear to vary depending on the nitrilase but include the cross-spiral D and F-surfaces, which may play some role in stabilizing the intact spiral, and the E-surface, which appears to stop further spiral extension (Figure 2.1) (Dent et al. 2009; Sewell et al. 2005; Thuku et al. 2007; Woodward et al. 2008).

The amino acids of the spiral forming nitrilases that comprise the putative C – surface have been identified by aligning the sequences of these enzymes to those of the members of the superfamily for which the crystal structures have been determined. (Figure 2.2) (Thuku et al. 2009). The alignment identifies two insertions relative to the non-spiral forming family members. Based on the fitted dimer model these two regions are proposed to lie in the C-surface interface (Sewell et al. 2005). 3D EM shows that the monomers on opposing sides of the C-surface interface are related to one another by a two-fold axis.

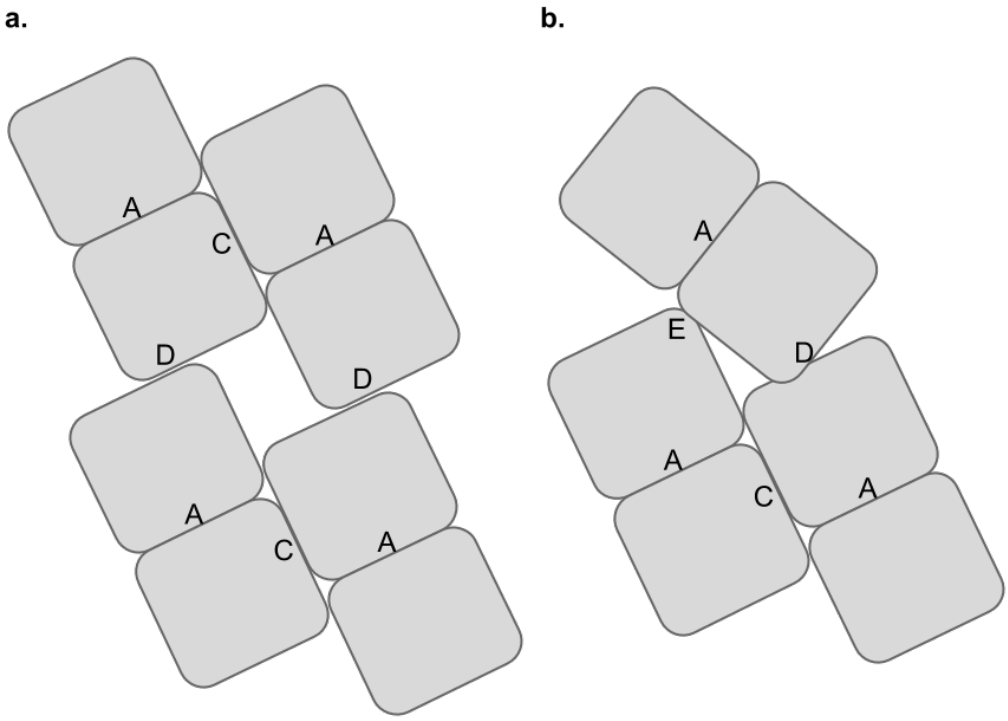

Figure 2.1 Diagram showing the position of oligomeric surfaces within the CynD spiral. Only two dimers are shown per turn. CynD monomers are represented by rectangles, which associate into dimers at the A-surface. The C-surface lies between adjacent dimers. (a) The D-surface interaction forms between adjacent turns of the spiral. (b) The terminal dimer at the end of the spiral forms the cross spiral E-surface interaction.

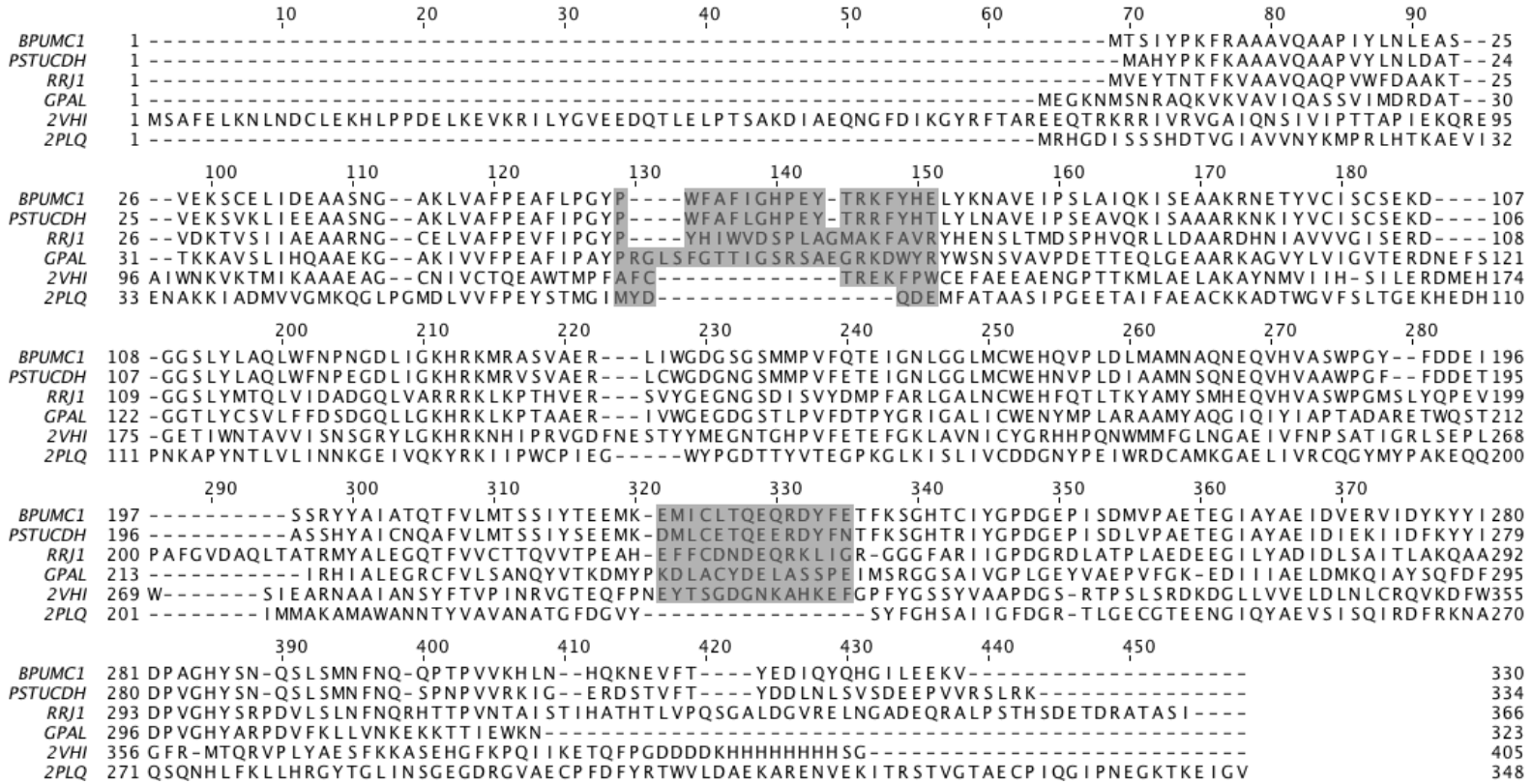

Figure 2.2 Multiple sequence alignment. Cyanide dihydratase from *B. pumilus* C1 and *P. stutzeri* (BPUMC1, PSTUCDH) (Jandhyala et al. 2003; Meyers et al. 1993; Sewell et al. 2003), Nitrilase from *R. rhodochrous* J1 (RRJ1) (Thuku et al. 2007), nitrilase from *G. pallidus* DAC521 (GPAL) (Williamson et al. 2010a), C-shaped β-alanine-synthase (βaS) from *D. melanogaster* (2VHI) (Lundgren et al. 2008), and non-spiral forming crystallized nitrilase superfamily member 2PLQ (Kimani et al. 2007; Kumaran et al. 2003; Nakai et al. 2000a; Pace et al. 2000; Wang et al. 2001a). Relative insertion regions in the spiral and C shaped nitrilases hypothesized to participate in oligomeric surfaces C-surface are highlighted. Multiple sequence alignment was constructed with ClustalW2 (Goujon et al. 2010; Larkin et al. 2007). Alignment was edited and exported using Jalview software (Waterhouse et al. 2009).

The crystal structure of the nitrilase-like beta-alanine synthase (βaS) from *Drosophila melanogaster* (Lundgren et al. 2008) enabled the first near atomic resolution visualization of this interface. βaS forms C-shaped oligomers that, if extended, could resemble the spiral of the nitrilases. Similar to the spiral forming nitrilases, βaS has an insertion (corresponding to residues 222-235 in CynD) relative to the other crystallized nitrilase-superfamily members. The insertion in βaS lies at an intermolecular interface that corresponds to the C-surface identified in the extended spirals. Interestingly the loop containing the insertion is disordered in the unmatched dimers at the ends of the βaS oligomer. Once folded in a paired C-surface these regions form the ceiling of the active site pocket, which could explain the link between activity and quaternary structure in the nitrilase enzymes (Lundgren et al. 2008). The βaS structure is less informative on the role the other insertion region(P55-E72) in the spiral nitrilases, as βaS does not have this relative insertion.

In a prior study investigating the oligomeric surfaces in cyanide dihydratase from *B. pumilus* (CynD), the C-surface region 2 (residues 222-235), missing in the non-spiral forming crystallized nitrilase-superfamily members, was deleted. This lead to complete loss of activity but the effect on oligomerization was not examined (Sewell et al. 2005). The other insertion C-surface region 1 (P55-E72) has not to-date been analyzed. To test the involvement of these putative C-surface regions in spiral formation we scanned the two regions in CynD for mutations affecting the oligomeric state or activity of the protein. Individual cysteine substitutions at each residue within these two putative C-surface regions were initially constructed to search for disulfide bridgeable positions.

Here each of these mutants was characterized for effects on the proteins activity and the oligomeric state as predicted by native protein size was examined by size exclusion chromatography.

METHODS

Media and reagents

Luria broth and plates were used for the growth of all bacterial strains, supplemented as needed with 25μg/ml chloramphenicol or 25μg/ml kanamycin. Phusion High Fidelity DNA polymerase master mix and restriction enzymes were purchased from New England Biolabs (NEB; Ipswich, MA). B-PER® extraction reagents, HisPur™ Cobalt Spin Columns, and Zeba Desalting Columns were obtained from Thermo-Scientific (Pierce Biotechnology; Rockford, IL).

Bacterial strains plasmids

Escherichia coli strain MB3436 (Δ*endA thiA hsdR17 supE44 lacI*^{q}*ZΔm15*) was used for cloning and mutant construction. Plasmids were transformed into *E. coli* BL21(DE3) pLysS for expression. All substitution mutants were constructed in pMB4407, which is pET28a containing CynD as a NdeI-XhoI insertion (Abou Nader 2012).

Scanning mutagenesis

Mutants were constructed by site directed mutagenesis following QuickChange® protocol (Stratagene, La Jolla, CA) using mutagenic primers (Table 2.1) and Phusion DNA polymerase and confirmed by sequencing. Mutagenic primers were designed using the program PrimerX (http://www.bioinformatics.org/primerx/).

Table 2.1 Primers used in the construction of the substitution mutations in insertion region 1.

Primers	Sequence
Pum Y54C F	GAAGCATTTTTACCTGGTTGCCCTTGGTTTGCTTTTATTG
Pum Y54C R	CAATAAAAGCAAACCAAGGGCAACCAGGTAAAAATGCTTC
Pum P55C F	GCATTTTTACCTGGTTATTGCTGGTTTGCTTTTATTGG
Pum P55C R	CCAATAAAAGCAAACCAGCAATAACCAGGTAAAAATGC
Pum W56C F	CCTGGTTATCCTTGCTTTGCTTTTATTGG
Pum W56C R	CCAATAAAAGCAAAGCAAGGATAACCAGG
Pum F57C F	CTGGTTATCCTTGGTGTGCTTTTATTGGTC
Pum F57C R	GACCAATAAAAGCACACCAAGGATAACCAG
Pum A58C F	GGTTATCCTTGGTTTTGTTTTATTGGTCATCC
Pum A58C R	GGATGACCAATAAAACAAAACCAAGGATAACC
Pum F59C F	CCTTGGTTTGCTTGTATTGGTCATCC
Pum F59C R	GGATGACCAATACAAGCAAACCAAGG
Pum I60C F	GTTATCCTTGGTTTGCTTTTTGTGGTCATCCAGAATATACG
Pum I60C R	CGTATATTCTGGATGACCACAAAAAGCAAACCAAGGATAAC
Pum G61C F	CCTTGGTTTGCTTTTATTTGTCATCCAGAATATACG
Pum G61C R	CGTATATTCTGGATGACAAATAAAAGCAAACCAAGG
Pum H62C F	GTTTGCTTTTATTGGTTGTCCAGAATATACGAG
Pum H62C R	CTCGTATATTCTGGACAACCAATAAAAGCAAAC
Pum P63C F	GTTTGCTTTTATTGGTCATTGCGAATATACGAGAAAGTTC
Pum P63C R	GAACTTTCTCGTATATTCGCAATGACCAATAAAAGCAAAC
Pum E64C F	GCTTTTATTGGTCATCCATGTTATACGAGAAAGTTCTATC
Pum E64C R	GATAGAACTTTCTCGTATAACATGGATGACCAATAAAAGC
Pum Y65C F	GGTCATCCAGAATGTACGAGAAAGTTC
Pum Y65C R	GAACTTTCTCGTACATTCTGGATGACC
Pum T66C F	GGTCATCCAGAATATTGCAGAAAGTTCTATCATG
Pum T66C R	CATGATAGAACTTTCTGCAATATTCTGGATGACC
Pum R67C F	GTCATCCAGAATATACGTGCAAGTTCTATCATG
Pum R67C R	CATGATAGAACTTGCACGTATATTCTGGATGAC
Pum K68C F	GTCATCCAGAATATACGAGATGCTTCTATCATGA
Pum K68C R	TCATGATAGAAGCATCTCGTATATTCTGGATGAC

Table 2.1 continued

Pum F69C F	ATCCAGAATATACGAGAAAGTGCTATCATGAATTAT
Pum F69C R	ATAATTCATGATAGCACTTTCTCGTATATTCTGGAT
Pum Y70C F	CAGAATATACGAGAAAGTTCTGCCATGAATTATATAAAAATGC
Pum Y70C R	GCATTTTTATATAATTCATGGCAGAACTTTCTCGTATATTCTG
Pum H71C F	TATACGAGAAAGTTCTATTGCGAATTATATAAAAATGCCG
Pum H71C R	CGGCATTTTTATATAATTCGCAATAGAACTTTCTCGTATA
Pum E72C F	CGAGAAAGTTCTATCATTGCTTATATAAAAATGCCG
Pum E72C R	CGGCATTTTTATATAAGCAATGATAGAACTTTCTCG
Pum E222C F	CGGAAGAAATGAAATGCATGATTTGTTTAACG
Pum E222C R	CGTTAAACAAATCATGCATTTCATTTCTTCCG
Pum M223C F	GAAATGAAAGAGTGCATTTGTTTAACGCAG
Pum M223C R	CTGCGTTAAACAAATGCACTCTTTCATTTC
Pum I224C F	GAAATGAAAGAGATGTGCTGTTTAACGCAG
Pum I224C R	CTGCGTTAAACAGCACATCTCTTTCATTTC
Pum C225A F	GAAAGAGATGATTGCTTTAACGCAGGAG
Pum C225A R	CTCCTGCGTTAAAGCAATCATCTCTTTC
Pum L226C F	GAGATGATTTGTTGCACGCAGGAGCAAAG
Pum L226C R	CTTTGCTCCTGCGTGCAACAAATCATCTC
Pum K221C F	TACGGAAGAAATGTGCGAGATGATTTG
Pum K221C R	AACAAATCATCTCGCACATTTCTTCCG
Pum T227C F	GATGATTTGTTTATGCCAGGAGCAAAGAG
Pum T227C R	CTCTTTGCTCCTGGCATAAACAAATCATC
Pum Q228C F	GATGATTTGTTTAACGTGTGAGCAAAGAGATTAC
Pum Q228C R	GTAATCTCTTTGCTCACACGTTAAACAAATCATC
Pum E229C F	GATTTGTTTAACGCAGTGCCAAAGAGATTACTTTG
Pum E229C R	CAAAGTAATCTCTTTGGCACTGCGTTAAACAAATC
Pum Q230C F	GTTTAACGCAGGAGTGCAGAGATTACTTTG
Pum Q230C R	CAAAGTAATCTCTGCACTCCTGCGTTAAAC
Pum R231C F	AACGCAGGAGCAATGCGATTACTTTGAAAC
Pum R231C R	GTTTCAAAGTAATCGCATTGCTCCTGCGTT
Pum D232C F	CGCAGGAGCAAAGATGTTACTTTGAAAC
Pum D232C R	GTTTCAAAGTAACATCTTTGCTCCTGCG
Pum Y233C F	CAGGAGCAAAGAGATTGTTTTGAAACATTTAAG
Pum Y233C R	CTTAAATGTTTCAAAACAATCTCTTTGCTCCTG
Pum F234C F	GCAAAGAGATTACTGCGAAACATTTAAGAGC
Pum F234C R	GCTCTTAAATGTTTCGCAGTAATCTCTTTGC
Pum E235C F	CAAAGAGATTACTTTTGCACATTTAAGAGCGG
Pum E235C R	CCGCTCTTAAATGTGCAAAAGTAATCTCTTTG

Primers designed using PrimerX (http://www.bioinformatics.org/primerx/)

Protein expression and purification

Protein was produced from *E. coli* BL21(DE3) pLysS transformed with pMB4407 or its derivatives. Cells were grown at 37°C to an OD600 between 0.4-0.6, and induced by adding IPTG to 1mM and transferred to 30°C for 2-3 hours. Enzyme activities in whole cells were examined immediately after the end of induction.

Cells destined for lysate production and/or protein purification were pelleted at 5,000g for 10 min and frozen at -20°C. Lysates were prepared using B-PER II Reagent® with added lysozyme and DNase, according to protocol (Pierce Biotechnology; Rockford, IL). Lysates were diluted with an equal volume of wash buffer (50mM sodium phosphate, 300mM sodium chloride, 10mM imidazole; pH 7.4). This was added to pre-equilibrated HisPur™ Cobalt 0.2ml resin bed Spin Columns (Pierce Biotechnology; Rockford, IL) in two to three 600µl applications. Each application of lysate was mixed end over end for 30 minutes on the sealed column. Columns were washed with 400µl wash buffer three times, and the protein was eluted in 600µl elution buffer (300mM sodium chloride, 150mM imidazole; pH7.4). Purified protein was exchanged into 0.1M MOPS buffer ph7.7 using 2ml Zeba™ Spin Desalting Columns 7K MWCO (Pierce Biotechnology; Rockford, IL) and stored on ice. Protein concentrations were measured by Bradford assay. Sample stored longer than overnight were divided into 200µl aliquots and frozen at -80°C.

Chromatography

Purified protein samples in 0.1M MOPS pH7.7 were separated at 0.5ml/min on a Superdex™ 200 10/300 GL column (Amersham Biosciences; Uppsala, Sweden) equilibrated with 0.1M MOPS pH7.7 using a BioRad BioLogic DuoFlow®. Protein elution was monitored by absorbance at 220 and 280nm using a BioRad BioLogic QuadTec® UV-Vis detector. Dilute samples were first concentrated using Amicon Ultra-4 centrifugal filter devices 10,000 MWCO (Millipore; Billerica, MA). The column was calibrated using Sigma-Aldrich gel filtration marker kit containing; Carbonic Anhydrase, bovine erythrocytes (29,000 Da), Albumin, bovine serum (66,000Da), Alchohol Dehydrogenase, yeast (150,0000 Da), β-Amylase, sweet potato (200,000 Da), Apoferritin, horse spleen (443,000 Da), Thyroglobulin, bovine (669,000 Da).

Purification for EM

Preparation of samples for EM was performed by Andani Mulelu. Aliquots of the purified protein samples in 0.1M MOPS pH7.7 were exchanged into 50 mM Tris pH 7.7, 150 mM NaCl, buffer using spin columns (Microsep Pty Ltd., South Africa). The protein was then separated at 0.5ml/min on a Superdex™ 200 10/300 GL column (Amersham Biosciences; Uppsala, Sweden) equilibrated with 50 mM Tris pH 7.7, 150 mM NaCl. Samples corresponding to the various elution peaks were collected and incubated overnight at 4°C before preparation of grids for electron microscopy.

Electron microscopy

Electron microscopy of CynD protein was performed by Andani Mulelu. The sample (3 µl) was incubated for 30 s on a glow-discharged carbon-coated copper grid, washed twice with deionized water, blotted with filter paper, and stained with three drops of 2% uranyl acetate, blotting between drops. Grids were examined using Tecnai T20 transmission electron microscopes operated at 200 kV, at a magnification of 69,000× and a nominal defocus of 3.0–5.0 µm. Images were recorded using a Gatan US1000 CCD camera.

Activity test

Activity was assayed using a picric acid assay to detect remaining cyanide (Wang et al. 2012). Purified protein was diluted to 50µg/ml in 100mM MOPS pH7.7. From this dilution 10µl was added to 80µl of 100mM MOPS pH7.7 in 96 well plates and allowed to incubate for 20 minutes at room temperature. To start the reaction 20µl of 25mM KCN in 100mM MOPS was added. The plate was covered with parafilm, which was pressed onto the wells to prevent evaporation of cyanide. The reaction was terminated at 20 minutes by adding 80µl of alkaline picric acid (0.5% picric acid in 0.25 M sodium carbonate). To develop the color, the plate was incubated at 60°C for 20 minutes. Absorbance was measured at OD520 in a Bio-Rad Benchmark Plus microplate spectrophotometer.

Activity from whole cells was measured similarly. 100µl of culture was mixed with 100µl of 6mM KCN in 0.1M MOPS pH 7.7 and the reaction was allowed to

proceed at room temperature. Remaining cyanide was detected by adding 100µl of the reaction to 100µl of alkaline picric acid (0.5% picric acid in 0.25 M sodium carbonate) in a 96 well plate and the absorbance was measured at OD520 in a Bio-Rad Benchmark Plus microplate spectrophotometer.

RESULTS

Effect of C-surface mutations on activity

To investigate the involvement of individual residues within the two putative C-surface regions of CynD from *B. pumilus*, each residue in C-surface region 1 (P55-E72) and C-surface region 2 (E222-E235) was individually replaced with cysteine except the native cysteine (C225) was changed to alanine. The activity of each purified CynD mutant protein was tested and CynD was found sensitive to cysteine substitution at several positions in C-surface region 1 (Figure 2.3a). Cysteine substitutions at P55, F57, G61, E64, Y65, T66, R67, F69, and Y70 reduced activity to ≤ 50% of wild type. Two of the mutants, R67C and Y70C, had no detectable activity when purified. R67C did have partial activity in whole cells but this activity was lost upon cell lysis, though the protein was readily purified. In contrast to region 1, there were only two mutations, Q230 and E235, in the C-surface region 2 that reduced CynD activity to ≤ 50% (Figure 2.3b).

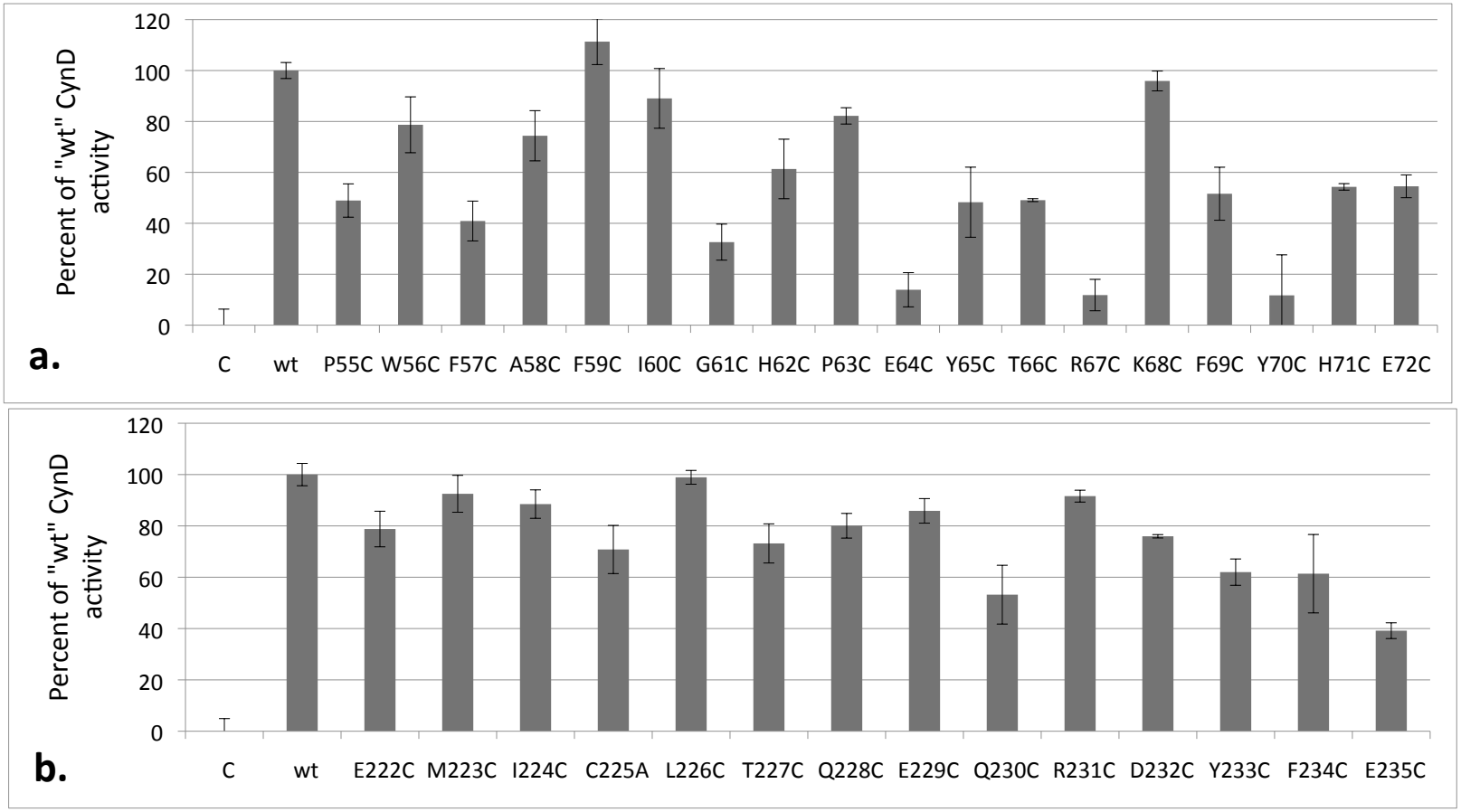

Figure 2.3 Activity of purified CynD proteins relative to wt CynD and buffer only controls (C) measured by picric acid CN assay. Activity for each substitution mutant in the C-surface regions 1 (a) and 2 (b). Error bars show standard deviation from three samples.

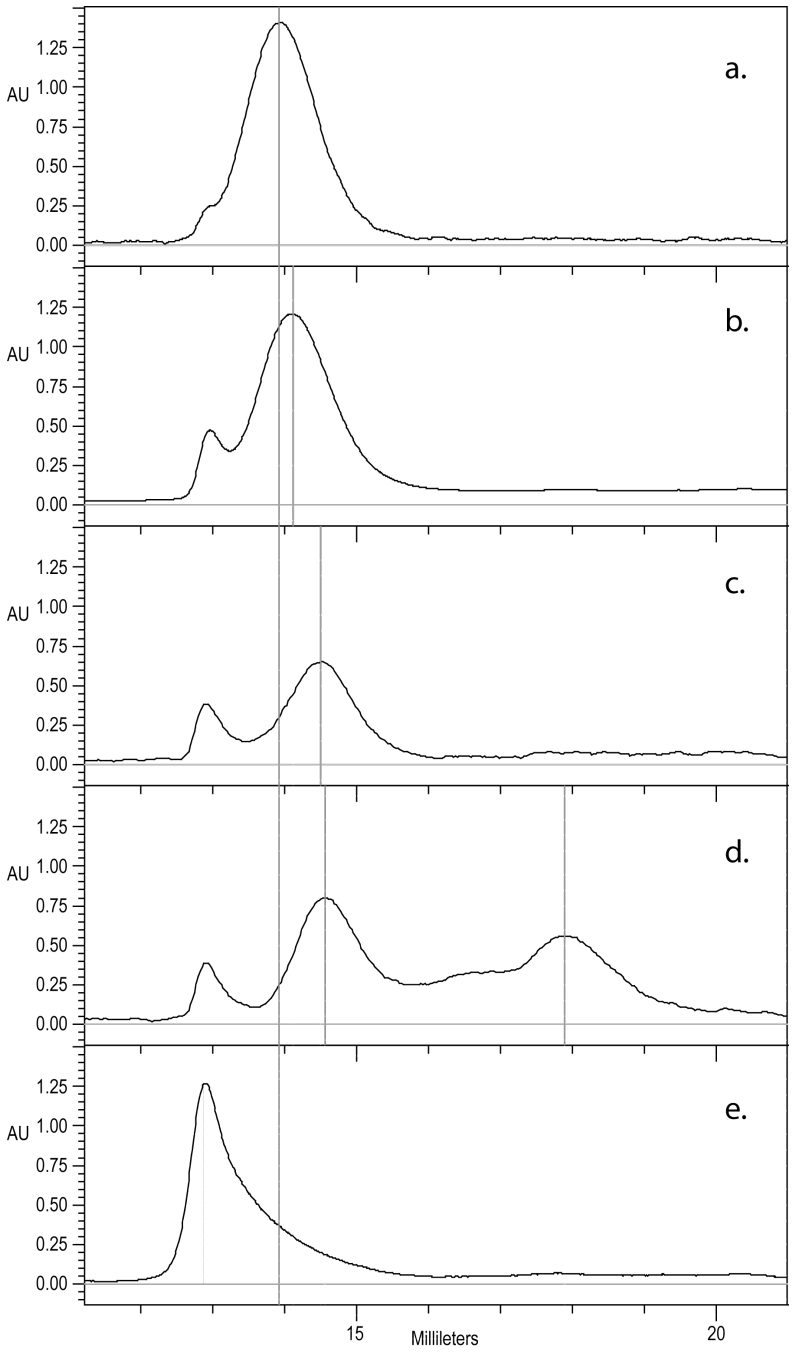

Figure 2.4 Size exclusion chromatography of C-surface mutants. Analysis on Superdex 200 10/300 GL of purified CynD protein in 100 mM MOPS pH 7.7. Elution monitored as absorbance at 220nm. Vertical gray lines highlight prominent peaks. Continuous gray line indicates wild-type CynD elution peak. Representative elution patterns of substitution mutants in CynD; a) wild type 18-mer CynD, b) intermediate 16-mer mutants (F69C shown) [see Table 2.2], c) *P. stutzeri* CynD 14-mer-like F57C, d) multiple elution peaks of R67C [also see Figure 2.5a], e) sloping void peak of Q228C.

Table 2.2 Elution patterns of each mutant investigated by gel filtration.

Elution/Mutant	wt	P55C	W56C	F57C	A58C	F59C	I60C	G61C	H62C	P63C	E64C	Y65C	T66C	R67C	K68C	F69C	Y70C	H71C	E72C
18-mer	X	X			X	X	X		X	X		X			X				X
~16-mer			X								X		X			X	X	X	
14-mer				X				X						X					
Multiple small														X					
Void																			

Elution/Mutant	wt	E222C	M223C	I224C	C225A	L226C	T227C	Q228C	E229C	Q230C	R231C	D232C	Y233C	F234C	E235C
18-mer	X	X	X	X	X	X	X		X	X	X	X			X
~16-mer													X	X	
14-mer															
Multiple small															
Void								X							

Representative chromatographs of each elution pattern shown in Figure 2.3.

Size analysis

His-tag purified protein from each of the C-surface region mutants was examined by size exclusion chromatography to determine the sizes and distribution of oligomeric variants present. The wt CynD from *B. pumilus* (Jandhyala et al. 2003) eluted as a single peak and was used as a marker for the normal CynD 18-mer (Figure 2.4a). CynD from *Pseudomonas stutzeri* (Sewell et al. 2003) eluted as a single peak but was delayed relative to the *B. pumilus* enzyme, as expected for a 14-mer spiral (Figure 2.4c). The elution patterns of the substitution mutants fell into a few categories (Table 2.2). The majority eluted similar to wild type *B. pumilus* CynD with a single strong peak consistent with a self-terminating 18-mer (Figure 2.4a). Eleven out of fourteen substitutions in C-surface region 2 had wild type elution patterns. Among the C-surface region 1 mutants only half of the 18 positions tested eluted like the wild type CynD 18mer. Two mutants (F57C, G61C) eluted similar to the *P. stutzeri* enzyme suggesting a failure to extend longer than the *P. stutzeri* CynD 14-mer (Figure 2.4c). Eight mutants eluted intermediate to the wild type CynD 18-mer and the *P. stutzeri* 14-mer (Figure 2.4b). These mutants may represent a 16-mer spiral, though this would be a break from the symmetry of other terminating spiral nitrilases (Wang et al. 2012). One mutant (Q228C) eluted primarily in the void volume but the signal trailed off resulting in a down sloping void peak and it remained active (Figure 2.4e). This sloping void peak is consistent with large variable length oligomers that no longer self-terminate, observed previously with other mutants (Wang et al. 2012). Alternatively aggregation could be

causing this elution pattern, but the near wild type activity of this mutant would argue against this.

One mutant, R67C, eluted as multiple peaks (Figure 2.4d). The largest peak eluted similar to the *P. stutzeri* CynD 14-mer at about 518kDa. Another distinct peak appears in the range of a dimer (74-111kDa). Between the two prominent peaks there was significant signal as well. This intermediate signal appeared as a shoulder in the range of decamer (370kDa) or a hexamer (222kDa) (Figure 2.4d and 2.5a). R67C is the first C-surface mutation in a spiral forming nitrilase to show a defect in association of dimer into the larger oligomer.

The elution of CynD R67C as multiple peaks could indicate that the protein is freely assembling and disassembling into varied sizes of oligomers. Alternatively this elution pattern might represent varied but fixed sizes that are not assembling or disassembling into other sizes at any appreciable rate. To distinguish between these two explanations protein was collected from the different elution peaks CynD R67C (Figure 2.5a). Fractions were collected from the 14-mer peak (minute 27-31), the intermediate elution volume (minute 31-34), and from the late peak (minute 34-40). Each fraction was concentrated to 2.00 mg/ml and stored overnight at 4°C to allow any redistribution of the oligomer sizes to occur. Each fraction was then subjected to a second round of gel filtration to see if the fractions had redistributed or remained primarily in the size ranges they were isolated from.

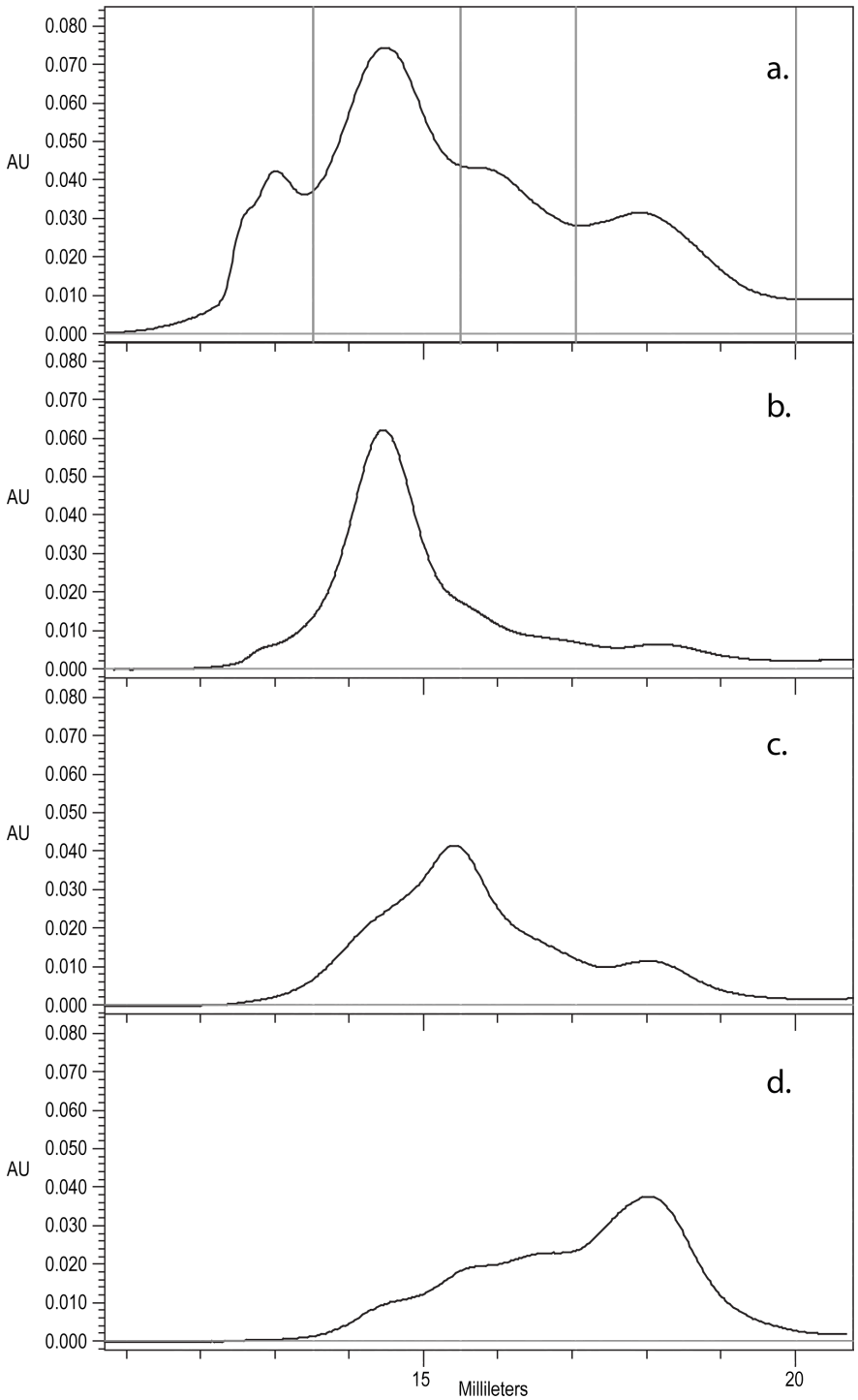

Figure 2.5 Size exclusion chromatography analysis and fraction collection of CynD R67C. (a) CynD R67C protein analyzed on Superdex 200 10/300 GL. Collection periods shown by vertical lines. (b-d) Gel filtration of concentrated fractions; (b) 14-mer like 13.5-15.5 ml, (c) intermediate decamer-hexamer range 15.5-17 ml, (d) dimer 17-20 ml.

Upon re-chromatography the first fraction remained mostly as the large peak about 518kDa with a shoulder into the intermediate sized oligomers and some signal through the lower ranges (Figure 2.5b). The intermediate (Figure 2.5c) and the late fraction (Figure 2.5d) separated into multiple peaks but the signal was primarily concentrated within the collected range of the fractions. For all three fractions the majority of the protein retained the original oligomeric size through a second round of gel-filtration. Protein outside the target range in the re-separation is likely due to incomplete resolution of the initial sample. The initial samples and all subsequent fractions of CynD R67C were inactive. These results suggest that the varieties of oligomers formed from CynD R67C are stable, inactive, and any disassociation/re-association is very gradual under the conditions tested.

Electron microscopy

For three mutants (R67C, Y70C, and Q228C), fractions were collected during gel filtration and examined by transmission electron microscopy (TEM) to confirm oligomer size and to observe their shape. For CynD R67C early fractions (Figure 2.6a & b) showed small terminated spirals and lock-washer rings, while later factions (Figure 2.6c & d) showed a mixture of C-shaped and smaller oligomers. This is consistent with the multiple peaks seen during size exclusion (Figure 2.4d). The peak fraction of CynD Y70C revealed well formed, self terminated spiral oligomers (Figure 2.7). Surprisingly the Q228C protein was observed to be aggregated and not form extended oligomers (Figure 2.8) yet was still active (Figure 2.3b).

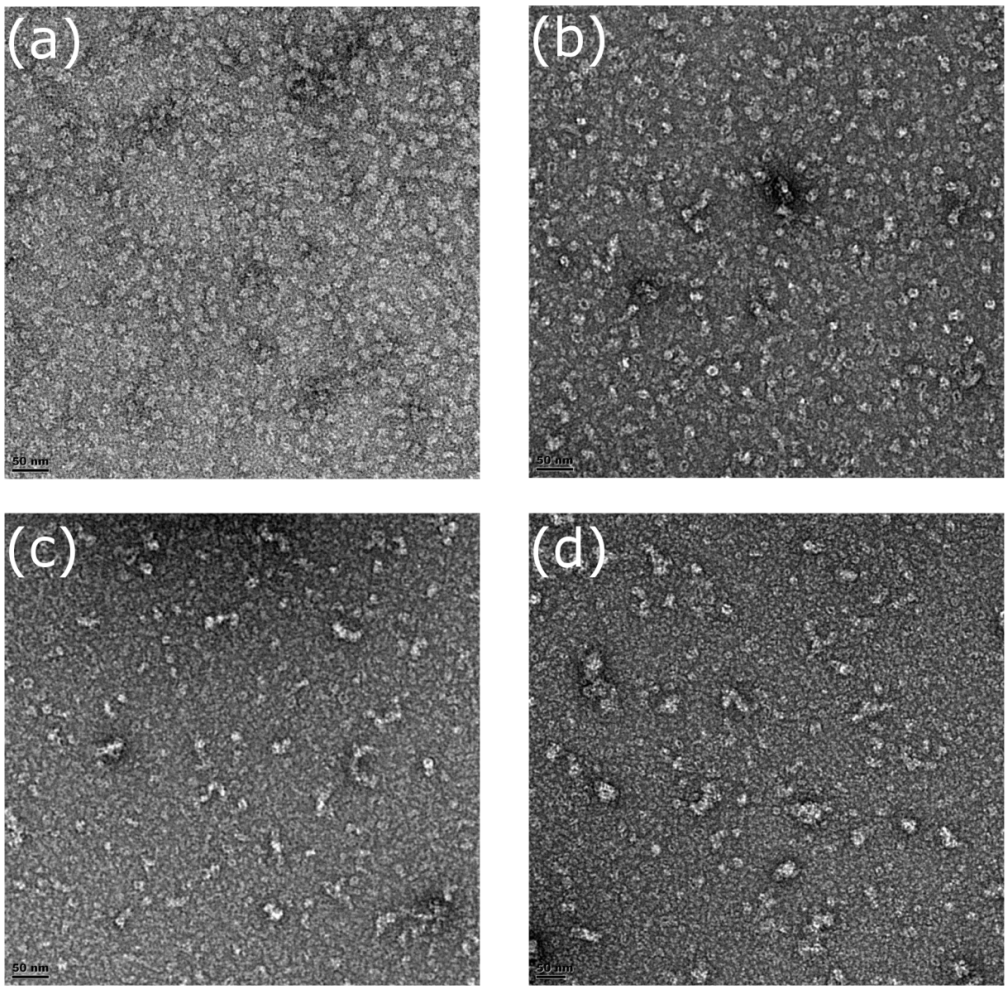

Figure 2.6 Fractions of CynD R67C from gel filtration incubated at pH 8.0, stained with 2% uranyl acetate and examined by transmission electron microscopy (courtesy of Andani Mulelu).

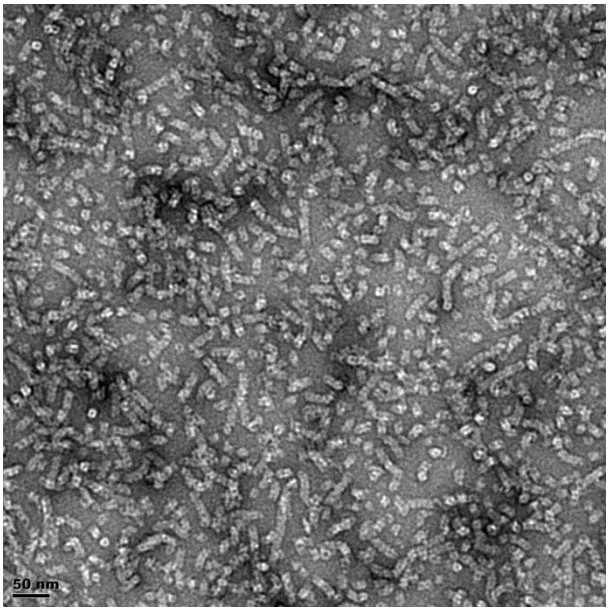

Figure 2.7 Fractions of CynD Y70C from gel filtration incubated at pH 8.0, stained with 2% uranyl acetate and examined by transmission electron microscopy (courtesy of Andani Mulelu).

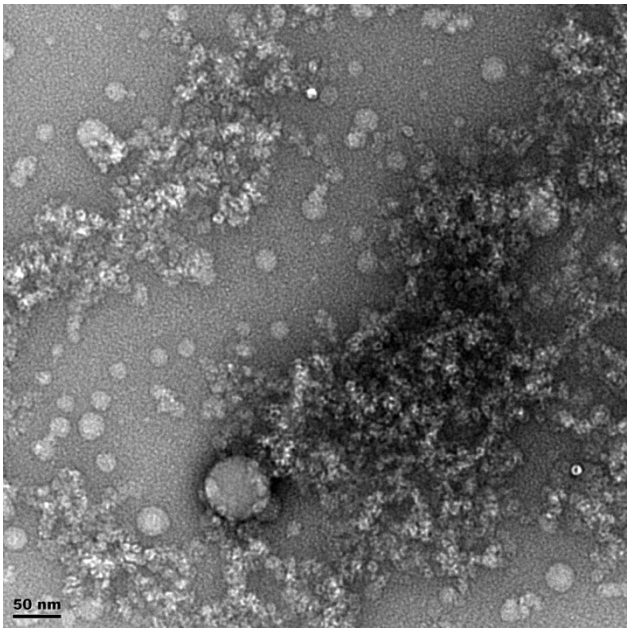

Figure 2.8 Fractions of CynD Q228C from gel filtration incubated at pH 8.0, stained with 2% uranyl acetate and examined by transmission electron microscopy (courtesy of Andani Mulelu).

DISCUSSION

All crystal structures from the nitrilase-superfamily have a common αββα monomer, which pair to form αββα-αββα dimers (Kimani et al. 2007; Kumaran et al. 2003; Lundgren et al. 2008; Nakai et al. 2000a; Pace et al. 2000; Wang et al. 2001a). Among members of the nitrilase branch of this superfamily, this basic dimer structure is expanded to form large spiral shaped homo-oligomers (Dent et al. 2009; Sewell et al. 2003; Sewell et al. 2005; Thuku et al. 2007; Williamson et al. 2010a; Woodward et al. 2008). The interaction between adjacent dimers in these spiral structures is thought to occur at the C-surface and is proposed to be the primary contributor to spiral formation (Sewell et al. 2003). Two regions of the protein are predicted by modeling to participate in the C-surface interaction (Sewell et al. 2003). These regions are missing from the non-spiral crystallized relatives (Figure 2.2) (Sewell et al. 2003). An interaction similar to one of these C-surface regions (222-235) was observed in the one crystallized homolog, the C shaped oligomer of β-alanine synthase (βaS) from *Drosophila melanogaster* (Lundgren et al. 2008).

Utilizing cysteine scanning mutagenesis, we probed the residues across these C-surface regions. With these mutants we investigated if the putative C-surface regions contained positions critical for CynD activity. Further we examined each mutant for effects on the oligomeric state of CynD. From these experiments a relationship between changes in oligomer size and their activity was observed.

Both C-surface regions influence the oligomeric state of CynD

From cysteine substitutions in the C-surface regions, three types of changes were seen in CynD's oligomeric state. These included reduction in oligomer size, extension or aggregation, and a partial defect in oligomerization.

Substitutions in both regions revealed mutants that reduced the size of the spiral oligomer from the normal 18-mer of CynD from *B. pumilus* C1. Three mutants (F57, G61, and R67C) eluted with a profile similar to the 14-mer of CynD from *P. stutzeri* (Jandhyala et al. 2003; Sewell et al. 2003) whereas other mutants (W56, E64, T66, F59, Y70, H71, Y233, and F234) were intermediate between these two. Spiral termination that defines oligomer size in the CynD enzymes is attributed to the alignment and interaction of the E-surface seen in 3D EM reconstructions (Sewell et al. 2005). The twist of the spiral determines when these E-surfaces align across the spiral groove. The mutants in the C-surface regions may have changed the spiral length by altering the angle of the dimer-dimer interaction, and thus the pitch of the spiral, leading to the E-surface terminating the oligomer prematurely.

Another possibility is the C-surface mutants having a more direct influence on the terminating interactions. Mutants leading to loss of self-termination have also previously been identified during screens for activity at high pH. One mutant Q86R resulted in a loss of self-termination and a dramatic increase in oligomer size. The residue Q86 is thought to participate in the D-surface, which is a cross-spiral interaction that occurs between subunits in adjacent turns of the spiral (Wang et al. 2012). The

change in the D-surface could prevent the self-termination by either perturbing or misaligning the E-surfaces.

Although mutants altering self-termination shortened the spiral, no mutants were found that resulted in extension or loss of self-termination in the C-surfaces. The mutant Q228C was initially thought to form extended oligomers because it eluted primarily in the void fraction and trailed off sloping away from the void volume through the peak of the wild-type protein. This pattern was suggestive of variable length non-terminated oligomers, but could also have been due to aggregation. Mutants from other studies have changed the twist or the rise of the spiral and moved the terminating E-surface interactions completely out of alignment, resulting in such variable length non-terminating oligomers (Wang et al. 2012). Spiral extension has also been observed in the wild type C1 nitrilase upon reduction in pH to below 6 (Jandhyala et al. 2003). However in this case TEM data suggests that the elution pattern of CynD Q228C was due to aggregation (Figure 2.8).

Apart from changing the size of the oligomer, mutant R67C in C-surface region 1 causes a partial defect in spiral formation. This mutant eluted as a 14-mer followed by possible; decamer, hexamer, and dimer peaks (Figure 2.4d). TEM of the different fractions of CynD R67C showed short spirals, ring and C-shaped oligomers, and smaller oligomers (Figure 2.6), consistent with the elution pattern (Figure 2.4d). This pattern indicates that R67C is the first mutation in the C-surface demonstrated to disrupt the oligomerization of dimers. Re-chromatography of each size variant peak of R67C indicated that the altered forms were stable and do not re-associate back into the other

variant forms (Figure 2.5). The presence of these smaller oligomers may be due to misfolding of the C-surface in a portion of the dimers, resulting in a mixture of prematurely terminated oligomers.

C-surface regions contain multiple positions critical for CynD activity

Several mutations at positions within region 1 (55-72) showed at least a 50% reduction in activity (P55, F57, G61, E64, Y65, T66, R67, F69, and Y70)(Figure 2.3a). In contrast only two mutated positions (Q230, E235) in region 2 (222-235) reduced activity by ≥50%. Kimani *et al* proposed that folding of the C-surface during oligomerization could be activating the nitrilase by positioning a glutamate residue in active site (Kimani et al. 2007). Changes in the folding of the C-surface in these CynD mutants may put the glutamate out of position sufficiently to slightly perturb activity. In the crystal structure of βaS the C-surface insertion region, when oligomerized, forms the ceiling of the active-site cavity (Lundgren et al. 2008). Changes in the C-surface may therefore prevent the substrate from accessing the active-site cavity even without directly altering oligomerization.

Many positions that altered oligomerization also showed reduced activity.

Of the twelve substitutions that caused changes in oligomerization (Table 2.2), ten (F57C, G61C, E64C, T66C, R67C, F69C, Y70C, H71C, Y233C, and F234C) had activity at or below 60% of wild type CynD (Figure 2.3ab), supporting the notion that activation and oligomerization are linked.

Consistent with the relationship between the C-surface and active site cavity in βaS, changes to the twist of the spiral many restrict the active site cavity. From comparisons of plant nitrilases, a correlation was found between spiral twist and substrate size. Woodward *et al* suggested that the tight spiral twist of CynD is responsible for its high specificity for cyanide (Woodward 2011). Of the mutants with reduced activity, five (E64C, T66C, R67C, Y70C, and H71C) (Figure 2.3) had shortened oligomer sizes (Table 2.2). If these shortened oligomers are due to changes in the angle at the C-surface, the active-site cavity may be restricted to limit access of cyanide.

One mutant (Y70C) appears to have broken the link between oligomerization and activation. While other mutants with reduced oligomer size have reduced activity, CynD Y70C is completely inactive (Figure 2.3a) yet appears to form normal spiral oligomers as seen by TEM (Figure 2.7). This suggests that the defect in CynD Y70C's activity is due to a failure to activate upon oligomerization. Exploring other residues at this position and structural characterization by EM-tomography may indicate how this position influences activation of CynD oligomers.

On the other hand, CynD R67C, which demonstrated a partial defect in oligomerization, is also completely inactive as purified protein (Figure 2.3a). The activity defect in this mutant is likely directly related to improper oligomerization. While completely inactive as purified protein CynD R67C does show partial activity in cells. The cellular conditions may be allowing CynD R67C to partially oligomerize in an active form, which is disrupted upon lysis, although the protein does not appear to degrade more rapidly than wild type.

CONCLUSIONS

While fine resolution structural data for the C-surface of a nitrilase enzyme is currently unavailable, the mutations examined here support the involvement of the relative insertion regions in associating CynD dimers into the larger structure, as well as the activity of this structure. Mutations, such as CynD Y70C, affecting both the spiral size and the activity may guide future exploration of the relationships between the spiral formation and CynD activation. Finally the smaller oligomer variants seen in CynD R67C could be valuable in future structural studies, as crystallization of the intact spiral oligomers has yet to be achieved.

CHAPTER III

RESIDUE Y70 OF THE NITRILASE CYANIDE DIHYDRATASE FROM *BACILLUS PUMILUS* IS CRITICAL FOR FORMATION AND ACTIVITY OF THE SPIRAL OLIGOMER

SYNOPSIS

Nitrilases pose attractive alternatives to the chemical hydrolysis of nitrile compounds. Their activity towards nitrile groups is intimately tied with their formation of large spiral shaped oligomers. In the nitrilase cyanide dihydratase (CynD) from *Bacillus pumilus*, mutations in a predicted oligomeric surface region altered oligomerization and reduced activity. Only mutant CynD Y70C retained uniform oligomer formation, however it was inactive unlike other mutants in the region that had similar or greater changes in oligomer size. It was hypothesized that Y70 is playing an additional role in the activity CynD beyond influencing oligomer size. Here, we performed saturation mutagenesis at residue 70 and demonstrated that only tyrosine or phenylalanine are permissible for CynD activity. Further, we show that other residues at this position are not only inactive, but have altered or disrupted oligomer conformations. These results suggest that Y70's essential role in activity is secondary to a role in the formation and shape of the spiral oligomer.

INTRODUCTION

Cyanide is the simplest but also most environmentally hazardous nitrile compound. However it is used extensively in industries ranging from textile production to gold mining (Muezzinoglu 2003). The cyanide degrading nitrilase, cyanide dihydratase (CynD) from *Bacillus pumilus*, is being engineered for use in detoxifying cyanide laden industrial waste (Meyers et al. 1993; Wang et al. 2012). Currently, a lack of fine structural knowledge of nitrilase enzymes is the major hurdle to rationally manipulating these enzymes (Thuku et al. 2009).

Limited structural insights can be gleaned from a conserved dimer structure that is seen in crystal structures of enzymes from the larger superfamily (Pace and Brenner 2001). The conserved dimers have a basic αββα-αββα architecture (Kumaran et al. 2003; Pace et al. 2000) and a C-E-E-K active site (Kimani et al. 2007). From electron microscopy we know that CynD expands on the basic dimer building block to form large 18-subunit left-handed spiral oligomers (Jandhyala et al. 2003). Similar spiral structures have been seen in all active nitrilase enzymes examined so far (Thuku et al. 2009).

Modeling and fitting of CynD's dimer to the 3D shell created from EM data lead to the prediction of the primary interface between dimers, the C-surface (Sewell et al. 2003; Sewell et al. 2005). Two regions were predicted to participate in this C-surface interaction, as they stand out as relative insertions compared non-spiral forming superfamily members (Sewell et al. 2003; Sewell et al. 2005; Thuku et al. 2009).

We have previously tested the participation of these regions in spiral formation by scanning these two regions in CynD with cysteine substitutions to identify residues

critical for activity and proper oligomer formation. These cysteine substitutions revealed multiple residues in the CynD region 55-72 that influence the size and activity of CynD oligomers. Two of these mutants, R67C and Y70C, had no detectable activity. The mutant R67C blocked proper CynD oligomerization, resulting in a heterogeneous mixture of partially formed oligomer fragments. This indicates a critical role in oligomerization at the C-surface and emphasizes dependence of activity on proper oligomer formation. On the other hand the inactive mutant CynD Y70C forms homogeneous oligomers as detected by size exclusion chromatography, intermediate in size between the 18 subunit CynD from *B. pumilus* and the 14 subunit CynD from *P. stutzeri* (Figure 2.4b). Unlike CynD Y70C, other mutants in this region that had oligomers of intermediate size retained partial activity (Figure 2.3a). We hypothesized that Y70 may play an additional role in CynD's activity or oligomerization beyond its effect on oligomer size.

Here we perform site saturation mutagenesis at position 70 and examine how critical Y70 is for activity. A subset of mutants was selected and examined for changes in their quaternary state.

METHODS

Media and reagents

Bacterial strains were grown in Luria broth or on plates supplemented with 25μg/ml chloramphenicol or 25μg/ml kanamycin where appropriate. Phusion High Fidelity DNA polymerase master mix (NEB; Ipswich, MA) was used for site directed

mutagenesis. B-PER® extraction reagents, HisPur™ Cobalt Spin Columns, and Zeba Desalting Columns were obtained from Thermo-Scientific (Pierce Biotechnology; Rockford, IL).

Bacterial strains and plasmids

All substitution mutants were constructed in pMB5006, derived from pBC KS+ with CynD as an XbaI-XhoI insertion. Select mutants were independently reconstructed by site directed mutagenesis in pMB4407 for protein expression. pMB4407 is pET28a containing CynD as a NdeI-XhoI insertion (Abou Nader 2012). *Escherichia coli* strain MB3436 (Δ*endA thiA hsdR17 supE44 lacI*^{q}*ZΔm15*) was used for cloning, mutant construction, and expression of pBC based plasmid constructs. pET28a based plasmids were transformed into *E. coli* BL21(DE3) (pLysS) for expression.

Site saturation mutagenesis

Mutants were constructed by site directed mutagenesis following the QuickChange® protocol (Stratagene, La Jolla, CA) using mutagenic primers and Phusion DNA polymerase. Primers were designed to have a semi-random codon to mutate Y70 to all possible amino acids. Not all mutations were obtained from this reaction; the remainders were individually constructed using specific primers (Table 3.1). Mutagenic primers were designed using the program PrimerX (http://www.bioinformatics.org/primerx/). Mutants were identified and confirmed by sequencing.

Table 3.1 Site directed primers

Primer	Sequence
Y70(random)	GGT CAT CCA GAA TAT ACG AGA AAG TTC NNK CAT GAA TTA TAT AAA AAT GCC GTT GAA ATC CC
Y70(K,N,Q,H,D,E)	GGT CAT CCA GAA TAT ACG AGA AAG TTC VAK CAT GAA TTA TAT AAA AAT GCC GTT GAA ATC CC
Y70I	GGT CAT CCA GAA TAT ACG AGA AAG TTC ATT CAT GAA TTA TAT AAA AAT GCC GTT GAA ATC CC
Y70F	GGT CAT CCA GAA TAT ACG AGA AAG TTC TTT CAT GAA TTA TAT AAA AAT GCC GTT GAA ATC CC
Y70G	GGT CAT CCA GAA TAT ACG AGA AAG TTC GGT CAT GAA TTA TAT AAA AAT GCC GTT GAA ATC CC
Y70E	GGT CAT CCA GAA TAT ACG AGA AAG TTC GAA CAT GAA TTA TAT AAA AAT GCC GTT GAA ATC CC
Y70K	GGT CAT CCA GAA TAT ACG AGA AAG TTC AAA CAT GAA TTA TAT AAA AAT GCC GTT GAA ATC CC

Forward sequences shown, reverse primers used are reverse compliment of forward.

Protein expression

Activity from pBC-derived constructs was measured in MB3436. Overnight cultures were diluted 200ul into 3ml of media and grown at 37°C to OD600 between 0.5 and 0.7, at which time they were induced for expression by adding IPTG at > 1mM and transferred to 37°C for another 1-2 hour. CynD activity was tested immediately after the induction period.

Protein expression from pET28a-derived constructs was performed as previously described (Chapter II)

His-tagged purified CynD protein was produced, purified, and examined by gel filtration as previously described (Chapter II)

Activity assay

CynD activity from whole cells was measured by mixing 50µl of culture with 50µl of 6mM KCN in 0.1M MOPS pH 7.7. Each reaction was allowed to proceed at room temperature. Remaining cyanide was detected by adding 100µl of alkaline picric acid (0.5% picric acid in 0.25 M sodium carbonate) to the reaction. The terminated reactions were incubated on a 100°C heat block for five minutes to develop the reaction. Remaining cyanide was indicated by a red color. Culture positive for CynD activity had a visible difference in color relative to empty vector controls.

Activity assays performed with purified protein were previously described (Chapter II).

RESULTS

Activity of Y70-X substitutions

In our previous work many mutants across the predicted C-surface region showed altered mobility, suggesting a change in oligomer size or conformation, but retained partial activity. The mutant CynD Y70C was the only such mutant with a moderate change in mobility (migrating intermediate between the 18 subunit and the 14 subunit controls), but other similar mutants it had no measurable activity. To test if position 70 is critical for activity in CynD, we individually constructed all nineteen amino acid substitutions at this position. Expression of each mutant protein was verified by western blot and all mutants had reasonable protein levels (data not shown). From activity tests in whole cells only the phenylalanine and the native tyrosine at residue 70

were tolerated for activity (data not shown). The activities of *wt* CynD and CynD Y70F were compared using purified protein and the activity of CynD Y70F was not significantly different than the wild type enzyme (Figure 3.1). Activities of five other purified mutants (Y70C, G, I, K, E) were not measurably different than negative controls.

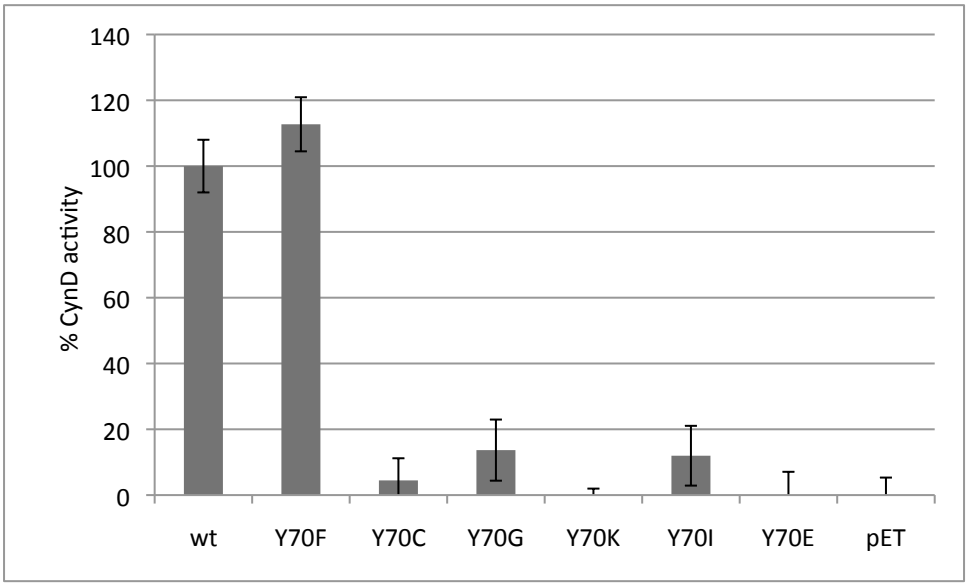

Figure 3.1 Activity of purified mutant CynD proteins. Measured relative to wt CynD and his-purified empty vector control measured by picric acid CN assay. Error bars show standard deviation from three samples.

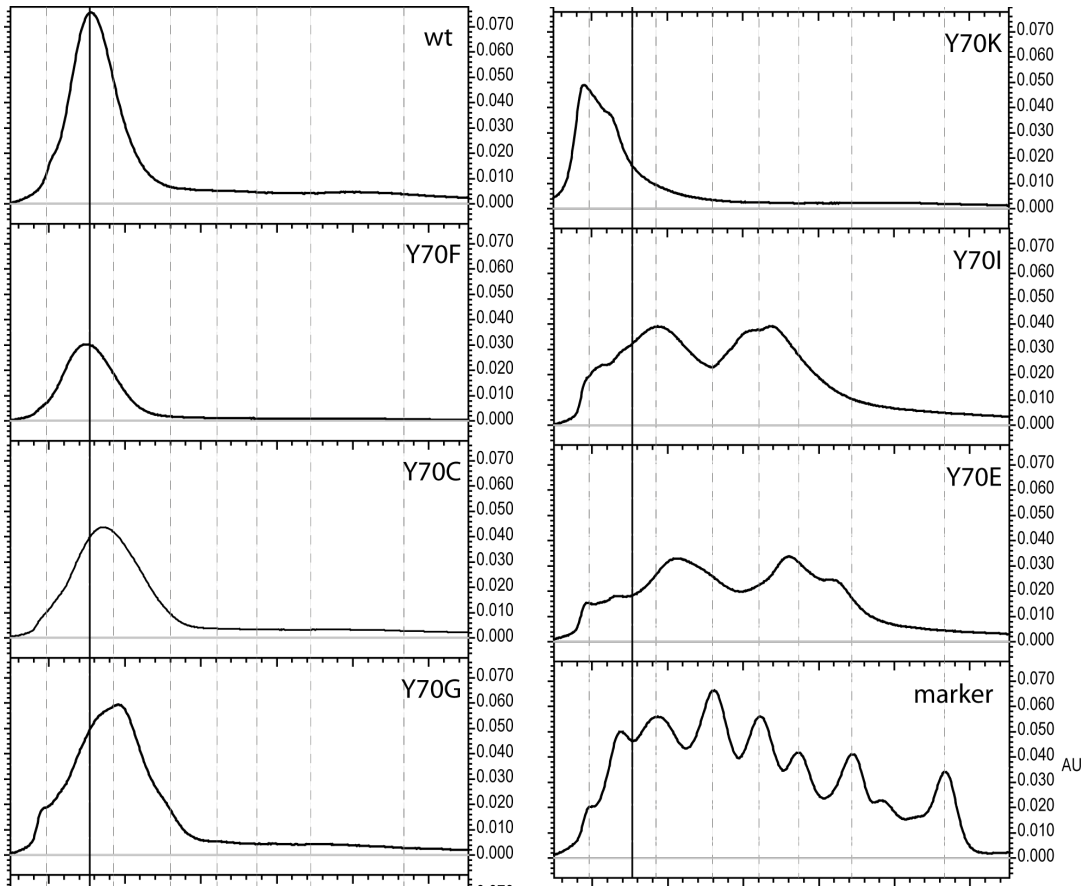

Figure 3.2 Size exclusion chromatography of Y70 mutants. Chromatographs of (wt) CynD, select Y70X mutants (Y70F, Y70C, Y70G, Y70K, Y70I, Y70E), and Sigma-Aldrich gel filtration marker (marker). Solid vertical line highlights the peak of the *wt* CynD 18-mer. The faint vertical dotted lines highlight the marker peaks of; void peak, ~669kDa, 443kDa, 200kDa, 150kDa, 66kDa, and 29kDa from left to right.

Size exclusion

To test if the Y70 mutants were altered in mobility, suggesting changes to their oligomeric structures, selected mutants (Y70C, G, I, K, E, F) were purified and examined by size exclusion (Figure 3.2). These mutants represented a range of amino acid characteristics. The active Y70F eluted as a single peak similar to the "wt" 18-subunit oligomer (Figure 3.2wt,Y70F). CynD Y70C and Y70G also eluted as single

peaks, but were delayed relative to the normal 18-mer, migrating with a size intermediate to the 18 and 14-mer controls (Figure 3.2Y70C,Y70G). The mutant Y70K eluted from the column in the void fraction indicating aggregation or extended non-terminated spirals (Figure 3.2Y70K). Two mutants Y70I and Y70E blocked normal oligomer formation and eluted as multiple peaks. The peaks from Y70I resemble possible 14, 10, and 8 subunit oligomers (Figure 3.2Y70I). CynD Y70E eluted slower with a range of 10-12, 6, and 2 subunit complexes (Figure 3.2Y70E).

DISCUSSION

In the oligomeric nitrilases examined to date the formation of a spiral oligomeric structure is needed for activation of the enzyme (Thuku et al. 2009). It is hypothesized that interactions at the C-surface region upon oligomerization influence the conformation of the active site (Kimani et al. 2007; Lundgren et al. 2008). The residue Y70 in CynD is predicted to lie at this interface by its location within the loop region 55-72, which is an insertion relative to the non-spiral forming nitrilase homologs (Sewell et al. 2003; Sewell et al. 2005). The mutation, R67C, also in this region, has been shown to disrupt proper oligomerization and activity (Figure 2.3, 2.4d).

Saturation mutagenesis at position 70 revealed that having either tyrosine or phenylalanine is essential for activity of CynD and furthermore there was no significant difference in activity between the CynD and CynD Y70F (Figure 3.1). This is not surprising given the similarity between the residues. However analysis of related

nitrilase sequences by Blast homology searching showed that Y70 was strictly conserved at this position and F70 was not found.

Similarly, the Y70F mutant was not altered in the size of the CynD oligomer, which eluted consistent with the wild type 18-mer (Figure 3.2Y70F). By comparison, all five of the inactive mutants examined by size exclusion showed notable change in their elution profile relative to wild type (Figure 3.2Y70C-E). The most dramatic changes were seen with CynD Y70I and CynD Y70E. These mutants eluted as multiple peaks, though the estimated size of the different oligomers present differed between them (Figure 3.2Y70I,Y70E). Similar to CynD R67C (Figure 2.4d), these mutants were blocked for proper oligomerization, indicating that position 70 is critical for oligomerization as well as activity.

CynD Y70K eluted in the void fraction during size exclusion (Figure 3.2Y70K). The upper limit of our chromatography column was about 1MDa, therefore we were unable to distinguish between extended non-terminating oligomers and large protein aggregates. If Y70K had changed the twist of the spiral so that the terminating interactions no longer align, this would yield an oligomer that failed to terminate, thereby explaining its elution in the void fraction. This has been seen for CynD at pH 5.4 as well as in mutants that similarly lead to spiral extension (Jandhyala et al. 2003; Wang et al. 2012). However in those cases the protein retained activity unlike CynD Y70K. Given the disruptive pattern of other mutations at this position it is more likely that CynD Y70K is forming protein aggregates. In our previous work the mutation Q228C in

region 221-235 eluted similarly and was shown by electron microscopy to aggregate (Figure 2.8).

The other inactive mutants examined (Y70C and Y70G) had less dramatic alterations to the oligomer, similar to the cysteine scanning mutants from C-surface regions 55-71 and 221-235 (Figure 2.4b,c). As in our previous work, CynD Y70C eluted at a position delayed relative to the wild type 18-mer indicating an altered or shorter oligomer (Figure 3.2Y70C). CynD Y70G eluted even at a position corresponding to a possible 14-mer (Figure 3.2Y70G). These mutants could alter the angle across the C-surface and the overall twist of the spiral. This could change the alignment of the terminating interactions and the size of the spiral. The altered size of these oligomers indicates that Y70C and Y70G may change the spiral's conformation. The shortening of the spiral is insufficient to explain the loss of activity in Y70C and Y70G, as mutants from our previous work that also reduced oligomer size remained partially active (F57C, G61C, T66C, and H71C) (Figure 2.3a).

The preservation of uniform oligomerization in CynD Y70C as seen by size exclusion led to us to hypothesize that Y70 is playing a role in activation of the oligomeric spiral, but not in the formation of the oligomer its self (Figure 2.4b). Abundant evidence suggests that dimers are inactive and only upon assembly to the oligomer is the enzyme activated (Kimani et al. 2007; Lundgren et al. 2008; Nagasawa et al. 2000; Thuku et al. 2007). Oligomerization may cause a change in the conformational change of the active site, possibly transmitted upon assembly through Y70.

However the loss of proper oligomer formation in both CynD Y70I and Y70E seemingly refutes this initial hypothesis Figure 3.2Y70I,Y70E) instead indicating that position 70 is either critical to oligomer formation or these changes at this position block assembly. Other mutants Y70C, Y70G, and possibly Y70K, are able to form oligomers but all differ from the native CynD 18-mer and remain inactive.

In our previous work on the C-surface region 55-72, six other cysteine substitutions (F57C, G61C, E64C, T66C, and H71C) altered oligomer sized (16 or 14-mers) also caused a reduction in CynD activity. We conclude that Y70 (or F70) is at the oligomerization interface and changes at Y70 either block assembly or prevent activation by blocking a needed conformational change.

CHAPTER IV

PROBING C-TERMINAL INTERACTIONS FROM THE CYANIDE DEGRADING CynD PROTEIN OF *PSEUDOMONAS STUTZERI* CynD ACTIVITY

PREFACE

This chapter contains contributions from Dr. Mary Abou Nader Crum and myself. Mary investigated how the C-terminus of cyanide dihydratase (CynD) from *P. stutzeri* and *B. pumilus*, and of cyanide hydratase from *N. crassa* influences activity and thermal stability. Furthermore she identified a region of the C-terminus required for activity in CynD from *P. stutzeri*. Her data are presented in figures and tables on pages 83, 85, 87, 88, and 90-94. I extended her work by probing interactions between the C-terminus and other regions of the CynD protein. I identified a specific interaction between the C-terminus and the A-surface region 2, which is predicted to participate in dimer formation. The data I contributed are shown in figures and tables on pages 96 and 97.

SYNOPSIS

The cyanide dihydratase from *Bacillus pumilus* and *Pseudomonas stutzeri* share high amino acid sequence similarity. However deletion or exchange of these divergent domains had different effects upon each enzyme. Here we extended those studies and investigated how the C-terminus affects the activity and stability of three nitrilases, the cyanide dihydratases from *Bacillus pumilus* ($CynD_{pum}$) and *Pseudomonas stutzeri*

($CynD_{stut}$) and the cyanide hydratase from *Neurospora crassa* following amino acid deletions within their C-terminal domain. Increasing deletion size generally decreased both stability and the activity of the enzymes but each enzyme tolerated noticeably different sizes of deletions. A domain in the *P. stutzeri* $CynD_{stut}$ C-terminus not found in the other enzymes, 306GERDST311, was shown to be necessary for its functionality and explains the inactivity of the $CynD_{stut-pum}$ hybrid described previously. This suggests the *B. pumilus* C-terminus may have specific interactions elsewhere in the protein. Introducing the dimerization interface A-surface region 195-206 (A2) $CynD_{pum}$ into the inactive $CynD_{stut-pum}$ hybrid. However this A2 region did not rescue activity in C-terminally truncated $CynD_{stut}\Delta302$ or enhance the activity of full length $CynD_{stut}$. These phenotypes suggest a specific interaction of the $CynD_{pum}$ C-terminus with the $CynD_{pum}$ A-surface.

INTRODUCTION

The cyanide dihydratase enzymes are members of the nitrilase branch of the nitrilase superfamily (Pace and Brenner 2001). Nitrilases hydrolyze organic nitriles to carboxylic acids and ammonia under mild acidic or basic reaction conditions (Thimann and Mahadevan 1964), in this instance cyanide to formate (Meyers et al. 1993). Although no member of the nitrilase branch has had a crystal structure solved, other members of the superfamily have solved structures such as a Dcase (N-carbamoyl-D-amino acid amidohydrolase) from *Agrobacterium* sp. strain KNK712 (Nakai et al. 2000b), a NitFhit (nit-fragile histidine triad fusion) protein from *Caenorhabditis elegans*

(Pace et al. 2000), a putative cyanide hydrolase from *Saccharomyces cerevisiae* (Kumaran et al. 2003) and several amidases (Hung et al. 2007; Kimani et al. 2007).

Based on low resolution electro-microscopy and alignment of sequences to related crystallographically determined structures, a model has been predicted for several members of the branch (Sewell et al. 2003; Thuku et al. 2009; Thuku et al. 2007). Members of the larger superfamily all possess similar monomer and dimer structures (Pace and Brenner 2001). The monomers fold into an αββα structure and then pair across the A surface to form αββα-αββα dimmers. In nitrilases these dimers act as the building blocks by interacting at the C surface to form higher order oligomeric structures. These structures in CynD from *Pseudomonas stutzeri* AK47 or *Bacillus subtilis* C1 are of 14 or 18 subunits respectively (Jandhyala et al. 2003; Sewell et al. 2003).

A notable variation is seen in alignments of nitrilases with other members of the superfamily at the carboxyl-terminus. The microbial nitrilases from *B. pumilus* (Jandhyala et al. 2003), *P. stutzeri* (Sewell et al. 2003), *Neurospora crassa*, *Gloeocercospora sorghi* and other microbes (Basile et al. 2008) and the crystalline amidases from *Helicobacter pylori* (Hung et al. 2007), *Geobacillus pallidus* (Agarkar et al. 2006; Kimani et al. 2007) and *Pseudomonas aeruginosa* (Andrade et al. 2007a; Andrade et al. 2007b) all show an extension of their C-terminus. This extension varies in length between the members of the superfamily as well as in sequence, with no preserved similarity even among closely related enzymes as well as no preserved predicted secondary structure (Thuku et al. 2009). Thus, the role or potential interaction this region may have elsewhere in the protein remains elusive.

Several studies point to the importance of the C-terminus. The nitrilase from *Rhodococcus rhodochrous* J1 is normally found as inactive dimers (Nagasawa et al. 2000). Following post-translational deletion of 39 C-terminal amino acids, the enzyme formed stable active helices (Thuku et al. 2007). This natural process is thought to be autocatalyzed and deletion of more or fewer than the 39 residues led to formation of inactive "c" shaped aggregates, thus implying this region is important for the oligomerization and activity of the enzyme. Similar observations were noted with C-terminal deletions of an arylacetonitrilase from *Pseudomonas fluorescens* EBC191 (Kiziak et al. 2007).

The very similar cyanide dihydratases from *B. pumilus* C1 ($CynD_{pum}$) and *P. stutzeri* ($CynD_{stut}$) also show significant difference in sequence and behavior of their C-termini. Alignment of $CynD_{pum}$ (330 aa) and $CynD_{stut}$ (334 aa) protein sequences reveals over 80% identity for the first 300 residues but only 25% for the C-terminal region. Truncations of their C-termini yielded discrepant results for the two enzymes (Sewell et al. 2005). $CynD_{pum}$ could tolerate truncation to residue 303 ($CynD_{pum}$ Δ303) with apparently normal activity, further deletion to residue 293 yielded partial activity and deletion beyond that point rendered the enzyme inactive. In contrast $CynD_{stut}$ became inactive with deletion to 310. The study also described the creation of hybrid enzymes (Sewell et al. 2005) where the C-terminus of $CynD_{pum}$ was replaced with that of $CynD_{stut}$ which yielded an active enzyme ($CynD_{pum\text{-}stut}$), as well as the converse ($CynD_{stut\text{-}pum}$) which had no detectable activity. These results emphasized the importance of this highly variable region, especially on the activity of $CynD_{stut}$, yet did little to clarify its role.

The C-terminus of $CynD_{pum}$ has also been proposed to play a role in its oligomerization. At pH 8 $CynD_{pum}$ formed 18-subunits spirals whereas at pH 5 the protein was found as elongated spirals (Jandhyala et al. 2003). The change in oligomer size was reversible and pH dependent. CynD from a different *B. pumilus* strain, strain 8A3, is nearly identical to C1 (97% identical) with only 10 out of 330 residues differing (Jandhyala et al. 2003). Among the differences 7 out of the 10 are found in the C-terminus, and notably $CynD_{pum}$ 8A3 has no histidine residues nor does it show a transition to long spirals at pH 5.4. This led to the suggestion that at pH 5.4 the protonated histidines cause a repulsion of adjacent subunits leading to an expansion of the diameter and subsequent disruption of the spiral terminating E surface resulting in elongation (Thuku et al. 2009). Oligomerization is thought to be required for catalytic activity by helping position the catalytic residues, especially E137 (in the case of $CynD_{pum}$ C1), in the active site. Thus, a slight observed increase in specific activity that was observed at pH 5.4 was proposed to be the result of activation of the terminal monomers of the short spiral by their incorporation into longer oligomers, resulting in fewer terminal monomers.

Participation of the C-terminus in oligomerization is seen in a few crystal structures from superfamily member that have extended C-termini. The C-terminus of amidase from *G. pallidus* folds into interlocking alpha helixes at the A-surface (Kimani et al. 2007). Based on the amidase structure, modeling of the C-terminus in CHT from *N. crassa* suggests that C-terminus may also participate in oligomerization at the C-surface (Dent et al. 2009). Though not as extended as the C-termini in the nitrilase and amidase

sequences, the C-terminus in the structure of the C-shaped β-alanine synthase (βaS) from *D. melanogaster* interacts with the A surface and then is anchored at its C surface (Lundgren et al. 2008).

This study aims to further explore the role of the C-terminus in determining the stability and the activity of these enzymes and to better explain the results of the hybrids with interchanged C-termini.

MATERIALS AND METHODS

Culture media and reagents

All strains were grown in LB broth or plates with antibiotics at concentrations of 100 μg /ml of ampicillin, 25 μg/ml of kanamycin or 25 μg/ml of chloramphenicol added as needed.

Bacterial strains and plasmids

E. coli strain MB3436 [Δ*endA thiA hsdR17 supE44 lacI*^{q}*ZΔM15*] was the host strain for DNA manipulations and expression of protein from pBC vectors and *E. coli* strain MB1837 [BL21 (DE3) pLysS] for protein expression from pET vectors. A synthetic gene encoding the *P. stutzeri* cyanide dihydratase but with *E. coli* optimized codons and additional restriction sites was used. Plasmids are described in Table 4.1.

Table 4.1 List of plasmids used in this study.

Plasmids	Description	Reference
pMB2784	pET26b carrying *P. stutzeri cynD*	Sewell *et al.* 2003
pMB4276	pET26b carrying synthetic *P. stutzeri cynD*	This work Abou-Nader
pMB5277	pET28a pMB4276	This work Abou-Nader
pMB2890	pET26b carrying *B. pumilus* C1 *cynD*	Jandhyala *et al.* 2003
pMB4406	pET28a carrying pMB2890	This work Abou-Nader
pMB3418	pBS carrying *N. crassa cht*	Basile *et al.* 2008
pMB4951	pMB3418 BstBI	This work Abou-Nader
pMB3460	pET26b carrying *N. crassa cht*	Basile *et al.* 2008
Tail deletions		
pMB3326	pMB2890 Δ279	Sewell *et al.* 2005
pMB3052	pMB2890 Δ293	Sewell *et al.* 2005
pMB3319	pMB2890 Δ303	Sewell *et al.* 2005
pMB4948	pMB3460 Δ307	This work Abou-Nader
pMB4949	pMB3460 Δ323	This work Abou-Nader
pMB4950	pMB3460 Δ339	This work Abou-Nader
pMB3328	pET26b carrying *P. stutzeri cynD* Δ302	Sewell *et al.* 2005
pMB5067	pMB4276 Δ310	This work Abou-Nader
pMB4959	pMB4276 Δ330	This work Abou-Nader
Hybrids		
pMB3407	pET26b carrying Stut-Pum	Sewell *et al.* 2005
pMB3411	pET26b carrying Pum-Stut	Sewell *et al.* 2005
pMB4956	pET26b carrying Cras-Stut	This work Abou-Nader
pMB4972	pET26b carrying Stut-Cras	This work Abou-Nader
pMB4993	pET26b carrying Pum-Cras	This work Abou-Nader
pMB5026	pET26b carrying Cras-Pum	This work Abou-Nader
pMB5389	pET28a carrying Pum-Stut	This work Abou-Nader
pMB5383	5389 K93R	This work Abou-Nader
P. stutzeri CynD alanine scanning		
pMB5158	pMB4276 G306A	This work Abou-Nader
pMB5159	pMB4276 E306A	This work Abou-Nader
pMB5160	pMB4276 R306A	This work Abou-Nader

Table 4.1 Continued

pMB5161	pMB4276 D306A	This work Abou-Nader
pMB5162	pMB4276 S306A	This work Abou-Nader
pMB5163	pMB4276 T306A	This work Abou-Nader
C-terminal mutants		
pMB5042	pMB3407 322HGILto 322VSDE	This work Abou-Nader
pMB5044	pMB5042 306NHQKNE to 306GERDST	This work Abou-Nader
pMB5046	pMB3407 306NHQKNE to 306GERDST	This work Abou-Nader
pMB5100	pMB3407 H307D Q308K K309E	This work Abou-Nader
pMB5182	pMB3407 N306G Q308R E311T	This work Abou-Nader
pMB5214	pMB3407 N306G K309D	This work Abou-Nader
pMB5244	pMB3407 N306G H307E	This work Abou-Nader
pMB5249	pMB4972 306VDRNGG to 306GERDST	This work Abou-Nader
pMB5250	pMB5046 306GERDST to 306 NHQKNE	This work Abou-Nader
pMB5253	pMB3407 H307E	This work Abou-Nader
pMB5365	pMB5046 320YQHGILEEK to 320LSVSDEEPV	This work Abou-Nader
pMB5367	pMB3407 320YQHGILEEK to 320LSVSDEEPV	This work Abou-Nader
Oligomer surface swaps		
pMB6007	pBC SK carrying *P. stutzeri cynD*	This work Park
pMB6018	pBC SK carrying Stut-Pum	This work Park
pMB6037	pMB6018 59LGHPEYTRRFYHT71 to IGHPEYTRKFYHE (C1)	This work Park
pMB6020	pMB6018 167NVPLDIAAMNS177 to QVPLDLMAMNA (A1)	This work Park
pMB6040	pMB6018 195TASSHYAICNQA206 to ISSRYYAIATQT (A2)	This work Park
pMB6038	pMB6018 221DMLCETQEEYFN234 to EMICETQEQYFE (C2)	This work Park
pMB6022	pMB6007 195TASSHYAICNQA206 to ISSRYYAIATQT (A2)	This work Park
pMB6033	pMB6007 Δ302	This work Park
pMB6028	pMB6022 Δ302	This work Park
pMB6056	pET28a carrying *P. stutzeri cynD*	This work Park
pMB6082	pMB6056 195TASSHYAICNQA206 to ISSRYYAIATQT (A2)	This work Park

C-terminal amino acids deletion

Nitrilase alleles with deletions in their C-termini were constructed using Phusion High-Fidelity PCR Master Mix (New England Biolabs) and the primers listed in Table 4.2. The primers were designed to incorporate a stop codon at the desired position along with deletion of the coding region beyond to avoid any read-through expression of the wild-type protein. The mutations were confirmed by DNA sequencing.

Table 4.2 Primers used for C-terminal deletions.

Primers	Sequence
Cras BstBI F	CTTTGCTGGACACTATTCGAACCCGGATCTCATTCGTCT
Cras d307 R	AAGTGAAGCTTAGAGATCCGGCCGCATGTAG
Cras d323 R	AAGTGAAGCTTACACCTCGGTGACGAGCTC
Cras d339 R	AAGTGAAGCTTAGCCCAAGCGCTCGCGC
Stut d310 R	CTAATCGTCTCGAGTTAATCGCGTTCACCGATTTTGCG
Stut d330 R	CATAATGAGCTCACACAACAGGTTCCTCATCAG

Hybrid constructs

The BstBI restriction site was introduced in cht_{cras}, $cynD_{pum}$ and $cynD_{stut}$ at nucleotides position 903, 858, 855 respectively which represent identical positions based on protein alignments. C-terminal swaps were constructed using this BstBI site and a XhoI site at the end of each gene and as described previously in Sewell *et al.* 2005. Hybrids are named designating the N-terminal region followed by the C-terminal, so for example $CynD_{pum\text{-}stut}$ would represent the body of the enzyme from *B. pumilus* and the C-terminus from *P. stutzeri*.

Mutagenesis

In order to introduce different mutations in the C-terminal region of the $CynD_{stut\text{-}pum}$ and the $CynD_{stut\text{-}cras}$ hybrids, the C-terminal sequence was divided into 3 parts beginning with a BstBI restriction site introduced at nucleotide position 855 in the $cynD_{stut}$ gene. Then three sets of overlapping oligonucleotides were annealed to reconstitute the C-terminal domain and introduced by restriction digestion and ligation. A list describing the DNA oligonucleotides and their sequences is shown in Table 4.3.

Site-directed mutagenesis reactions were carried out using 25µl Phusion High-Fidelity PCR Master Mix with HF Buffer (New England Biolabs), 150 ng dsDNA template and 100ng of each of the forward and reverse primers. MQH_2O was added to the reaction mixture for a total volume of 50µl. Each reaction was run for 18 cycles. The mutagenic primers are listed in Table 4.4. The mutations were confirmed by DNA sequencing.

Table 4.3 Primers used for C-terminal mutagenesis.

Overlapping Primers	Sequence
Pum tailA F	CGAATCAAAGTTTGAGTATGAATTTTA ATCAGCAGCCCACTCCTGTTGTGAAA
Pum tailA R	CTGCTGATTAAAATTCATACTCAAACTTTGATT
Pum tailB F	CATTTAAATCATCAAAAAAATGAAGTATTCACcTATGA GGACATT
Pum tailB R	TACTTCATTTTTTTGATGATTTAAATGTTTCACAACAGGA GTGGG
Pum tailC F	CAATATCAACATGGTATACTGGAAGAAAAAGTTTAAGAA TTCc
Pum tailC R	TCGAGGAATTCTTAAACTTTTTCTTC CAGTATACCATGTTGATATTGAATGTCCTCATAGGTGAA
$CynD_{pum}$ 307NHQKNE to 307GERDST	
muttailB F	CATTTAGGTGAACGCGATAGCACCGTATTCACcTATGAG GACATT
muttailB R	TACGGTGCTATCGCGTTCACCTAAATGTTTCACAACAGGA GTGGG
$CynD_{pum}$ 323HGIL to 323VSDE	
muttailC F	CAATATCAAGTTTCTGATGAGGAAGAAAAAGTTTAAGA ATTCC
muttailC R	TCGAGGAATTCTTAAACTTTTTCTTCCTCATCAGAAACTT GATATTGAATGTCCTCATAGGTGAA
$CynD_{pum}$ 320YQHGILEEK to 320LSVSDEEPV	
tailC mut2 F	CAATTGTCGGTTTCTGATGAGGAACCAGTCGTTTAAGAAT TCC
tailC mut2 R	TCGAGGAATTCTTAAACGACTGGTTCCTCATCAGAAACCG ACAATTGAATGTCCTCATAGGTGAA
CHT_{cras} 322VDRNGG to 322GERDST	
muttail B F	CGCAAGGAGCTCGTCACCGAGGGTGAACGCGATAGCACGATCGT GCAGTACTCGACGCGC
muttail B R	GCGCGTCGAGTACTGCACGATCGTGCTATCGCGTTCACCC TCGGTGACGAGCTCCTTGCG

Table 4.4 Site directed mutagenesis primers.

Primers	Sequence
Pum 308DKE F	GTTGTGAAACATTTAAATGATAAAGAAAATGAAGTATTCACGTATGAGGACATTCAATAT
Pum 308DKE R	ATATTGAATGTCCTCATACGTGAATACTTCATTTTCTTTATCATTTAAATGTTTCACAAC
Pum N307G K310D F	TGTTGTGAAACATTTAGGTCATCAAGACAATGAAGTATTCACGTATGAGGACATTCAATA
Pum N307G K310D R	TATTGAATGTCCTCATACGTGAATACTTCATTGTCTTGATGACCTAAATGTTTCACAACA
Pum N307G Q309R E312T F	CTGTTGTGAAACATTTAGGTCATCGAAAAAATACAGTATTCACtTATGAGGACATTCA
Pum N307G Q309R E312T R	TGAATGTCCTCATAAGTGAATACTGTATTTTTTCGATGACCTAAATGTTTCACAACAG
Pum N307G H308E F	GTTGTGAAACATTTAGGTGAGCAAAAAAATGAAGTATTCACGTATGAGGACATTCAA
Pum N307G H308E F	TTGAATGTCCTCATACGTGAATACTTCATTTTTTTGCTCACCTAAATGTTTCACAAC
Pum H308E F	GTGAAACATTTAAATGAGCAAAAAAATGAAGTATTCACCTATGAGGACATTCAA
Pum H308E R	TTGAATGTCCTCATAGGTGAATACTTCATTTTTTTGCTCATTTAAATGTTTCAC

Table 4.5 Overlapping primers used for $CynD_{stut}$ C-terminus alanine scanning.

Overlapping primers	Sequence
Stut tailA F	CGAACCAGTCTCTGTCCATGAACTTTAACCAATCTCCGAACCCGG TTGTTCGCAAAATC
Stut tailA R	GGTTCGGAGATTGGTTAAAGTTCATGGACAGAGACTGGTT
Stut tailC F	AGGAACCTGTTGTGCGTTCCCTGCGTAAATGACCATGGAAGCTTG CTATTGC
Stut tailC R	GCAATAGCAAGCTTCCATGGTCATTTACGCAGGGAACGCACAACA GGTTCCTCATCAGAAACGGACAGG
G306A F	GCCGAACGCGATAGCACCGTATTCACTTACGACGACCTGAACCTG TCCGTTTCTGATG
G306A R	TTCAGGTCGTCGTAAGTGAATACGGTGCTATCGCGTTCGGCGATT TTGCGAACAACCG
E307A F	GGTGCCCGCGATAGCACCGTATTCACTTACGACGACCTGAACCTG TCCGTTTCTGATG
E307A R	TTCAGGTCGTCGTAAGTGAATACGGTGCTATCGCGGGCACCGATT TTGCGAACAACCG
R308A F	GGTGAAGCCGATAGCACCGTATTCACTTACGACGACCTGAACCTG TCCGTTTCTGATG
R308A R	TTCAGGTCGTCGTAAGTGAATACGGTGCTATCGGCTTCACCGATT TTGCGAACAACCG
D309A F	GGTGAACGCGCCAGCACCGTATTCACTTACGACGACCTGAACCTG TCCGTTTCTGATG
D309A R	TTCAGGTCGTCGTAAGTGAATACGGTGCTGGCGCGTTCACCGATT TTGCGAACAACCG
S310A F	GGTGAACGCGATGCCACCGTATTCACTTACGACGACCTGAACCTG TCCGTTTCTGATG
S310A R	TTCAGGTCGTCGTAAGTGAATACGGTGGCATCGCGTTCACCGATT TTGCGAACAACCG
T311A F	GGTGAACGCGATAGCGCCGTATTCACTTACGACGACCTGAACCTG TCCGTTTCTGATG
T311A R	TTCAGGTCGTCGTAAGTGAATACGGCGCTATCGCGTTCACCGATT TTGCGAACAACCG

For alanine scanning overlapping primers were used to reconstitute the $CynD_{stut}$ C-terminus with mutations G306A, E307A, R308A, D309A, S310S or T311A. The different primers and their sequences are listed in Table 4.5.

Substitution of the A and C surface regions in $CynD_{stut}$ for the $CynD_{pum}$ sequence was done by overlap extension PCR using primers listed in (Table 4.6). The products of these reactions were cloned into pBC-SKII+ between XbaI and XhoI.

Table 4.6 Primers used to exchange $CynD_{stut}$ oligomeric regions for the $CynD_{pum}$ sequence

Primer	Sequence
Stut (C1 pum) F	ATT GGT CAT CCA GAA TAT ACG AGA AAG TTC TAT CAT GAA CTC TAT CTG AAC GCA GTC GAG ATT CCG AGC GAG
Stut (C1 pum) R	TTC ATG ATA GAA CTT TCT CGT ATA TTC TGG ATG ACC AAT GAA TGC GAA CCA TGG ATA TCC CGG AAT AAA TGC CTC CG
Stut (A1 pum) F	CAA GTC CCA CTT GAT CTT ATG GCG ATG AAT GCC CAG AAC GAG CAG GTT CAT GTG GCT GCA TGG
Stut (A1 pum) R	GGC ATT CAT CGC CAT AAG ATC AAG TGG GAC TTG GTG TTC CCA GCA CAT CAG GCC TCC GAG
Stut (A2 pum) F	ATA TCA AGT AGA TAT TAT GCT ATC GCG ACA CAG ACA TTC GTG CTG ATG ACG TCG TCC ATC TAT TCA GAA G
Stut (A2 pum) R	TGT CTG TGT CGC GAT AGC ATA ATA TCT ACT TGA TAT TTC ATC GTC GAA GAA TCC GGG CCA TGC AG
Stut (C2 pum) F	GAG ATG ATT TGT TTA ACG CAG GAG CAA AGA GAT TAC TTT GAA ACA TTC AAA AGC GGT CAC ACC AGG ATC TAT GGG C
Stut (C2 pum) R	TTC AAA GTA ATC TCT TTG CTC CTG CGT TAA ACA AAT CAT CTC CTT CAT TTC TTC TGA ATA GAT GGA CGA CGT CAT CAG CAC G

Activity and stability measurements of deletion mutants

Overnight cultures of BL21 (DE3) cells transformed with each expression plasmid were diluted 1:100 in 3ml LB kanamycin and grown to an OD600 of 0.3 at 37^{o}C. IPTG was added to 1 mM for induction and incubation continued for 3-4 hours at 30^{o}C. One ml of cells carrying wild-type or variant genes was diluted to a similar OD600 of 0.3 and 200µl were added to 800 µl of 50 mM MOPS pH 7.7. Cyanide was added to 4mM and the reaction was maintained at room temperature, a 100µl aliquot was removed every 2 min and the reaction terminated by adding 100µl of picric acid reagent (0.5% picric acid in 0.25 M sodium carbonate), incubated at 100^{o}C in a dry block for 5 min to allow color development and the absorbance was measured at 540 nm. Routine enzyme activity was measured similarly incubating for 30 min at room temperature.

To test stability, the cells were lysed at room temperature with B-PER II Protein Extraction Reagent (Thermo Scientific). Two mL of B-PER II reagent per gram of cell pellet was used supplemented with 0.5 mg/ml lysozyme, 10µg/ml DNase and 1X EDTA-free protease inhibitors as recommended by the manufacturer. The cell lysate was centrifuged at 13,000 rpm for 15 min at 4^{o}C and 80 µl of each lysate was resuspended in 4 ml 50 mM MOPS pH 7.7 and the tubes were placed in a water bath at 38^{o}C (CynD) or 42^{o}C (CHT). At different time points, 0.5 ml aliquots were removed into new 1.5 ml microfuge tubes and left to equilibrate at room temperature for 3 min before adding cyanide to a final concentration of 4 mM. The reaction continued at room temperature and the activity was monitored for the first 5 min with time points taken every minute. Ammonia production was measured by using Nessler reagent (Nichols and Willits 1934)

and measuring absorbance at 420 nm for $CynD_{pum}$, $CynD_{pum}\Delta303$, $CynD_{stut}$ and $CynD_{stut}\Delta330$ whereas a picric acid assay (Jandhyala et al. 2005) was used to measure cyanide degradation by the cyanide hydratases CHT_{cras} and $CHT_{cras}\Delta339$, which do not produce ammonia. Ammonia production and cyanide loss are co-linear but ammonia production can be measured more accurately at early reaction times.

Activity and stability measurements of $CynD_{stut}$ alanine mutants

Wild-type $CynD_{stut}$ along with the alanine mutants were grown in LB kanamycin and induced as described above. Cells were adjusted to a similar OD600 of 0.3 and 200µl was added to 800 µl of 50mM MOPS pH 7.7 and cyanide added to 4 mM and incubated at room temperature. At each time point 100µl of the reaction was removed and combined in a 1.5 ml microfuge tube with 100µl picric acid reagent and incubated on a heat block at 100^{o}C for 5 min to allow color development. 100 µl of the mixture was then transferred into 96-wells plate and absorbance was determined at OD540 nm using the microplate reader Benchmark Plus (BioRad). The reaction rate of the mutants was then compared to wild-type $CynD_{stut}$. The stability test was performed as described above using cleared cell lysates, 80 µl of lysate was added to 4 ml of 0.1 M MOPS pH 7.7 and placed in a water bath at 39^{o}C. For each time point 500µl of the mixture was removed to which 4 mM cyanide was added and ammonia production was monitored as above.

Activity of A and C surface mutants in $CynD_{stut}$, $CynD_{stut}\Delta302$, and $CynD_{stut\text{-}pum}$

The active oligomer surface mutant in the $CynD_{stut\text{-}pum}$ background did not tolerate over-expression, so activity was tested from non-induced pBC constructs. MB3436 cells were freshly transformed with pBC-based plasmids and cultures were inoculated from the single colonies and allowed to grow to saturation without induction. Activities of the CynD mutants were tested using 50µl of culture in 1.5ml micro-centrifuge tubes by adding 50µl of 6mM KCN in 0.1M MOPS (pH7.7) to the culture samples and were terminated after 20 minutes with 100µl of picric acid reagent (0.5% picric acid in 0.25 M sodium carbonate). Tubes were incubated on a 100°C heat block for 5 minutes and the assays were read as described above.

Protein purification and size exclusion chromatography

His-tagged $CynD_{stut}$ and $CynD_{stut}A2_{pum}$ in pET 28 was expressed and purified as previously described in Chapter II.

The relative sizes of the $CynD_{stut}$ oligomers were measured by gel filtration. Protein samples were prepared in 0.1M MOPS pH7.7 and separated on a Superdex™ 200 10/300 GL column (Amersham Biosciences; Uppsala, Sweden) at 0.5ml/min equilibrated with 0.1M MOPS pH7.7 using a BioRad BioLogic DuoFlow® HPLC.

RESULTS

Effect of C-terminal deletions on nitrilase activity

A previous study looked at the effect of mutating interfacial residues on nitrilase activity, including deletions in the C-terminal region of two cyanide dihydratases, $CynD_{pum}$ and $CynD_{stut}$ (Sewell et al. 2005). Despite their high amino acid sequence identity, the two enzymes differed dramatically in their tolerance to C-terminal truncation with $CynD_{pum}$ being notably more tolerant, retaining normal activity when deleted to 303 and partial activity at 293 whereas $CynD_{stut}$ lost all activity with similar deletions.

To extend this study to a cyanide hydratase (CHT), similar length deletions in CHT_{cras} (352aa) were created after residues 339, 323 and 307. Residue 307 is the position where the alignment with the bacterial CynDs diverge and align with residue 293 of *B. pumilus* CynD. Residue 323 is the position where the *N. crassa* CHT begins to diverge from other cyanide hydratases such as CHT of *G. sorghi* CHT. One further deletion site was chosen randomly at residue 339. Two additional deletions were also constructed in *P. stutzeri*, at residues 330 and 310. $CynD_{stut}$ is normally 334 aa with a C-terminus 5 aa longer than $CynD_{pum}$. Although $CynD_{stut}$ Δ310 was previously described (Sewell et al. 2005) it reconstructed by adding creating a stop codon with subsequent removal of the remaining ORF to avoid read-through, which remained in the prior construct.

Table 4.7 Cyanide degrading activity of C-terminal deletion mutants.

Mutant	Length of deletion (amino acids)	Reaction rate relative to wild-type (%)
B. pumilus		
Δ303	28	87 ± 5
Δ293	38	27 ± 2
Δ279	52	Undetectable
P. stutzeri		
Δ330	5	97 ± 3
Δ310	26	13 ± 5
Δ302	33	Undetectable
N. crassa		
Δ339	13	46 ± 8
Δ323	29	22 ± 5
Δ307	45	Undetectable

Proteins were expressed from constructs in pET26b in strain MB1837 cells. The cyanide degrading activity from whole cells was tested using 4mM cyanide in 0.1M MOPS at pH 7.7 at room temperature for 30 min. Cyanide degradation was measured using picric acid to detect the remaining cyanide and the reaction rate of the mutants was compared to wild-type. The reaction rate values represent the average and the standard deviation of the average from three separate experiments.

Not surprisingly, for all three enzymes activity declined with the deletions of increased size (Table 4.7). Similar to previous results (Sewell et al. 2005), $CynD_{pum}$ Δ303 retained about 87% of wild-type activity, this decreased to 27% when 39 amino acids were deleted ($CynD_{pum}$ Δ293) and no activity was observed with a larger deletion ($CynD_{pum}$ Δ279). In contrast the *P. stutzeri* enzyme only tolerated the shortest deletion of 5 residues, a longer deletion to 310 decreased activity to about 13%, and deletion to 302 abolished all activity. The CHT enzyme from *N. crassa* was somewhat intermediate between the two when considering length of deletion (Table 4.7).

Effect of C-terminal deletions on stability

Wang et al (2012) identified a high stability mutant located in the C-terminus suggesting a possible contribution of that region either to stability of the enzyme. This suggests that C-terminal deletions retaining activity might have reduced stability. Using survival at elevated temperature as our assay, the two active mutants of $CynD_{pum}$ were probed, $CynD_{pum}$ Δ303 which although nearly wild type in activity was very unstable losing 85% of its initial activity after 15 min incubation at 38^{o}C (Figure 4.1a), conditions where the wild type retained 100%. Similar but not as dramatic results were seen with the 5aa deletion of $CynD_{stut,}$ Δ330; after 90 min incubation at 38^{o}C, the mutant lost about 50% of its initial activity (Figure 4.1a) where the wild type only lost 5%.

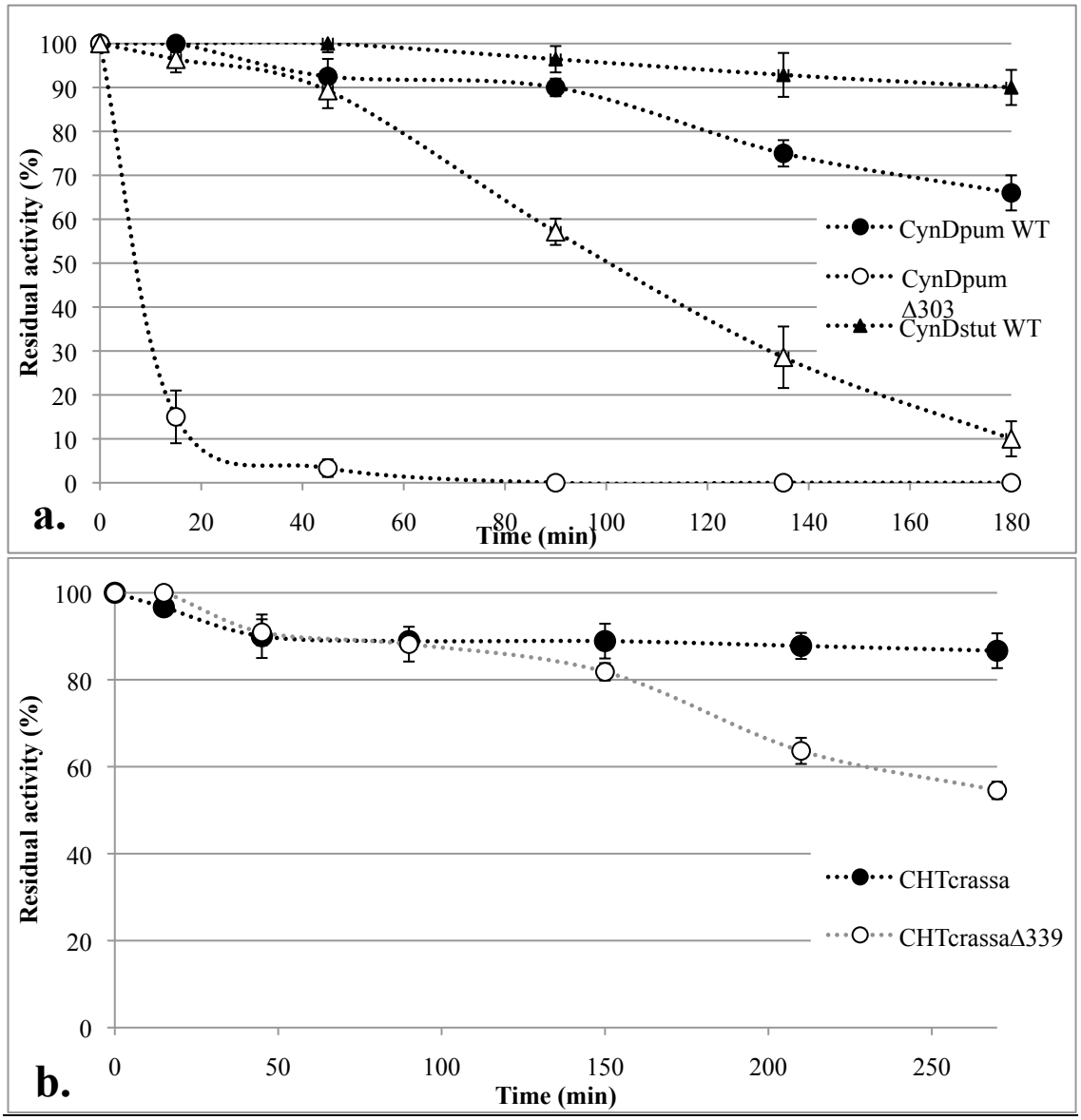

Figure 4.1 Effect of C-terminal deletions on nitrilase stability. (a) $CynD_{pum}$ and $CynD_{stut}$ stability. Cleared cell lysates with protease inhibitor were incubated in a water bath and 38°C and at different times the remaining enzyme activity was tested. (b) CHT_{cras} stability. Residual activity was tested at room temperature after cleared cell lysates were incubated at 42°C for the designated times. Error bars indicate the standard deviation of the average from three separate experiments.

In contrast CHT_{cras} Δ339 seemed to be more stable than deletions of the bacterial nitrilases. It was indistinguishable from wild type at 38°C (data not shown) and only at 42°C was a difference detectable with the deletion enzyme retaining nearly 60% of initial activity after 3h incubation at 42°C (Figure 4.1b).

Heterologous C-terminal domains

Sewell *et al*. (Sewell et al. 2005) described the construction of CynD hybrids between $CynD_{pum}$ and $CynD_{stut}$. The $CynD_{pum-stut}$ hybrid carried the N-terminus of $CynD_{pum}$ and its C-terminus was replaced with that of $CynD_{stut}$ after position 286. This enzyme retained normal activity, whereas the converse $CynD_{stut-pum}$ hybrid had no detectable activity.

In Table 4.8 is shown the activity of additional CynD and CHT hybrids, again $CynD_{stut}$ but also CHT_{cras} failed to have activity with a heterologous C-terminus, whereas $CynD_{pum}$ was tolerant to any C-terminal domain, not unexpected since it was also tolerant to deletion. It is important to note that the CynDpum was unable to tolerate deletions to residue 286, so the heterologous C-termini were playing a necessary role.

Table 4.8 Cyanide degrading activity of hybrid nitrilases.

Hybrid	Residues	Reaction rate (%) compared to corresponding wild-type
$CynD_{pum-stut}$	Residues1-286 from *B. pumilus,* 287-end from *P. stutzeri*	103 ± 3
$CynD_{pum-cras}$	Residues1-286 from *B. pumilus,* 287-end from *N. crassa*	59 ± 2
$CynD_{stut-pum}$	Residues 1-287 from *P. stutzeri,* 288-end from *B. pumilus*	Undetectable
$CynD_{stut-cras}$	Residues 1-287 from *P. stutzeri,* 288-end from *N. crassa*	Undetectable
$CHT_{cras-stut}$	Residues 1-303 from *N. crassa,* 304-end from *P. stutzeri*	Undetectable
$CHT_{cras-pum}$	Residues 1-303 from *N. crassa,* 304-end from *B. pumilus*	Undetectable

The activity was tested as in Table 4.7.

C-terminal residues required for $CynD_{stut}$ activity

The inability of the *P. stutzeri* CynD to tolerate deletion or a heterologous C-terminus suggests that residues specific to the $CynD_{stut}$ C-terminus are necessary for its activity but are missing and not necessary for $CynD_{pum}$. Although the C-terminal sequences are highly diverged, we aligned the CyD_{pum} and $CynD_{stut}$ and compared amino acid side chain properties (Figure 4.2). Two regions that stand out as notably different are 306GERDST and 320LSVSDEEPV found in the *P. stutzeri* enzyme but missing in that of *B. pumilus*.

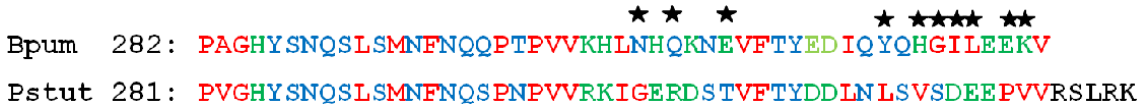

Figure 4.2 Alignment of $CynD_{pum}$ and $CynD_{stut}$ C-termini.

Table 4.9 $CynD_{stut\text{-}pum}$ hybrids activity.

Hybrid	Mutation	Activity *in vivo*
$CynD_{stut\text{-}pum}$		Undetectable
$CynD_{stut\text{-}pum}$ GERDST	306NHQKNE → 306GERDST	Active
$CynD_{stut\text{-}pum}$ VSDE	322HGIL → 322VSDE	Undetectable
$CynD_{stut\text{-}pum}$ LSVSDEEPV	320YQHGILEEK → 320LSVSDEEP	Undetectable
$CynD_{stut\text{-}pum}$ NHQKNE	306GERDST → 306NHQKNE	Undetectable

The activity was tested as in Table 4.7.

The inactive $CynD_{stut\text{-}pum}$ hybrid was used as a platform to test whether either of these domains was sufficient to restore activity. The domain GERDST was introduced at position 306 to 311, residues VSDE at position 322 to 325, and residues LSVSDEEPV at position 320 to 328. The cyanide degrading activity of $CynD_{stut\text{-}pum}$ carrying each was then tested (Table 4.9).

Restoring amino acids 306GERDST311 to the $CynD_{stut\text{-}pum}$ hybrid partially rescued the activity of the enzyme to about 30% of wild-type $CynD_{stut}$ (Figure 4.3), however neither 322VSDE325 nor 320LSVSDEEPV328 had any effect. Replacing both domains to create $CynD_{stut\text{-}pum}$ 306GERDST311/322VSDE325 showed no additional activity and was similar to $CynD_{stut\text{-}pum}$ 306GERDST311 (Figure 4.3).

As confirmation the GERDST domain in the active $CynD_{stut\text{-}pum}$ 306GERDST311 was restored back to NHQKNE and the protein lost its activity again (Table 4.9). These results suggest that some or all of the 306GERDST region is required for activity of the $CynD_{stut\text{-}pum}$ hybrid and presumably of $CynD_{stut}$.

Surprisingly activity was observed in whole cells but was rapidly lost in cell lysates. This might indicate a rapid unfolding or aggregation of the mutant hybrids once the cells are lysed, or perhaps increased susceptibility to proteolysis.

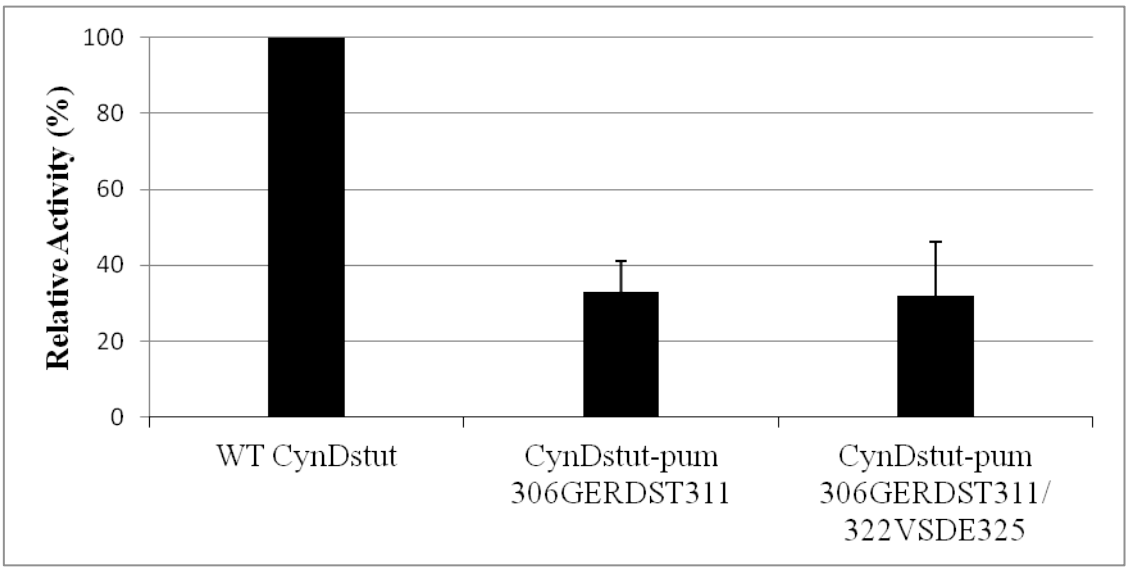

Figure 4.3 Comparison of cyanide degrading activity of $CynD_{stut\text{-}pum}$ 306GERDST and $CynD_{stut\text{-}pum}$ 306GERDST/322VSDE to wild-type $CynD_{stut}$. Cells were adjusted to similar OD600 of 0.3 and the cyanide degradation was monitored using the picric acid assay. The $CynD_{stut}$ wild type reaction rate was taken as 100% and the relative activity of the mutants was then calculated. Error bars indicate the standard deviation of the average from three experiments.

Alanine scanning of $CynD_{stut}$ GERDST region

Alanine scanning through the GERDST region in the wild type $CynD_{stut}$ was performed and the activity of each mutant was tested. Each of the 6 mutants remained active, but their activity differed (Figure 4.4). $CynD_{stut}$ G306A and D309A had only about 40-50 % of wild type activity, $CynD_{stut}$ R308A retained about 60% activity and the other 3 mutants, E307A, S310A and T311A retained more than 80% of wild type activity.

The stability of these mutants was also probed by incubating cell lysates in 50 mM MOPS pH 7.7 at 39^{o}C and testing remaining activity after different times of incubation (Figure 4.5). $CynD_{stut}$ G306A was highly unstable. It was completely

inactivated within minutes. Similarly, $CynD_{stut}$ R308A, $CynD_{stut}$ D309A and $CynD_{stut}$ T311A were significantly reduced in stability, all three mutants lost 90% of their activity after 45 min of incubation at 39°C. $CynD_{stut}$ E307A was similar but slightly less stable than wild type, losing 50% of its activity after 1h incubation at 39°C, conditions where the wild-type $CynD_{stut}$ lost 30% of its activity. The S310A mutant was indistinguishable from wild type.

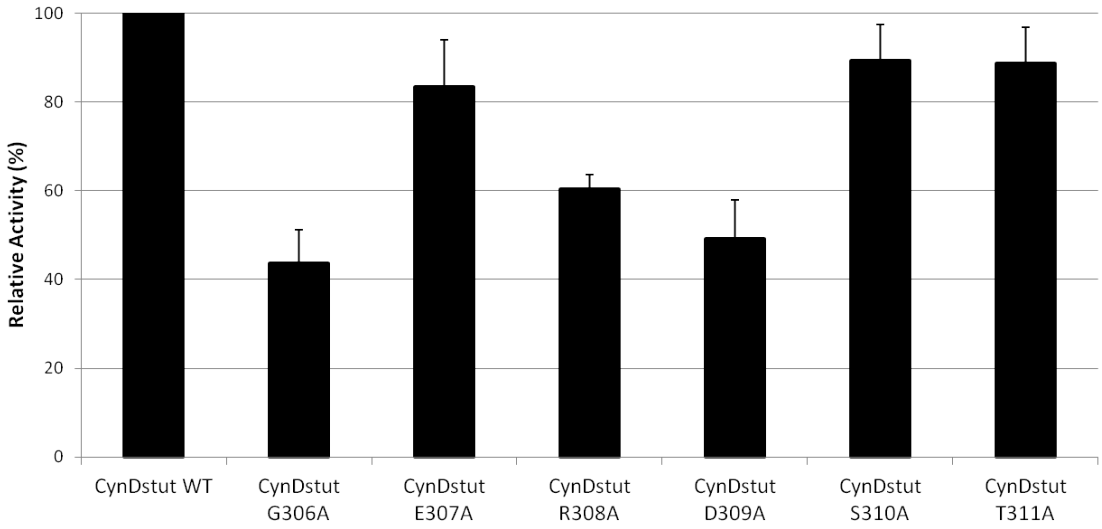

Figure 4.4 Comparison of cyanide degrading activity of $CynD_{stut}$ alanine mutants to the wild type enzyme. Relative activity as a percent of wild type was determined as in Figure 4.3.

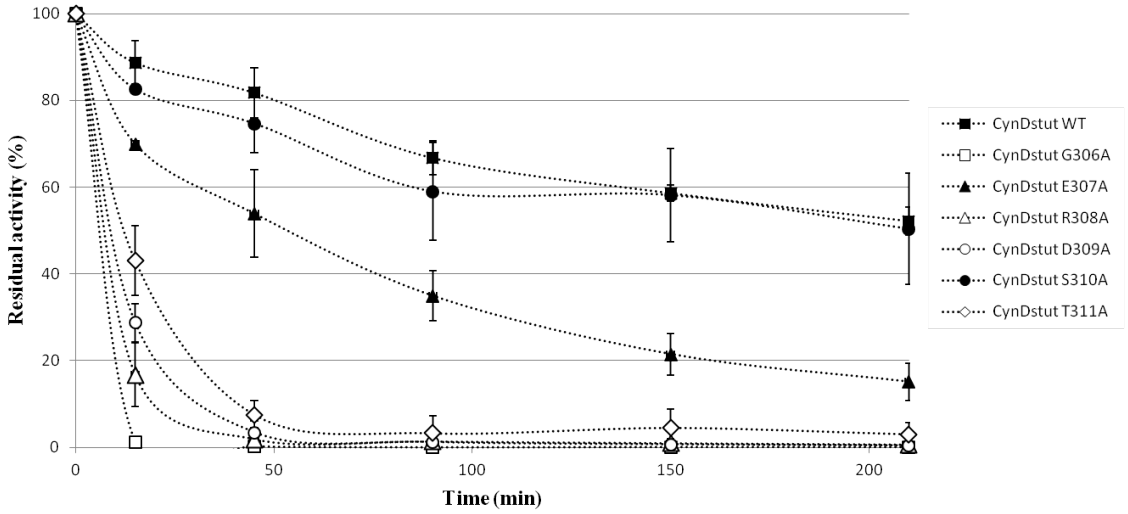

Figure 4.5 Thermostability of $CynD_{stut}$ alanine mutants. Cell lysates were incubated at 39^{o}C in a water bath and the residual activity was tested at specified time points by detecting ammonia production. Activity at time 0 was considered 100%. Error bars indicate the standard deviation of the average from three experiments.

Restoring the activity of $CynD_{stut\text{-}pum}$ hybrid

Using the inactive $CynD_{stut\text{-}pum}$ hybrid as a platform the six residues in GERDST were investigated in various combinations by site directed mutagenesis for restoration of activity to $CynD_{stut\text{-}pum}$.

The side chain charges of $CynD_{stut}$ and $CynD_{pum}$ at position 307, 308 and 309 are reversed. $CynD_{stut}$ has a negative residue (E307) followed by a positive (R308) then a negative residue (D309). However, $CynD_{pum}$ has a positive residue (H307) then a neutral (Q308) and a positive residue (K309). If $CynD_{stut\text{-}pum}$ hybrid was inactive due to this inversion of charges in this important region, then mutationally reinstating the negative-positive-negative amino acids should restore the activity. This proved not to be true; $CynD_{stut\text{-}pum}$ 306NDKENE was inactive (Table 4.10).

Moving to the other residues in the essential 306GERDST region, the G306A mutation greatly affected both activity and stability of $CynD_{stut}$ suggesting its importance. Similar but lesser effects were seen for R308A, D309A and somewhat for T311A. Therefore the restoration of these residues in $CynD_{stut-pum}$ was conducted in combination with G306. Both $CynD_{stut-pum}$ GHRKNT or $CynD_{stut-pum}$ GHQDNE were inactive (Table 4.10).

Table 4.10 Site directed mutagenesis of CynDstut-pum GERDST domain.

Mutant	Amino acid change	Activity in cells
$CynD_{stut-pum}$ (NHQKNE)	306GERDST311→306NHQKNE311	Inactive
$CynD_{stut-pum}$ NDKENE	H307D Q308K K309E	Inactive
$CynD_{stut-pum}$ GHRKNT	N306G Q308R E311T	Inactive
$CynD_{stut-pum}$ GHQDNE	N306G K309D	Inactive
$CynD_{stut-pum}$ GEQKNE	N306G H307E	Active
$CynD_{stut-pum}$ NEQKNE	H307E	Inactive

Changes made to the parent sequence NHQKNE in $CynD_{stut-pum}$ are underlined. The activity was tested as in Table 4.7.

Another residue, E307 also altered the stability $CynD_{stut}$ when it was replaced by an alanine even though it had similar activity to wild-type. Therefore, $CynD_{stut\text{-}pum}$ GEQKNE was constructed. This mutant had some activity, about 15% of wild type (Figure 4.6) and only 2-fold less than $CynD_{stut\text{-}pum}$ GERDST. However, mutation H307E was unable to restore activity to the hybrid. These results indicate the importance of two residues in the $CynD_{stut}$ C-terminus, G306 and E307. In addition other as yet unknown residues outside the GERDST region of the C-terminus are required to restore full activity to the $CynD_{stut\text{-}pum}$ hybrid.

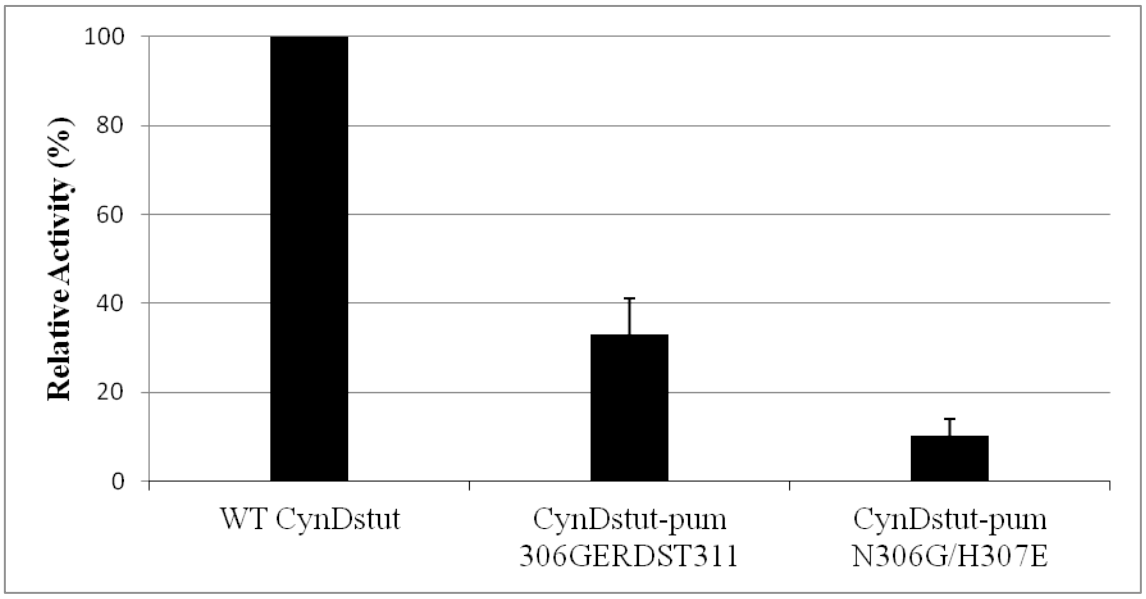

Figure 4.6 Reaction rate comparison of $CynD_{stut\text{-}pum}$ active mutants. Relative activity as a percent of wild type was determined as in Figure 4.3.

Identifying an interaction of the C-terminus with the A surface

The restoration of partial activity by substituting only a few residues in the C-terminus of $CynD_{stut\text{-}pum}$ raises the question whether mutants elsewhere in the protein could restore activity by repairing interactions with the C-terminus? Because, the C-terminus has been seen interacting with both the A and C-surfaces in structures from the larger superfamily (Kimani et al. 2007; Lundgren et al. 2008; Pace et al. 2000), four regions of CynD were predicted to participate in the oligomeric surfaces (Sewell et al. 2003; Sewell et al. 2005). These regions (native to $CynD_{pum}$) were introduced individually into the inactive $CynD_{stut\text{-}pum}$ hybrid. Exchanging either of the C surface ($CynD_{stut\text{-}pum}$ $C1_{pum}$ and $CynD_{stut\text{-}pum}$ $C2_{pum}$) did not restore detectable activity. Similarly, the $CynD_{pum}$ A surface region 167-177 (A1) had no effect on activity ($CynD_{stut\text{-}pum}$ $A1_{pum}$) (Table 4.11). However, $CynD_{stut\text{-}pum}$ carrying the *B. pumilus* A2 surface region 195-206 ($CynD_{stut\text{-}pum}$ $A2_{pum}$) did have activity (Table 4.11) although only about 10% that of wildtype $CynD_{stut}$ activity (Figure 4.7). This result indicates that the $CynD_{pum}$ A2 region is able to partially suppress the disruptive effect of the $CynD_{pum}$ C-terminus in $CynD_{stut\text{-}pum}$.

Table 4.11 $CynD_{stut\text{-}pum}$ with $CynD_{pum}$ oligomer surface regions

Hybrid	Mutation	Activity in cells
$CynD_{stut\text{-}pum}$ $C1_{pum}$	59LGHPEYTRRFYHT71 to IGHPEYTRKFYHE	Inactive
$CynD_{stut\text{-}pum}$ $A1_{pum}$	167NVPLDIAAMNS177 to QVPLDLMAMNA	Inactive
$CynD_{stut\text{-}pum}$ $A2_{pum}$	195TASSHYAICNQA206 to ISSRYYAIATQT	Active
$CynD_{stut\text{-}pum}$ $C2_{pum}$	221DMLCETQEEYFN234 to EMICETQEQYFE	Inactive

Proteins were expressed from non-induced constructs of pBC SK in MB3436 cells. The cyanide degrading activity from 50µl saturated culture mixed with 50µl 0.1M MOPS pH 7.7 6mM cyanide at room temperature for 20 min. Cyanide degradation was measured using picric acid to detect the remaining cyanide and the activity of the of the mutants was compared to wild-type. The reaction rate values represent the average and the standard deviation of the average from three experiments.

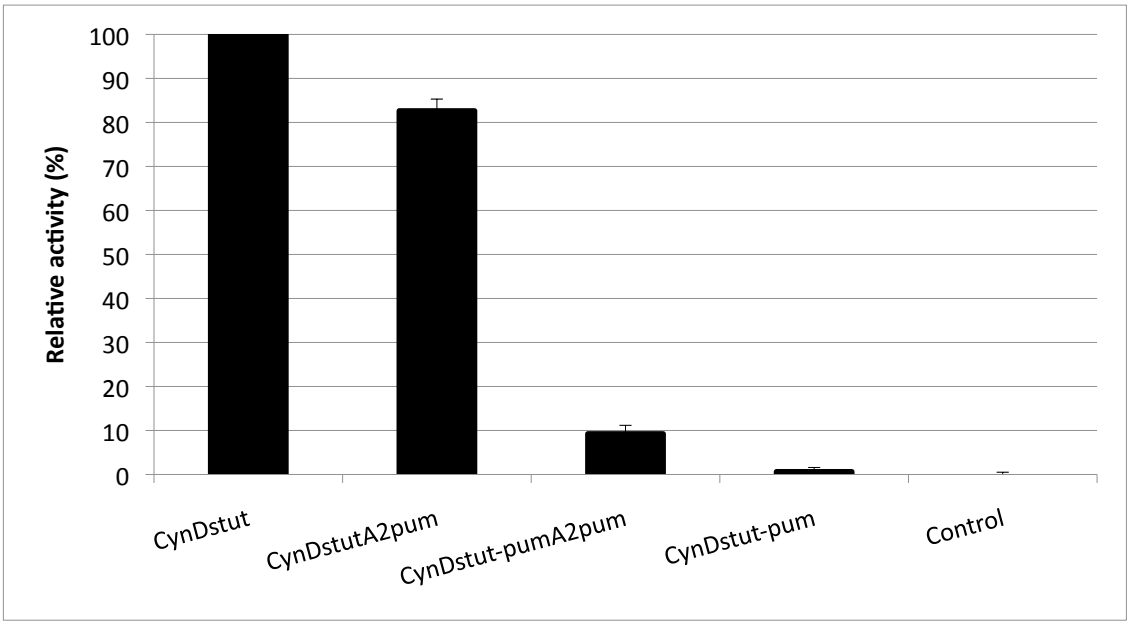

Figure 4.7 Relative activity of A surface region 2 substitution mutants in $CynD_{stut}$ and $CynD_{stut\text{-}pum}$ compared to $CynD_{stut}$ and empty vector control. Cyanide degradation was monitored using the picric acid assay. Error bars indicate the standard deviation from three independent cultures.

Characterization of the A surface substitution

To test if the $CynD_{pum}$ A2 region was specific to the $CynD_{pum}$ C-terminus and not a general stability suppressor, it was also tested in the non-hybrid $CynD_{stut}$ background ($CynD_{stut}A2_{pum}$). $CynD_{stut}A2_{pum}$ did retain activity but it was significantly lower (~16%) than wild type $CynD_{stut}$ (Figure 4.7).

It was also tested whether the $CynD_{pum}$ A2 region made $CynD_{stut}$ tolerant to C-terminal deletions, similar to the $CynD_{pum}$ protein. $CynD_{pum}$ A2 region did not restore activity to deletions at aa 302 in $CynD_{stut}$ ($302CynD_{stut}\Delta302+A2_{pum}$) (Table 4.12), indicating that it does not remove the need for the C-terminal tail.

Table 4.12 $CynD_{stut}\Delta302$ with $CynD_{pum}$ A-surface 195-206

Hybrid	Mutation	Activity *in vivo*
$CynD_{stut}$		Active
$CynD_{stut}\Delta302$	Δ302	Undetectable
$CynD_{stut}\Delta302+A2_{pum}$	Δ302 195TASSHYAICNQA206 to ISSRYYAIATQT (A2)	Undetectable

The activity was tested as in Table 4.11.

Examining the size of $CynD_{stut}A2_{pum}$

$CynD_{pum}$ and $CynD_{stut}$ form 18 and 14 subunit spirals respectively (Jandhyala et al. 2003; Sewell et al. 2003). We investigated if the A2 region play a role in this difference. The elution pattern from size exclusion chromatography of $CynD_{stut}A2_{pum}$ was compared to those of $CynD_{stut}$ and $CynD_{pum}$. $CynD_{stut}A2_{pum}$ eluted from the column

similar to the wild type $CynD_{stut}$ indicating no change in oligomer size (data not shown). Similarly the reverse hybrid CynDpum-stut migrates like CynDpum, suggesting that neither A2 nor the C-terminus are themselves determinants for oligomer size (Chapter V).

DISCUSSION

The cyanide dihydratases from *B. pumilus* and *P. stutzeri* share a very high level of sequence identity (80%) over most of their amino acid sequence. This strong conservation remains, although at a lower level, when comparing cyanide dihydratases to cyanide hydratases such as from *N. crassa* and *G. sorghi*. However, in all cases the C-termini are highly divergent both in sequence and in length (Basile et al. 2008). $CynD_{stut}$ has 5 additional residues relative to $CynD_{pum}$ and CHT_{sorghi} has an extension of 10 carboxy-terminal amino acids compared to CHT_{cras}. Even more striking is the divergence seen in the CynD proteins of two different but closely related from two *B. pumilus* strains, C1 and 8A3, out of only 10 variant amino acids over the whole sequence, 7 are found in the C-terminus (Jandhyala et al. 2003).

This divergence translates into differences in the properties of the protein. For example, $CynD_{pum}$ C1 formed long spirals at pH 5.5 instead of the 18-subunit short helix found at neutral pH (Jandhyala et al. 2003). However, $CynD_{pum}$ 8A3 does not undergo such transformation (Jandhyala et al. 2003). This reversible and pH dependent structural change may be due to histidines protonation at pH 5.5, there are 3 histidines in the $CynD_{pum}$ C-terminus, H305, H308 and H323 whereas $CynD_{pum}$ 8A3 has none (Jandhyala

et al. 2003). The positive charge on the histidines was proposed to lead to repulsion of the monomer C-terminus, expansion of the spiral's diameter and elongation of the spiral. CHT_{cras} and $CynD_{stut}$ also do not show pH-dependent structural changes, keeping the same extended oligomers of variable length or 14-subunits respectively (Dent et al. 2009; Sewell et al. 2003).

Another significant difference is seen in enzyme activity following truncation of the C-terminus. $CynD_{pum}$ is more tolerant to deletion than either $CynD_{stut}$ and CHT_{cras} (Table 4.7). With 28 carboxy-terminal amino acids deleted, $CynD_{pum}$ Δ303 had a reaction rate comparable to wild type (Table 4.7), whereas $CynD_{stut}$ and CHT_{cras} were essentially inactivated by a similar deletion. Although $CynD_{pum}$ tolerates deletions in its C-terminus, they did have an effect on stability. The C-terminus may help stabilize the oligomeric structure of the enzyme, thereby suggesting that loss of activity with deletion might simply be the result of destabilizing the oligomeric structure.

The localization of the C-terminus in the folded protein is not yet clear. No structural data for this region is available due to the lack of sequence identity with related crystallographically determined structures, but it is thought that this domain is found in the center of the helix where is could be interacting with oligomeric A and/or C-surfaces. Structural information from the known crystal structure of amidase might help predict the interfaces where the C-terminus could be interacting. Based on the visible C-terminal region of the amidase from *G. pallidus* (Kimani et al. 2007), Dent *el al*. have suggested that in *N. crassa* the C-terminus interacts with the C surface and then reaches across to the A surface (Dent et al. 2009). Similarly, in the C-shaped β-alanine

synthase (βaS) from *D. melanogaster* the C-terminus has interactions at both the A-surface and C-surface interfaces. Both these surface are essential for oligomerization of the spiral and the activity of the nitrilase, thus the importance of the C-terminus may be at these interfaces.

Our result from substituting putative A and C-surface regions in $CynD_{stut\text{-}pum}$ for the $CynD_{pum}$ sequences suggest a specific interaction of the C-terminus with the A-surface region 2 (195-206). Substituting the A2 region for the $CynD_{pum}$ sequence in $CynD_{stut\text{-}pum}$ ($CynD_{stut\text{-}pum}A2_{pum}$) restored partial activity (Figure 4.7). Further, this region did not enhance activity of the full length $CynD_{stut}$ or remove the need for the C-terminus all together. The *B. pumilus* A2 region actually reduced activity in $CynD_{stut}$, suggesting some specificity for the *B. pumilus* C-terminus. In crystal structures form the larger superfamily, the A-surface is structurally linked to the positioning of the catalytic cysteine in the active site (Kumaran et al. 2003). The loss of activity in the $CynD_{stut}$ C-terminal deletions and $CynD_{stut\text{-}pum}$ hybrid may stem from a loss of an interaction with the A-surface.

Neither the A surface interaction or the GERDST domain completely explain the incompatibility of the $CynD_{stut\text{-}pum}$ hybrid. Either region was only able to restore partial activity to $CynD_{stut\text{-}pum}$. $CynD_{stut\text{-}pum}$GERDST and $CynD_{stut\text{-}pum}A2_{pum}$ also had apparent defects in stability, with $CynD_{stut\text{-}pum}A2_{pum}$ not tolerating over-expression and $CynD_{stut\text{-}pum}$GERDST losing activity upon cell lysis. Other interactions between the C-terminus and the rest of the protein are unclear. The other oligomer surface regions and C-terminal segments examined did not restore detectable activity to $CynD_{stut\text{-}pum}$ when

added individually. Another possibility comes from $CynD_{pum}$'s tolerence to C-terminal deletions. Perhaps the *B. pumilus* enzyme is inherently more stable than the *P. stutzeri* version and therefore does not require the C-terminus for activity. However, loss of the interaction between the C-terminus and the A-surface could explain the drop in stability seen in $CynD_{pum}\Delta303$.

A notable difference between $CynD_{stut}$ and $CynD_{pum}$ has been the size of their oligomers. $CynD_{stut}$ terminates at 14 subunits, while $CynD_{pum}$ extends to an 18-subunit oligomer (Jandhyala et al. 2003; Sewell et al. 2003). We tested if the A2 region was influencing the terminal size of the oligomer. The elution pattern of $CynD_{stut}A2_{pum}$ protein from size exclusion was consistent with the normal $CynD_{stut}$ 14 subunit oligomer, indicating that variation in self-termination stems from elsewhere in the protein. The Oligomer size of $CynD_{stut\text{-}pum}$GERDST and $CynD_{stut\text{-}pum}A2_{pum}$ were not examined because the proteins did not survive cell lysis or over-expression.

Alterations to the C-terminal tail have been observed to affect activity and quaternary structure in both CynD and other nitrilases (Kiziak et al. 2007; Thuku et al. 2007; Wang et al. 2012), but a lack of clear conserved sequence or secondary structure has made it difficult to predict a common role in nitrilases (Thuku et al. 2009). Interaction between the C-terminal tail and the A-surface are seen in multiple crystal structures of greatly diverged enzymes from the nitrilase superfamily. The interaction seen between these regions in CynD suggests that placement of the C-terminal tail at the A-surface by be common despite the sequence divergence seen in this region.

CHAPTER V

C-TERMINAL HYBRID MUTANT OF *BACILLUS PUMILUS* CynD DRAMATICALLY ENHANCES STABILITY AND pH TOLERANCE BY REINFORCING OLIGOMERIZATION

PREFACE

This chapter contains contributions from Dr. Mary Abou Nader Crum and myself. While investigating the C-terminus of cyanide dihydratase (CynD) from *P. stutzeri* ($CynD_{stut}$) and *B. pumilus* ($CynD_{pum}$), she discovered that switching the C-terminal regions in $CynD_{pum}$ for the $CynD_{stut}$ sequence ($CynD_{pum\text{-}stut}$) dramatically increase the proteins thermal stability and pH tolerance. Her data are presented in figures and tables on pages 112 and 114-116. Together we characterized the oligomerization of the $CynD_{pum\text{-}stut}$ hybrid and the C-terminally truncated $CynD_{pum}\Delta303$ by size exclusion chromatography, shown page 118. I built off Dr. Mary Abou Nader Crum's work by examining mutations known to disrupt oligomer formation in $CynD_{pum}$ (Chapter II) in combination with the C-terminus of $CynD_{stut}$. I found that the C-terminus of $CynD_{stut}$ enhances stability in $CynD_{pum\text{-}stut}$ by supporting oligomerization. The data I contributed independently are presented in figure on pages 119 and 120.

SYNOPSIS

The C-terminal domain of nitrilase, although highly variable, has significant impact on cyanide dihydratase activity and stability. The lack of structural data and of sequence similarity makes it difficult to hypothesize possible mechanisms. We previously showed that CynD from *Pseudomonas stutzeri* is dependent on its native C-terminus, whereas CynD from *Bacillus pumilus* can both tolerate deletions as well as replacement of its C-terminus. Here we further characterize a cyanide dihydratase hybrid, $CynD_{pum\text{-}stut}$, constructed with the N-terminal from $CynD_{pum}$ from *B. pumilus* and C-terminal from $CynD_{stut}$ *P. stutzeri*. The $CynD_{pum\text{-}stut}$ hybrid was found to be significantly more stable than its parent $CynD_{pum}$. This hybrid also exhibited full activity at pH 9, a pH where the parent enzyme is essentially inactive, and retained 40% of its activity at pH 9.5 making it a unique pH tolerant mutant. Gel filtration chromatography of the C-terminal deletion mutant, $CynD_{pum}\,\Delta 303$, revealed a defect in oligomerization. The CynD from *P. stutzeri* in the hybrid $CynD_{pum\text{-}stut}$ restored the wild-type oligomer size. The $CynD_{pum\text{-}stut}$ hybrid was also able to suppress the C-surface mutation R67C, which blocks activity and proper oligomerization. This indicates that the C-terminus from *P. stutzeri* stabilizes CynD by supporting oligomerization between dimers at the C-surface.

INTRODUCTION

Biological detoxification of cyanide contaminated waste-water is of significant interest both due to the dangerous effects of cyanide as well as the cost of chemical detoxification (Mosher and Figueroa 1996), bioremediation promises a safer and potentially less expensive process. Several enzymes capable of degrading cyanide have been found in bacteria, fungi and plants (Knowles 1976; Poulton 1990) that use diverse reaction mechanisms with varied requirements for cofactors or secondary substrates (Dash et al. 2009; Gupta et al. 2010). Cyanide dihydratase (CynD), a member of the nitrilase enzyme superfamily, hydrolyses cyanide into formate and ammonia (Pace and Brenner 2001). The reaction does not require any cofactors or additional substrates during the hydrolysis process, making it among the best prospects for cost-effective bioremediation. CynD has been described from *Alcaligenes xylosoxidans subsp. denitrificans, Pseudomonas stutzeri* AK61 (Watanabe et al. 1998) and *Bacillus pumilus* strains C1 and 8A3 (Meyers et al. 1993), the AK61 and C1 enzymes being the best characterized. Likely homologues are found only in about a dozen genomes to date, making this a relatively rare enzyme.

Bacillus pumilus C1 was isolated by enrichment from a cyanide wastewater dam in South Africa (Meyers et al. 1991). The CynD protein from this bacteria forms a 18-subunit spiral shaped oligomer, only the oligomeric form has activity. This protein has optimal activity between 37°C and 42°C and in the pH range of 7-8 (Jandhyala et al. 2005), activity dramatically falls off above pH 8.5. This presents a major drawback for

its application to cyanide waste-water treatment since cyanide solutions are kept highly alkaline to avoid formation of hydrogen cyanide gas which occurs at neutral pH.

The CynD C-terminus is an extension not found in other members of the superfamily whose crystal structures are solved. This lack of structural information prevents its localization in CynD structural models but some predictions on its role have been proposed based on mutational studies (Sewell et al. 2005; Thuku et al. 2009). A mutation (E327G) in the C-terminus increased the thermostability of the enzyme (Wang et al. 2012) whereas deletion of the C-terminal 28 amino acids, while not affecting the activity of $CynD_{pum}$, notably reduced its stability (Abou Nader 2012). The E327G mutant is also associated with an extension of the CynD oligomer beyond the wild-type 18 subunits.

The creation of hybrid CynD proteins where the C-termini were exchanged between the highly similar cyanide dihydratases *P. stutzeri* and *B. pumilus* revealed that each behaved uniquely (Sewell et al. 2005). A hybrid carrying the N-terminus from the *B. pumilus* enzyme and the C-terminal domain from the *P. stutzeri* ($CynD_{pum-stut}$) retained full activity relative to the parent whereas the converse $CynD_{stut-pum}$ hybrid had no detectable activity (Sewell et al. 2005). The enzyme from *P. stutzeri* also fails to tolerate any significant deletions within it. The high amino acid identity between these two enzymes is not shared in their C-termini, although some conservation of residues with like polarity or charge can be seen (Abou Nader 2012). Only $CynD_{pum}$ shows a tolerance for alterations of its C-terminus.

Two possible interpretations might arise from these observations. First $CynD_{stut}$ is inherently unstable and requires the stabilizing effect of its C-terminus. This might involve a unique interaction between the two; hence the $CynD_{pum}$ C-terminus fails to stabilize the $CynD_{stut}$ protein. Alternatively the $CynD_{stut}$ C-terminus is a super-stabilizer that suppresses the instability of the protein, and the $CynD_{pum}$ C-terminus is only a weak stabilizer that does contribute somewhat to stability of the *B. pumilus* enzyme but is insufficient to suppress the $CynD_{stut}$ instability.

The phenotype of the $CynD_{pum-stut}$ hybrid was not known other than it remained active. If the first model above was correct, then since $CynD_{pum}$ activity does not require a C-terminus, the hybrid $CynD_{pum-stut}$ could have a phenotype similar to a short C-terminal deletion and remain active but unstable. The alternative model suggests that the $CynD_{stut}$ C-terminus might have general instability suppressing properties and make the hybrid protein more stable. In this study we set out to distinguish between these hypothesis and better characterize the $CynD_{pum-stut}$ hybrid protein. We further investigate if C-terminus participates in the oligomeric structure of CynD.

MATERIALS AND METHODS

Culture media and reagents

All strains were grown in LB broth or on plates. Antibiotics were used at concentrations of 100 ug/ml of ampicillin, 25 ug/ml of kanamycin or 25 ug/ml of chloramphenicol.

Bacterial strains and plasmids

E. coli strains MB3436 [Δ*endA thiA hsdR17 supE44 lacI*^{q}*ZΔM15*] was used as the host strain for DNA manipulations and MB1837 [BL21 (DE3) pLysS] was used to produce protein. The plasmids used are described in Table 5.1.

Table 5.1 List of plasmids used in this study

Plasmid	Description	Reference
p5277	pET28 carrying synthetic *P. stutzeri cynD*	Abou-Nader
p2890	pET26b carrying *B. pumilus* C1 *cynD*	Jandhyala *et al.* 2003
p4406	pET28a carryimg *B. pumilus* C1 *cynD*	Abou-Nader
p3411	pET26b carrying $CynD_{pum\text{-}stut}$	Sewell et al. 2005
p5389	pET28a carrying $CynD_{pum\text{-}stut}$	Abou-Nader
p5383	5389 K93R	Abou-Nader
p5467	pET28b carrying $CynD_{pum}$ 306GERDST311	Abou-Nader
p5585	p4406 R67C	Park Chapter II
p5523	p4406 Y70C	Park Chapter II
p5954	p5389 R67C	Park This work
p6015	p5389 Y70C	Park This work

Protein expression and purification

Genes were cloned into pET28a to create expression constructs with an N-terminal his-tag, and transformed into MB1837 for expression. Overnight cultures were diluted 1:100 in 50ml LB + kanamycin and grown to an OD600 of 0.3 at 37°C at which point IPTG was added to 1mM and growth continued at 30°C for 3-4 hours. Cells were pelleted by centrifugation and washed twice with 0.1 M MOPS pH 7.7 and the pellet was

stored at -20°C overnight. Cells were thawed and lysed at room temperature with B-PER II Protein Extraction Reagent (Thermo Scientific), 2mL of B-PER II reagent per gram of cell pellet was used with 0.5 mg/ml lysozyme, 10ug/ml DNase and 1X EDTA-free protease inhibitors as recommended by the manufacturer. The cell lysate was centrifuged at 13,000 rpm for 15 min at 4°C. Purification of hexahistidine-tagged proteins was performed at 4^{o}C using the *HisPur Cobalt Purification Kit (*Thermo Scientific). Buffer exchange of the purified protein at 4°C used Zeba Spin Desalting Columns (Thermo Scientific) and the protein was resuspended in 0.1 M MOPS pH 7.7. Purity was confirmed by SDS-page and protein concentration was determined by measuring absorbance at 280nm with a NanoDrop ND-1000 and using the predicted his-tagged protein extinction coefficient of 54770 cm^{-1} M^{-1} and molecular weight of 40,013 g/mol for the purified proteins. Select proteins were also checked by Bradford assay to confirm relative concentrations. Purified proteins were stored in aliquots at -80°C.

Kinetic measurements

Kinetic analysis used 3.9 µg of in 1 ml total volume adding cyanide from a stock solution of 1 M prepared in a 1 M MOPS pH 7.7. Reactions were done at room temperature in 50 mM MOPS at pH 7.7 at different concentrations of cyanide. Kinetic measurements were also repeated using 50 mM Tris-HCl at pH 7.7 and pH 9. Each reaction was run for 5 min with time points taken every 1 min. The reaction rates over the first 5 min were linear and $V_{initial}$ was calculated by monitoring ammonia produced in 100µl of reaction mixed with 100 µl of diluted Nessler reagent (1:3 in MQ H_2O) and

absorbance measured using a 96-well plate reader (Bio-Rad) at 420 nm to determine the ammonia produced. Lineweaver-Burk plots were used to calculated K_m and V_{max}. For each enzyme, the final K_m and V_{max} values are averages from 3 independent protein preps. V_{max} was used to calculate K_{cat}. All enzymes were considered as 18-subunits spirals with molecular weight of 713,772 g/mole.

pH activity measurements

Enzyme at 5.5 µg in 1ml total volume was used for pH activity analysis. Three 1M cyanide stock solutions were prepared: 1 M citric acid/Na_2HPO_4 at pH 5.5, 1 M MOPS pH 7.7 or 1 M CAPS at pH 9.5. The activity of the purified enzyme was measured over the pH range 4-10 using the following buffers; 50 mM citric acid/ Na_2HPO_4 (pH 4, 5 and 6), 50 mM MOPS (pH 7), 50 mM Tris HCl (pH 8) and 50 mM glycine/NaOH (pH 9 and 9.5). Reactions were done at room temperature in a fume hood at a final concentration of 4mM cyanide. The activity was monitored for the first 5 min and time points were taken every min. Ammonia production was measured as described above. Final values are averages from 3 independent protein preps.

Activity of C-surface mutants

Activity was assayed by picric acid endpoint assay for cyanide (Wang et al. 2012). Purified proteins were prepared at 50µg/ml in 100mM MOPS pH7.7. From these dilutions 10µl was added to 80µl of 100mM MOPS pH7.7 in triplicate wells on a 96 well plate. This was allowed to incubate for 20 minutes at room temperature. Reactions were

started by adding 20µl of 25mM KCN 100mM MOPS. The plate was covered with parafilm to prevent evaporation of cyanide. After 20 minutes 80µl of alkaline picric acid (0.5% picric acid in 0.25 M sodium carbonate) was added to terminate the reaction. The assay was developed by incubating at 60°C for 20 minutes. Remaining cyanide was measured by absorbance at 520nm in a Bio-Rad Benchmark Plus microplate spectrophotometer.

Enzyme stability

The thermostability of the enzyme was determined by incubating 80 µg of purified enzyme in a total volume of 8 ml of 50 mM MOPS pH 7.7 in a water bath at 42°C. At each time points 0.5 ml aliquots were removed into a new 1.5 ml microfuge tubes and left at room temperature for 3 min to equilibrate before adding cyanide from a 1M stock in 1 M MOPS pH 7.7 to a final concentration of 4 mM. The reaction continued at room temperature and the activity was monitored for the first 5 min with time points taken every min to measure ammonia production as described above. The reaction rate was calculated using the zero time value considered as 100% activity rate and the relative activity of the enzyme at the different incubation times was then calculated. Final values are averages from 3 independent protein preps.

Gel filtration

Size-exclusion chromatography of the purified enzymes used a Superdex 200 10/300 GL column and BioLogic DuoFlow chromatography system from Biorad equilibrated with 0.1 M MOPS pH 7.7. 200 µl of 2-3mg/ml purified enzyme resuspended in 0.1 M MOPS pH 7.7 were loaded on the column. 0.1 M MOPS pH 7.7 was used to as mobile phase to elute the protein and the elution was monitored by absorbance at 280 nm. The size standard kit used was Gel Filtration Markers Kit weights 29,000 – 700,000 daltons from Sigma (Carbonic Anhydrase 29 KDa, Albumin 66 KDa, Alcohol dehydrogenase 150 KDa, β-Amylase 200 KDa, Apoferritin 443 KDa, Thyroglobulin 669 KDa, Blue dextran, 2,000 KDa).

RESULTS

Characterizing the stability of $CynD_{pum\text{-}stut}$ hybrid

The hybrid protein ($CynD_{pum\text{-}stut}$) carrying the N-terminal ~300 residue body of $CynD_{pum}$ and the ~30 residue C-terminal tail from $CynD_{stut}$ had normal activity (Abou Nader 2012; Sewell et al. 2005) unlike the converse construct $CynD_{stut\text{-}pum}$ which had no detectable activity. Deletion of the C-terminus from the *B. pumilus* enzyme, $CynD_{pum}$ Δ303, retained high activity (87% of the parent) but was notably unstable. To analyze the stability of the $CynD_{pum\text{-}stut}$ hybrid, the purified enzymes $CynD_{pum}$, $CynD_{stut}$ and $CynD_{pum\text{-}stut}$ were incubated at 42°C in a water bath for various times and the fraction of enzyme activity remaining was determined.

The $CynD_{pum-stut}$ hybrid was significantly more stabile than either wild-type $CynD_{pum}$ or $CynD_{stut}$ (Figure 5.1) which were similar; 50% of initial activity was lost after 1 h of incubation at 42°C for the parent enzymes but 17 hours of incubation was needed for 50% loss with the $CynD_{pum-stut}$ hybrid. The hybrid retained about 10% of its activity after 48 h of incubation. The results supports the initial hypothesis that the *P. stutzeri* C-terminus acts as a general suppression of instability and suggests that the native C-terminus of $CynD_{pum}$ is not optimal for stability of that protein.

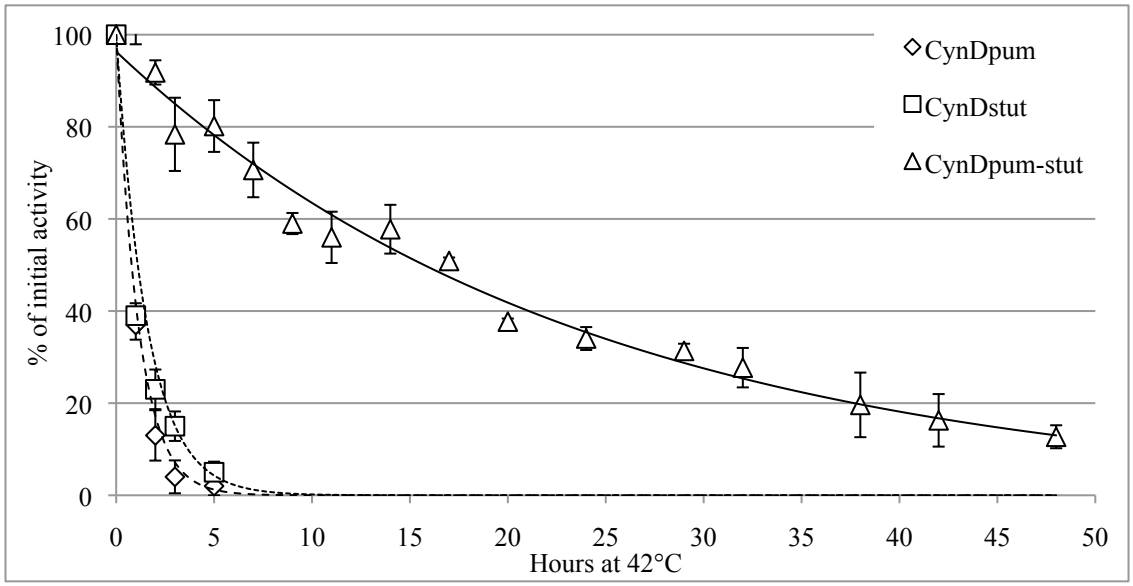

Figure 5.1 Comparison of $CynD_{pum-stut}$ hybrid and wild-type thermostability. Purified enzymes were incubated in a water bath at 42°C for designated times and aliquots removed to assay as described in Materials and Methods. Residual activity was tested at room temperature. Error bars indicate the standard deviation of the average from experiments conducted with three separate protein preps. Trend line highlights CynDpum-stut data.

In a previous study, we described other $CynD_{pum}$ mutants that increased its stability: E327K, D172N and K93R, with the latter having the largest effect (Abou Nader 2012). The $CynD_{pum-stut}$ is much more stable that any of the single mutants. We speculated that this mutation is involved in interactions at the A and D/E surfaces whereas the C-terminus is thought to interact with the A and C surface. Therefore we hypothesize that K93R mutation might have a synergistic effect with the C-terminus. To test this we constructed $CynD_{pum-stut}$ K93R mutant and tested its thermostability. $CynD_{pum-stut}$ K93R was somewhat more stable than $CynD_{pum-stut}$ (Figure 5.2).

A motif GERDST, located in the C-terminus of $CynD_{stut}$ at position 306 to 311, was previously shown (About Nader 2012) to be necessary for the activity and stability of $CynD_{stut}$. This motif is not found in the $CynD_{pum}$ C-terminus, instead a somewhat similar (by amino acid properties) motif NHQKNE is found at position 307 to 312. To see whether this motif was responsible for the stabilizing phenotype, a $CynD_{pum}$ GERDST mutant was constructed by replacing $CynD_{pum}$ residues 307NHQKNE312 with $CynD_{stut}$ sequence GERDST. This $CynD_{pum}$ GERDST was intermediate in stability (Figure 5.2), much more than wild type but less than the $CynD_{pum-stut}$ hybrid (which carries GERDST in its native context). $CynD_{pum}$ GERDST retained 50% activity after 7 h incubation at 42^{o}C, compared to K93R for example that lost 50% of activity within 2.5 h.

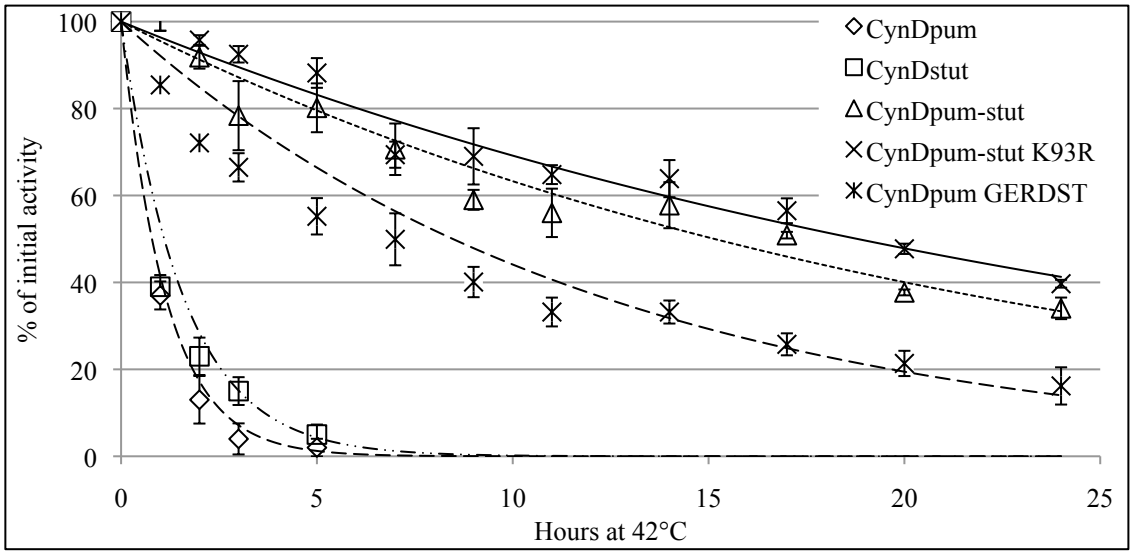

Figure 5.2 Thermostability of different $CynD_{pum}$ mutants. Purified enzymes were incubated in a water bath at 42°C for designated times and aliquots removed to assay as described in Materials and Methods. Residual activity was tested at room temperature. Error bars indicate the standard deviation of the average from experiments conducted with three separate protein preps.

pH activity profile

A link between stability and pH activity has been described for $CynD_{pum}$, a mutant was previously described that showed a slight increase in cyanide degrading activity at pH 9 *in vivo* as well as an increase in stability, at pH 9 the wild-type is inactive (Wang et al. 2012).

Wild-type $CynD_{pum}$ and $CynD_{pum}$ GERDST had a similar pH activity profile with both having maximal activity at pH 8; at pH 9 or above $CynD_{pum}$ was inactive and $CynD_{pum}$ GERDST had only 5% activity at pH 9 (Figure 5.3).

The $CynD_{pum\text{-}stut}$ hybrid displayed a very different pH activity profile. At alkaline pH, the effect was even more dramatic. The hybrid $CynD_{pum\text{-}stut}$ had its maximal activity

at pH 9 in contrast to wild-type $CynD_{pum}$, which was essentially inactive at pH 9. Even at pH 9.5 the hybrid $CynD_{pum\text{-}stut}$ retained about 40% to 50% of its maximal activity whereas the wild-type was completely inactive and at pH 10 about 5% of the activity remained. Similarly this enzyme had a notable increase in reaction rate in acidic solutions, 60% higher than wild-type at pH 4, 50% at pH 5 and 40% at pH 6. The K93R mutation had a slight but not a significant positive effect on the $CynD_{pum\text{-}stut}$ hybrid at the different pHs.

Although $CynD_{pum}$ GERDST was more stable than wild-type, it too was essentially inactive at pH 9 as was the parent enzyme and the K93R single mutant.

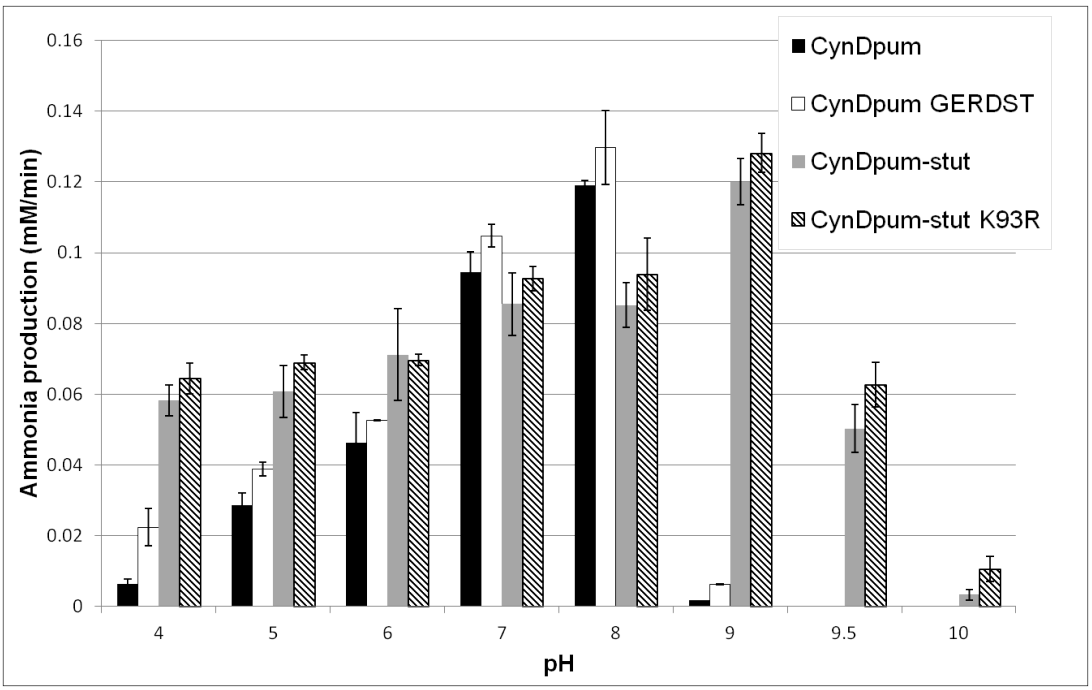

Figure 5.3 pH activity profile of $CynD_{pum}$ mutants. Purified enzyme was tested with 4 mM cyanide and the ammonia production was measured at different pHs as described in Materials and Methods. Error bars indicate the standard deviation of the average from experiments conducted with three separate protein preps.

Kinetic parameters at high pH

The increase in reaction rate seen in the previous experiment at pH 9 (Figure 5.3) suggested that the $CynD_{pum-stut}$ hybrid optimal pH shifted from pH 8 to pH 9. Kinetic parameters of the $CynD_{pum-stut}$ hybrid were measured at pH 7.7 and pH 9 and compared to that of wild-type $CynD_{pum}$ (Table 5.2). At pH 7.7, $CynD_{pum}$ and $CynD_{pum-stut}$ exhibited comparable kinetic properties. Both enzymes had similar K_m and V_{max} values. When tested at pH 9, $CynD_{pum-stut}$ hybrid displayed a 2-fold increase in affinity for the substrate but a slight decrease in V_{max}. The wild-type enzyme was inactive at pH 9 and therefore could not be measured.

Table 5.2 Kinetic measurement of $CynD_{pum-stut}$ at pH 7.7 and pH 9.

		$CynD_{pum}$	$CynD_{pum-stut}$
pH 7.7	K_m (mM)	2.9 ± 0.5	2.4 ± 0.8
	V_{max} (mmole/min.mg)	0.038 ± 0.004	0.03 ± 0.003
	K_{cat} (min^{-1})	2.63 $x10^4$	2.15 $x10^4$
pH 9	K_m (mM)	N/A	1.3 ± 0.3
	V_{max} (mmole/min.mg)	N/A	0.025 ± 0.002
	K_{cat} (min^{-1})	N/A	1.8 $x10^4$

Oligomerization state as probed by size exclusion chromatography

The role of the C-terminus in the oligomerization of the nitrilase has been observed for several members of the superfamily. $CynD_{pum}$ C1 changes its structure from an 18-subunit spiral at pH 8 to long helix at pH 5 (Jandhyala et al. 2003). This effect is thought to involve three histidines found in the C-terminus, which become

protonated at this pH. Thus, the C-termini from the different subunits located in the center of the spiral repulse, leading to an expansion of the spiral radius and elongation of the helix (Thuku et al. 2009). Another example comes from the nitrilase of *Rhodococcus rhodochrous* J1. Following the autocleavage of 39 C-terminal residues, the enzyme structure changed from inactive 80 KDa dimers to active 410 KDa helical oligomers (Nagasawa et al. 2000; Thuku et al. 2007). Wang et al. (Wang et al. 2012) described two C-terminal mutants of $CynD_{pum}$ that showed increased stability, using negative stain electron microscopy the protein displayed helices with an average of 2.5 times the length of wild-type.

We analyzed the oligomer size of the $CynD_{pum}$ Δ303 deletion, $CynD_{pum\text{-}stut}$ and wild-type $CynD_{pum}$ using the size exclusion chromatography to detect size changes. The $CynD_{pum}$ monomer has a size of 37 KDa and assembles into an 18-subunit spiral. Thus, the elution peak of $CynD_{pum}$ aligned with that of the protein standard of 669 KDa as expected (Figure 5.4a). The $CynD_{pum\text{-}stut}$ eluted with the same profile as $CynD_{pum}$ suggesting its structure is similar to the parent enzyme (Figure 5.4a,c) and therefore a change in oligomerization state does not explain its enhanced stability. However, $CynD_{pum}$ Δ303 showed multiple peaks, a small peak of the 18-subunit oligomer eluted at 669 KDa but the majority of the protein eluted in the 150-180 KDa range (Figure 5.4b) which would be the size of a tetramer.

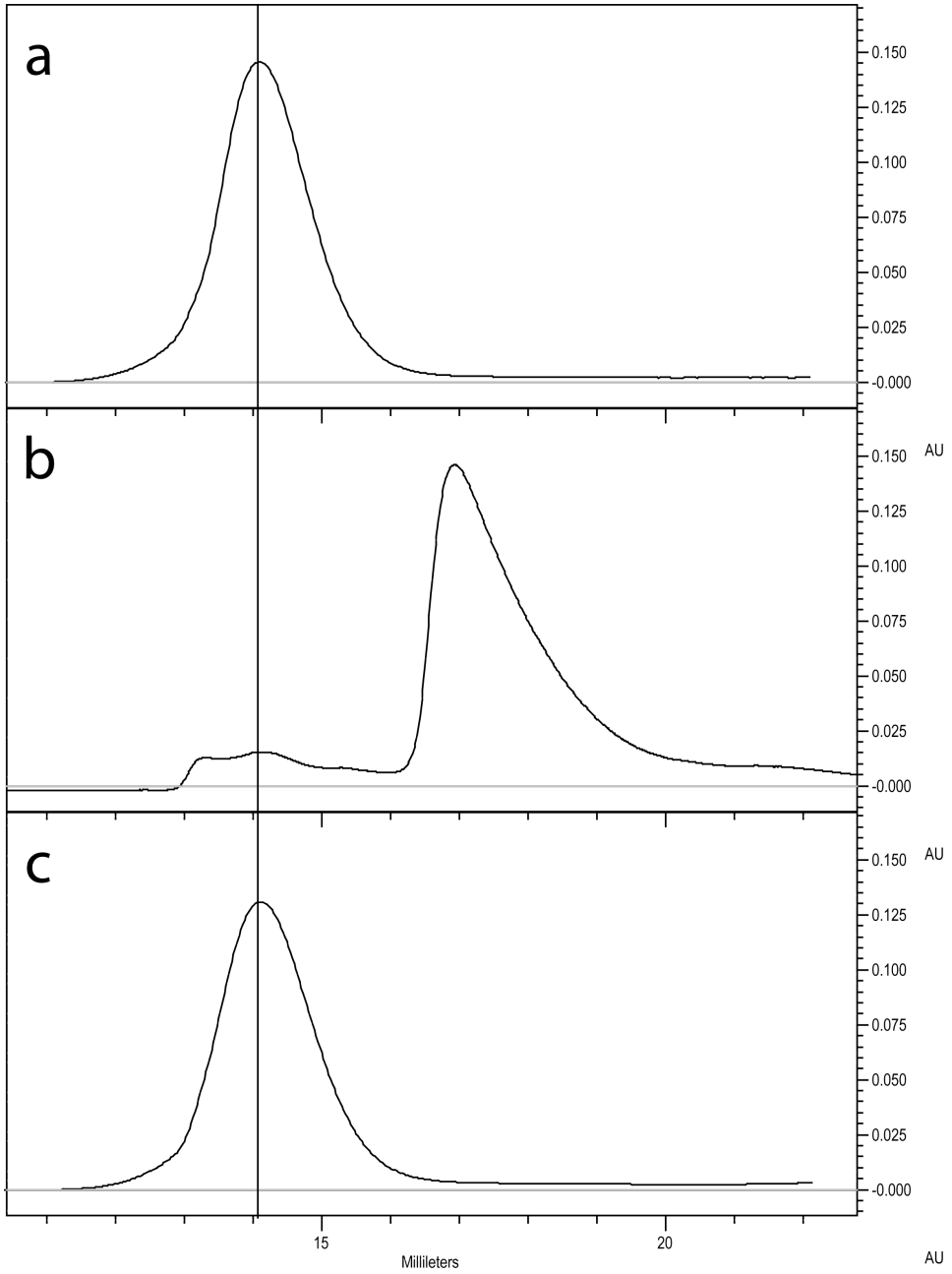

Figure 5.4 Gel filtration chromatography of (a) $CynD_{pum}$, (b) $CynD_{pum}$ Δ303, and (c) $CynD_{pum\text{-}stut}$. 2 to 3 mg/ml of purified enzymes were loaded on Superdex 200 10/300 GL column and 0.1 M MOPS was used as mobile phase. Elution was monitored by absorbance at 280 nm. Vertical line highlights the elution position of the $CynD_{pum}$ wild type enzyme.

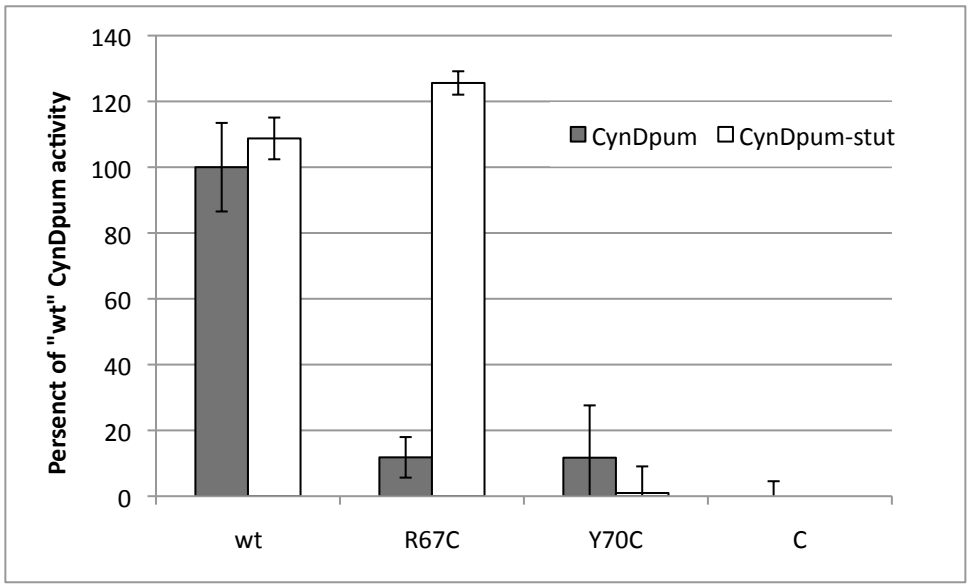

Figure 5.5 Activity of $CynD_{pum}$ and $CynD_{pum\text{-}stut}$ with C-surface mutations R67C and Y70C. Activity was assayed using purified enzyme by picric acid endpoint assay. Error bars indicate the standard deviation from the average of assays done in triplicate.

C-terminus interaction with C-surface mutants

In a concurrent study substitutions R67C and Y70C in the C-surface have been shown to abolish activity of $CynD_{pum}$ (Figure 5.5). These mutants as examined by size exclusion chromatography, shows that that $CynD_{pum}$R67C has a defect in oligomerization (Figure 5.6c). $CynD_{pum}$Y70C on the other hand forms uniform oligomers but remained inactive (in preparation Park *et al*). To test if the *P. stutzeri* C-terminus stabilizes $CynD_{pum}$ by promoting oligomerization, R67C and Y70C were examined with the *P. stutzeri* C-terminus. The *P. stutzeri* C-terminus fully restored activity in $CynD_{pum\text{-}stut}$R67C (Figure 5.5). Furthermore as examined by size exclusion chromatography $CynD_{pum\text{-}stut}$R67C oligomer formation was restored (Figure 5.6d). On

the other hand $CynD_{pum\text{-}stut}$Y70C showed no restoration of activity (Figure 5.5). This indicates that the C-terminus stabilizes CynD by supporting the oligomeric structure.

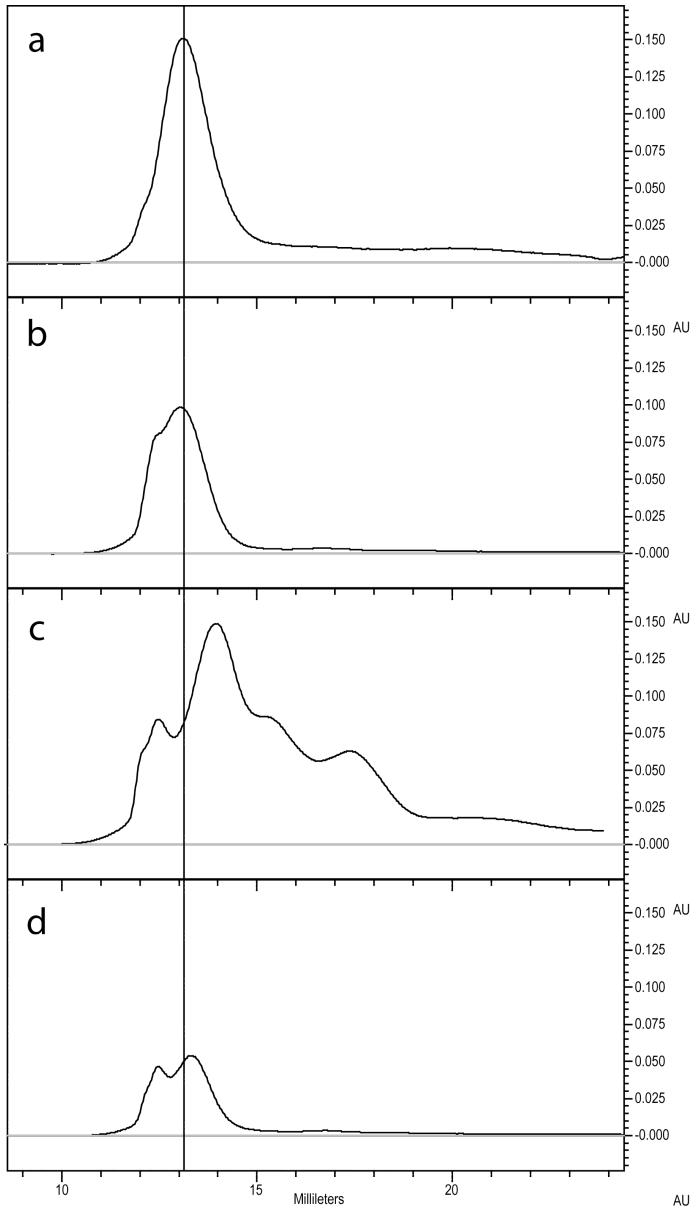

Figure 5.6 Gel filtration chromatography of (a) $CynD_{pum}$, (b) $CynD_{pum\text{-}stut}$, (c) $CynD_{pum}$R67C, and (d) $CynD_{pum\text{-}stut}$R67C. 2 to 3 mg/ml of purified enzymes were loaded on Superdex 200 10/300 GL column and 0.1 M MOPS was used as mobile phase. Elution was monitored by absorbance at 280 nm. Vertical line highlights the elution position of the $CynD_{pum}$ wild type enzyme.

DISCUSSION

The use of enzymes for the bioremediation of cyanide has been long discussed in the literature (Akcil 2003; Dash et al. 2009). Several enzymes capable of transforming cyanide to less toxic products exist (Gupta et al. 2010), cyanide dihydratases prominent among them since the end products of formate and ammonia are not especially toxic and additional cofactors are not required (Meyers et al. 1993). However to become practical an increase in enzyme stability would be useful to allow long term remediation but more importantly survival and activity at alkaline pH is essential. Cyanide contaminated wastewater is kept highly alkaline to prevent the production of poisonous hydrogen cyanide gas which occurs with neutral cyanide solutions (Akcil 2003) at room temperatures.

In this work we focused our attention on the potential contribution of the C-terminal domain on the cyanide degrading nitrilase, $CynD_{pum}$ from *B. pumilus*. Nitrilase C-termini are highly variable both in length, sequence, and tolerance to modification. Partial deletions of the C-terminus were tolerated by the $CynD_{pum}$ protein but are not tolerated by $CynD_{stut}$ nor CHT from *N. crassa* (Abou Nader 2012; Sewell et al. 2005). Mutations affecting substrate specificity and protein stability have also been found mapping to this domain in multiple nitrilases (Kiziak et al. 2007; Wang et al. 2012). Here we showed that the C-terminus of $CynD_{stut}$ acted as an enhancer of stability on the heterologous $CynD_{pum}$ nitrilase, in fact functioning better than the native C-terminus.

The $CynD_{pum-stut}$ hybrid demonstrated remarkable stability compared to wild-type (Figure 5.1), about 15-20 fold more than the parent in our 42°C thermostability

challenge. In addition, $CynD_{pum\text{-}stut}$ showed a shift of its optimal pH from pH 8 to pH 9 (Figure 5.4). Whereas $CynD_{pum}$ rapidly lost activity as the pH increased above pH 8, the hybrid had 100% activity at pH 9 and had nearly 50% activity at pH 9.5. No other previously described nitrilase mutants have shown such a dramatic improvement in stability or catalysis at alkaline pH.

The current model suggests that the C-terminus is involved in interactions with both the dimerization (A) surface and the oligomerization (C) surface. Both these surfaces were shown to be important for stability and activity of the enzyme (12). Another A surface mutant, D172N increased the stability of $CynD_{pum}$ and the affinity to the substrate at pH 7.7 (Abou Nader 2012). The C surface is not only important for oligomerization, but interactions at this interface help position a catalytic residue, E141 in the active site (20). Deletion or substitution of residues in this region destroyed activity (Sewell et al. 2005); Chapter II). The restoration of activity (Figure 5.5) and oligomerization (Figure 5.6) in $CynD_{pum\text{-}stut}$R67C indicates that the C-terminus exerts its effect by stabilizing the C-surface.

In a previous study, we showed $CynD_{pum}$ Δ303 to be highly unstable losing all of its activity within 30 minutes after a 38°C challenge (Abou Nader 2012). However, it retained nearly full activity in vivo, 86% that of wild-type, but this activity was lost following cell lysis. Gel filtration chromatography also showed loss of the 18-subunits oligomeric structure in purified $CynD_{pum}$ Δ303 protein (Figure 5.4b), leading to possible pentamers or more likely tetramers based on size. The high instability and reduced activity in lysates is likely due to unstable oligomer formation without participation of

the C-terminus in the C-surface. Unlike previously characterized stabilizing mutants (Wang et al. 2012), the highly stabilizing $CynD_{stut}$ C-terminus did not alter the size of the quaternary structure (Figure 5.4c), gel filtration data demonstrated the hybrid had a similar length as the wild-type.

CONCLUSION

Our data indicates that the influence of the nitrilase C-terminus on stability stems from its participation in oligomerization at the major C-surface interface. This surface is crucial for the activity and stability of CynD. Thus, it is not too surprising that this domain would have major effects on the enzyme parameters. While we can not know the precise nature of the C-terminus with the current lack of high resolution structural data, our studies on the C-terminus have enabled us to construct a novel protein with remarkable stability and tolerance to alkaline conditions, features essential for practical application.

CHAPTER VI

SUMMARY AND FURTHER QUESTIONS

Nitrile compounds are an industrially important class of chemicals with diverse applications from mining to fine chemical synthesis (Korte and Coulston 1995; Pollak et al. 2000). The hydrolysis of these nitriles allows for the production of valuable amide or acid products, as well as the remediation of extremely toxic nitrile wastes. An enzymatic approach to nitrile hydrolysis offers improvements to product purity, while significantly reducing the environmental impact relative to conventional chemical synthesis and waste degradation (Ramteke et al. 2013).

Nitrilase enzymes are particularly attractive for industrial application, as they require no additional substrates, metal cofactors, or specific anaerobic conditions (Banerjee et al. 2002). While characterizing and reengineering nitrilases, multiple characteristics such as activity, stability, substrate specificity, and pH tolerance were found to be influenced by the formation and shape of nitrilases' oligomeric spiral structure (Thuku et al. 2009). A lack of fine structural detail for any of these nitrilase enzymes has been a significant hurdle to rationally engineering these enzymes to improve and expand their industrial utility.

Comparisons of nitrilases to crystal structures from the larger superfamily (Kimani et al. 2007; Kumaran et al. 2003; Lundgren et al. 2008; Pace et al. 2000), and the characterization of nitrilase spiral structures by 3D electron microscopy, have identified putative surfaces responsible for oligomer formation (Dent et al. 2009; Sewell

et al. 2003; Sewell et al. 2005; Thuku et al. 2007; Woodward et al. 2008). In this study I tested the involvement of three regions in the oligomerization of the cyanide degrading nitrilase CynD. Two regions tested are insertions in the nitrilase sequence relative to the larger superfamily and were predicted to participate in the C-surface interaction (Sewell et al. 2003). The third region is the C-terminus, which was previously shown to influence the activity, stability, and oligomerization in various nitrilases (Abou Nader 2012; Kiziak et al. 2007; Sewell et al. 2005; Thuku et al. 2007). Regions of CynD that my work demonstrated to participate in oligomerization and activity are highlighted in Figure 6.1.

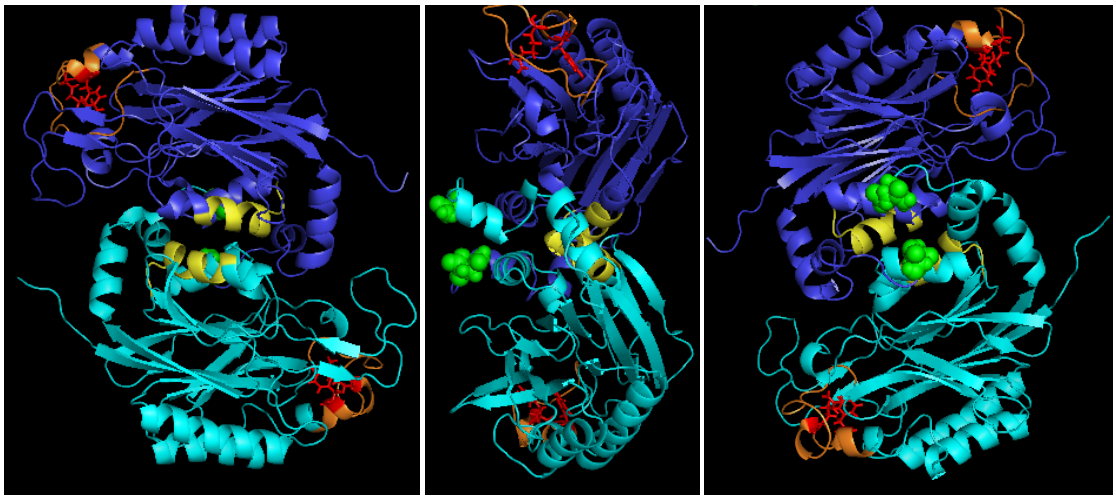

Figure 6.1 Summary of regions participating in oligomerization or activity. Front side and back view of the dimer model of $CynD_{pum}$ (B.T. Sewell, personal correspondence), from left to right. Monomers colored blue and light blue. Positions (R67 and Y70) capable to disrupting oligomerization upon mutagenesis are highlighted in red (Chapter II and III). C-surface regions 1, which was sensitive to cysteine substitutions, is highlighted in orange (Chapter II). A-surface region 2, which was shown to interact with the C-terminus, is highlighted in yellow (Chapter IV). The last residue modeled of the C-terminus (N293) is highlighted in green. This is also where the sequence begins to diverge between $CynD_{pum}$ and $CynD_{stut}$. The segment beyond this point was shown to be critical for oligomerization, activity, and stability. (Chapter IV and V). Figure generated in PyMol.

THE PARTICIPATION OF C-SURFACE REGION 1 AND 2 IN OLIGOMERIZATION

To test participation of two predicted C-surface regions in $CynD_{pum}$, I constructing cysteine substitutions at each residue in C surface region 1 (55-72) and C-surface region 2 (222-235). These mutants were characterized for activity and effects on oligomer size as determined by size exclusion chromatography.

The C-surface region 1 is critical for proper oligomerization

Overall C-surface region 1 was dramatically more sensitive to substitution than region 2. Half of the cysteine substitutions from aa 55-72 had altered mobility during size exclusion, indicating effects on oligomer size (Figure 2.4 Table 2.2). Further, the mutants with altered oligomer size all had reductions or loss of CynD activity (Figure 2.3). This emphasizes the requirement for correct conformation of the spiral oligomer for nitrilase activity, as seen in CynD and other nitrilases (Jandhyala et al. 2005; Kiziak et al. 2007; Thuku et al. 2007).

The most significant mutant from this cysteine scan was CynD R67C. It had not detectable activity as purified protein and separated into multiple smaller oligomers when examined by size exclusion chromatography (Figure 2.4d). Further characterization of these smaller oligomers showed them to be blocked for further association into the normal 18-subunit structure (Figure 2.5). This mutant strongly supports the model that C-surface region 1 is important to the formation of the functional oligomer.

Currently the interacting partner of this C-surface region 1 is not predicted in the CynD models. This CynD R67C mutant may be useful to identify other regions involved in oligomerization by screening for secondary mutations capable of suppressing R67C and restoring activity and oligomerization. Random mutagenesis by error-prone PCR has already proven useful for identifying important mutations in CynD and other nitrilases (Abou Nader 2012; Liu et al. 2013; Schreiner et al. 2010; Sosedov and Stolz 2013; Wang et al. 2012; Wu et al. 2007; Wu et al. 2008). Further, I have already shown R67C to be suppressible by the stabilizing C-terminus of $CynD_{stut}$ (discussed later). CynD R67C does have residual activity in whole cells, indicating that the intracellular environment is able to compensate for the mutants disruptive effect on activity. A search for second site suppressors of R67C may need to include a lysis step to remove the effect of the cell.

C-surface region 2 and comparison to βaS

C-surface region 2 had previously been compared to a similar C-surface region in the crystal structure of β-alanine synthase (βaS) from *D. melanogaster* (Thuku et al. 2009). In βaS this region forms much of the area in the C-surface and interacts with the same region in adjacent subunits through a pair of symmetric salt bridges. At the C-surface of βaS this region also forms the roof of the enzymes active site (Lundgren et al. 2008). Thus, it was expected that mutations in the C-surface region 2 of CynD would have profound effects on activity and oligomerization. Surprisingly, C-surface region 2 (222-235) only showed moderate sensitivity to cysteine substitutions (Figure 2.3b). Only

three mutants had altered oligomer sizes and all retained reasonable activity. Even CynD Q228C, which formed large protein aggregates, retained about 80% activity (Figure 2.3b).

The moderate reduction in oligomer size and activity in CynD Y233C and CynD F234C does suggest some influence on the oligomer size or conformation, but this C-surface region 2 is playing a much smaller role than predicted by comparisons to the βaS C-surface. If we instead compare the C-surface region 1 to the corresponding region in βaS, the CynD sequence contains an eight amino acid insertion relative to βaS (Thuku et al. 2009). Some residues from this region in βaS participate in the C-surface (Lundgren et al. 2008).

THE ROLE OF C-SURFACE RESIDUE Y70 ON ACTIVITY AND OLIGOMERIZATION

Apart from $CynD_{pum}$R67C, another mutant $CynD_{pum}$Y70C had no significant activity (Figure 2.3a). Unlike $CynD_{pum}$R67C however, this mutant still formed large oligomers. Its mobility on size exclusion chromatography was slightly altered relative to the wild type protein, and eluted as a single uniform peak, intermediate to the $CynD_{pum}$ 18-mer and the $CynD_{stut}$ 14-mer (Figure 3.2). Other mutations (F57C, G61C, T66C, and H71C) from the C-surface region also had reduced oligomer sizes, but unlike Y70C, retained partial activity. I hypothesized that Y70 plays an additional role in activity, beyond influencing the oligomer size.

From saturation mutagenesis at position 70, only wild type $CynD_{pum}$ and $CynD_{pum}$Y70F were active. Furthermore their activities were essentially identical. To examine the influence this residue has on oligomer formation and size, select mutants (Y70F, C, G, K, I, and E) were examined by size exclusion chromatography. $CynD_{pum}$Y70F eluted similar to the non-mutant CynD, consistent with an 18-subunit oligomer. The five inactive mutants examined (Y70C, G, K, I, and E) all had changes in mobility relative to the wild type $CynD_{pum}$ (Figure 3.2). Two mutants, $CynD_{pum}$Y70I and $CynD_{pum}$Y70E eluted as multiple peaks, indicating they are defective in proper oligomer formation. These mutants indicate that Y70 participates in oligomerization at the C-surface, and mutations at this position disrupt activity by either blocking assembly, or necessary conformational changes needed for activation.

This hypothesis could be examined further by testing whether the defect in oligomerization of $CynD_{pum}$Y70I or $CynD_{pum}$Y70E can be suppressed. The elution pattern of $CynD_{pum}$Y70I and $CynD_{pum}$Y70E resembles that of $CynD_{pum}$R67C. The oligomerization and activity defect of $CynD_{pum}$R67C can be suppressed by the stabilizing effect of the $CynD_{stut}$ C-terminus (discussed below). It would be interesting to test if the C-terminus could restore oligomerization to $CynD_{pum}$Y70I or $CynD_{pum}$Y70E as well. However given the phenotype of $CynD_{pum}$Y70C and $CynD_{pum}$Y70G, I do not expect the $CynD_{stut}$ C-terminus to restore activity. Additionally, I would expect that any oligomers of $CynD_{pum\text{-}stut}$Y70I or $CynD_{pum\text{-}stut}$Y70E to differ in size from wild type, similar to $CynD_{pum}$Y70C.

Without crystal structures of any nitrilase protein we lack the structural context to predict the exact mechanism by which Y70 affects activity. As discussed above, a region in βaS, similar to the CynD C-surface region 2, forms the roof of the active site. Given the sensitivity of Y70 and the C-surface region 1 in general, perhaps this region similarly forms part of the active site cavity in CynD. A tyrosine of phenylalanine at position 70 may be essential for proper conformation of this cavity.

A more specific mechanism was suggested by the crystal structure of the hexameric amidase from *Geobacillus pallidus* RAPc8 (Kimani et al. 2007). Kimani et al. proposed that an active site glutamate in close proximity to the C-surface may be positioned by oligomerization. Y70 may be critical for the conformation change needed to position the active site residue in CynD.

The behavior of the nitrilase from *R. rhodochrous* J1 indicates a two-way relationship between the active site and oligomerization. The native protein remains as dimers until triggered to oligomerize a specific substrate, benzonitrile. Once oligomerized the protein is active against benzonitrile and other substrates that do not trigger oligomerization themselves. Although CynD does not require substrate binding to trigger oligomerization, perturbation of the active site may still be able to affect oligomerization. An interesting experiment would be to examine the effect of mutating the active site residues on oligomerization. If mutating the active site glutamate alters or disrupts oligomerization it would demonstrate a structural link to the C-surface.

THE ROLE OF THE C-TERMINUS IN THE STRUCTURE OF CYND

To investigate how and where the C-terminus of CynD contributes to the structure and function of CynD, I exploited the phenotypes of mutants previously constructed in the lab (Sewell et al. 2005). This work first investigated the effects of removing or substituting the C-terminal tails in CynD from *B. pumilus* and *P. stutzeri* (Sewell et al. 2005). They found that $CynD_{pum}$ and $CynD_{stut}$ had different tolerances to C-terminal deletions. $CynD_{pum}$ remained fully active with truncation at position 303 of the 330 amino acid protein. $CynD_{stut}$ on the other hand retained no activity with comparable, or shorter truncations. Furthermore, exchanging the C-termini revealed a one sided specificity for this region. The $CynD_{pum}$ enzyme with the $CynD_{stut}$ C-terminus ($CynD_{pum\text{-}stut}$) was fully active. Conversely the $CynD_{pum}$ C-terminus on the other hand was not tolerated in the hybrid $CynD_{stut\text{-}pum}$.

The CynD C-terminus interacts with the A-surface region 2

Mary Abou-Nader further characterized the C-terminal hybrid $CynD_{stut\text{-}pum}$ (Abou Nader 2012). She investigated which region of the $CynD_{stut}$ C-terminus was missing in the $CynD_{stut\text{-}pum}$ hybrid. By introducing *P. stutzeri* sequences into the C-terminus of $CynD_{stut\text{-}pum}$ she found that the motif GERDST was able to partially restore activity. Furthermore, restoring only the glycine and glutamate was sufficient to gain about 10% of wild type activity (Figure 4.6).

I expanded Dr. Abou-Nader's study by asking if activity could be restored using the converse approach; testing whether substituting other $CynD_{pum}$ sequences elsewhere

into the $CynD_{stut\text{-}pum}$ hybrid could restore interactions with the C-terminus and activity. Because the C-terminus has been seen to interact with both the A and C-surfaces in crystal structures from nitrilase homologs, I focused on these regions. I individually exchanged the two A-surface regions and the two C-surface regions into the inactive $CynD_{stut\text{-}pum}$ hybrid. From these I was able to show the A-surface region 2 (195-206) restored partial activity to $CynD_{stut\text{-}pum}$ ($CynD_{stut\text{-}pum}A2_{pum}$) (Table 4.11). This A-surface region 2 did not remove the need for the C-terminus in $CynD_{stut}\Delta302+A2_{pum}$ but presumably restored a necessary interaction. Furthermore the $CynD_{pum}$ A-surface region 2 slightly reduced activity when put in $CynD_{stut}$ alone ($CynD_{stut}A2_{pum}$) (Figure 4.7), indicating the effect was not merely increased stability. Together, these results indicate a specific interaction between the C-terminus and A-surface of $CynD_{pum}$.

It is still not known which portion of the C-terminus is involved in this interaction with the A-surface region 2. Both the A2 region and the GERDST only restored partial activity to $CynD_{stut\text{-}pum}$ indicating that the C-terminus incorporates additional interactions as well. These two regions have also not been examined in combination. Incompatibility between the A surface region 2 from $CynD_{pum}$ and the GERDST motif from $CynD_{stut}$ would indicate that they are part of the same specific interaction. However, if combining these mutants into the $CynD_{stut\text{-}pum}$ hybrid ($CynD_{stut\text{-}pum}GERDST+A2_{pum}$) results in equivalent or greater activity than $CynD_{stut\text{-}pum}A2_{pum}$ or $CynD_{stut\text{-}pum}GERDST$, it would indicate that the two regions are involved in independent interactions. As discussed below, the GERDST motif alone confers increased stability

when introduced in the non-hybrid $CynD_{pum}$, suggesting that it is compatible with the presence of $CynD_{pum}$ A-surface region 2.

The CynD C-terminus supports oligomerization at the C-surface

In characterizing the stability of the active C-terminal deletions and hybrid mutants, Dr. Mary Abou-Nader found that the C-terminus had a large impact on the thermostability of CynD. She observed that the active C-terminal hybrid, $CynD_{pum\text{-}stut}$, was dramatically more stable than any other CynD variant or mutant identified to date. Further, an active C-terminal deletion mutant, $CynD_{pum}\Delta303$, was much less stable than the full length $CynD_{pum}$ (Figure 4.1) (Abou Nader 2012). Similar to the $CynD_{pum}$R67C (Chapter II) and $CynD_{stut\text{-}pum}$GERDST mutants (Chapter IV), $CynD_{pum}\Delta303$ lost the majority of its *in vivo* activity upon cell lysis.

Working together we compared the oligomer size of $CynD_{pum}$, $CynD_{pum\text{-}stut}$, and $CynD_{pum}\Delta303$ by their mobility during size exclusion chromatography (Figure 5.4). We found that wild type $CynD_{pum}$, and the hybrid $CynD_{pum\text{-}stut}$ had similar mobility, consistent with the known 18-subunit $CynD_{pum}$ oligomer. $CynD_{pum}\Delta303$ on the other hand had a very short peak in the range of the 18-mer, but mostly eluted from the column in the range of a tetramer and smaller (Figure 5.4b). This suggested that the C-terminus participates in the oligomeric structure of CynD, and that the stabilizing effect of the C-terminal swap in the $CynD_{pum\text{-}stut}$ hybrid is through supporting oligomerization. Lysis of the cell may have allowed the de-oligomerization of the $CynD_{pum}\Delta303$ protein and thus explain its loss of activity upon cell lysis.

I further tested this hypothesis by examining the mutants R67C and Y70C in the $CynD_{pum\text{-}stut}$ hybrid background. $CynD_{pum}$R67C is inactive, disrupted for proper oligomerization, and elutes in size exclusion chromatography as multiple smaller oligomers. $CynD_{pum}$Y70C is also inactive, but unlike $CynD_{pum}$R67C, still forms large oligomers (Chapter II)(Figure 2.4b). In the hybrid $CynD_{pum\text{-}stut}$ background the R67C mutants was fully restored for both activity and oligomerization, while Y70C was unaffected (Figure 5.5 and 5.6). This indicates that the C-terminus in the $CynD_{pum\text{-}stut}$ hybrid stabilized the protein by supporting oligomer formation at the C-surface.

Similar to the interaction of the $CynD_{pum}$ C-terminus with the $CynD_{pum}$ A2 region, it is unclear what region of the $CynD_{stut}$ C-terminus is stabilizing oligomerization in the $CynD_{pum\text{-}stut}$ hybrid. Dr. Abou-Nader found the GERDST motif to be partially responsible for the hybrid's stability (Figure 5.2), but it is untested if this motif in the $CynD_{stut}$ C-terminus is restoring oligomerization in $CynD_{pum\text{-}stut}$R67C. The compatibility of the GERDST motif with the $CynD_{pum}$ does however suggest that the specific interaction of the C-terminus with the A2 region is separate from the stabilizing effect of the GERDST motif.

CONCLUSION

Fitting of the CynD dimer model into the 3D EM structure had given us a picture of how these protein might oligomerize, but what regions are responsible for oligomerization had not previously been demonstrated. My results strongly implicate the C-surface region 1 and the C-terminus on the formation of and activity of the spiral CynD structure. These results may lead to the manipulation of the oligomeric structure in order to exploit its influence on activity and stability of CynD and other nitrilases.

REFERENCES

Abou Nader M (2012) Directed evolution of cyanide degrading enzymes. Doctoral dissertation Texas A&M University

Agarkar VB, Kimani SW, Cowan DA, Sayed MF, Sewell BT (2006) The quaternary structure of the amidase from *Geobacillus pallidus* RAPc8 is revealed by its crystal packing. Acta Crystallogr Sect F Struct Biol Cryst Commun 62(Pt 12):1174-8 doi:10.1107/S1744309106043855

Akcil A (2003) Destruction of cyanide in gold mill effluents: biological versus chemical treatments. Biotechnol Adv 21(6):501-511

Andrade J, Karmali A, Carrondo MA, Frazao C (2007a) Crystallization, diffraction data collection and preliminary crystallographic analysis of hexagonal crystals of *Pseudomonas aeruginosa* amidase. Acta Crystallogr Sect F Struct Biol Cryst Commun 63(Pt 3):214-6 doi:10.1107/S1744309107005830

Andrade J, Karmali A, Carrondo MA, Frazao C (2007b) Structure of amidase from *Pseudomonas aeruginosa* showing a trapped acyl transfer reaction intermediate state. J Biol Chem 282(27):19598-605 doi:10.1074/jbc.M701039200

Banerjee A, Sharma R, Banerjee UC (2002) The nitrile-degrading enzymes: current status and future prospects. Appl Microbiol Biotechnol 60(1-2):33-44 doi:10.1007/s00253-002-1062-0

Basile LJ, Willson RC, Sewell BT, Benedik MJ (2008) Genome mining of cyanide-degrading nitrilases from filamentous fungi. Appl Microbiol Biotechnol 80(3):427-35 doi:10.1007/s00253-008-1559-2

Dash RR, Gaur A, Balomajumder C (2009) Cyanide in industrial wastewaters and its removal: a review on biotreatment. J Hazard Mater 163(1):1-11 doi:10.1016/j.jhazmat.2008.06.051

Dent KC, Weber BW, Benedik MJ, Sewell BT (2009) The cyanide hydratase from *Neurospora crassa* forms a helix which has a dimeric repeat. Appl Microbiol Biotechnol 82(2):271-8 doi:10.1007/s00253-008-1735-4

Detzel C, Maas R, Tubeleviciute A, Jose J (2013) Autodisplay of nitrilase from *Klebsiella pneumoniae* and whole-cell degradation of oxynil herbicides and related compounds. Appl Microbiol Biotechnol 97(11):4887-4896 doi:10.1007/S00253-012-4401-9

Eijsink VG, Bjork A, Gaseidnes S, Sirevag R, Synstad B, van den Burg B, Vriend G (2004) Rational engineering of enzyme stability. J Biotechnol 113(1-3):105-20 doi:10.1016/j.jbiotec.2004.03.026

Fleming F (1999) Nitrile-containing natural products. Nat Prod Rep 16(5):597-606 doi:10.1039/a804370a

Gong JS, Lu ZM, Li H, Shi JS, Zhou ZM, Xu ZH (2012) Nitrilases in nitrile biocatalysis: recent progress and forthcoming research. Microb Cell Fact 11 doi:Artn 142 doi:10.1186/1475-2859-11-142

Gordon RD, Qiu W, Romanov V, Lam K, Soloveychik M, Benetteraj D, Battaile KP, Chirgadze YN, Pai EF, Chirgadze NY (2013) Crystal structure of the CN-hydrolase SA0302 from the pathogenic bacterium *Staphylococcus aureus* belonging to the Nit and NitFhit Branch of the nitrilase superfamily. J Biomol Struct Dyn 31(10):1057-1065 doi:10.1080/07391102.2012.719111

Goujon M, McWilliam H, Li W, Valentin F, Squizzato S, Paern J, Lopez R (2010) A new bioinformatics analysis tools framework at EMBL,ÄìEBI. Nucleic Acids Res 38(suppl 2):W695-W699 doi:10.1093/nar/gkq313

Gupta N, Balomajumder C, Agarwal VK (2010) Enzymatic mechanism and biochemistry for cyanide degradation: a review. J Hazard Mater 176(1-3):1-13 doi:10.1016/j.jhazmat.2009.11.038

Hung CL, Liu JH, Chiu WC, Huang SW, Hwang JK, Wang WC (2007) Crystal structure of *Helicobacter pylori* formamidase AmiF reveals a cysteine-glutamate-lysine catalytic triad. J Biol Chem 282(16):12220-9 doi:10.1074/jbc.M609134200

Jandhyala D, Berman M, Meyers PR, Sewell BT, Willson RC, Benedik MJ (2003) CynD, the cyanide dihydratase from *Bacillus pumilus*: gene cloning and structural studies. Appl Environ Microbiol 69(8):4794-805

Jandhyala DM, Willson RC, Sewell BT, Benedik MJ (2005) Comparison of cyanide-degrading nitrilases. Appl Microbiol Biotechnol 68(3):327-35 doi:10.1007/s00253-005-1903-8

Jenrich R, Trompetter I, Bak S, Olsen CE, Moller BL, Piotrowski M (2007) Evolution of heteromeric nitrilase complexes in *Poaceae* with new functions in nitrile metabolism. Proc Natl Acad Sci U S A 104(47):18848-18853 doi:10.1073/Pnas.0709315104

Kimani SW, Agarkar VB, Cowan DA, Sayed MF, Sewell BT (2007) Structure of an aliphatic amidase from *Geobacillus pallidus* RAPc8. Acta Crystallogr D Biol Crystallogr 63(Pt 10):1048-58 doi:10.1107/S090744490703836X

Kiziak C, Klein J, Stolz A (2007) Influence of different carboxy-terminal mutations on the substrate-, reaction- and enantiospecificity of the arylacetonitrilase from *Pseudomonas fluorescens* EBC191. Protein Eng Des Sel 20(8):385-396 doi:10.1093/Protein/Gzm032

Knowles CJ (1976) Microorganisms and cyanide. Bacteriol Rev 40(3):652-80

Korte F, Coulston F (1995) From single-substance evaluation to ecological process concept: the dilemma of processing gold with cyanide. Ecotoxicol Environ Saf 32(1):96-101 doi:10.1006/eesa.1995.1091

Kumaran D, Eswaramoorthy S, Gerchman SE, Kycia H, Studier FW, Swaminathan S (2003) Crystal structure of a putative CN hydrolase from yeast. Proteins: Struct, Funct, Genet 52(2):283-291 doi:10.1002/Prot.10417

Larkin MA, Blackshields G, Brown NP, Chenna R, McGettigan PA, McWilliam H, Valentin F, Wallace IM, Wilm A, Lopez R, Thompson JD, Gibson TJ, Higgins DG (2007) Clustal W and Clustal X version 2.0. Bioinformatics 23(21):2947-2948 doi:10.1093/bioinformatics/btm404

Liu ZQ, Baker PJ, Cheng F, Xue YP, Zheng YG, Shen YC (2013) Screening and improving the recombinant nitrilases and application in biotransformation of iminodiacetonitrile to iminodiacetic acid. PLoS One 8(6):e67197 doi:10.1371/journal.pone.0067197

Lundgren S, Lohkamp B, Andersen B, Piskur J, Dobritzsch D (2008) The crystal structure of beta-alanine synthase from *Drosophila melanogaster* reveals a homooctameric helical turn-like assembly. J Mol Biol 377(5):1544-59 doi:10.1016/j.jmb.2008.02.011

Mahadevan S, Thimann KV (1964) Nitrilase. Ii. Substrate specificity and possible mode of action. Arch Biochem Biophys 107:62-8

Matamá T, Carneiro F, Caparrós C, Gübitz GM, Cavaco-Paulo A (2007) Using a nitrilase for the surface modification of acrylic fibres. Biotechnol J 2(3):353-360 doi:10.1002/biot.200600068

Meyers PR, Gokool P, Rawlings DE, Woods DR (1991) An efficient cyanide-degrading *Bacillus pumilus* strain. J Gen Microbiol 137(6):1397-400

Meyers PR, Rawlings DE, Woods DR, Lindsey GG (1993) Isolation and characterization of a cyanide dihydratase from *Bacillus pumilus* C1. J Bacteriol 175(19):6105-12

Mosher JB, Figueroa L (1996) Biological oxidation of cyanide: A viable treatment option for the minerals processing industry? Miner Eng 9(5):573-581 doi:10.1016/0892-6875(96)00044-1

Mueller P, Egorova K, Vorgias CE, Boutou E, Trauthwein H, Verseck S, Antranikian G (2006) Cloning, overexpression, and characterization of a thermoactive nitrilase from the hyperthermophilic archaeon *Pyrococcus abyssi*. Protein Expr Purif 47(2):672-681 doi:10.1016/J.Pep.2006.01.006

Muezzinoglu A (2003) A Review of Environmental Considerations on Gold Mining and Production. Crit Rev Env Sci Technol 33(1):45-71 doi:10.1080/10643380390814451

Nagasawa T, Wieser M, Nakamura T, Iwahara H, Yoshida T, Gekko K (2000) Nitrilase of *Rhodococcus rhodochrous* J1. Conversion into the active form by subunit association. Eur J Biochem 267(1):138-44 doi:10.1046/j.1432-1327.2000.00983.x

Nakai T, Hasegawa T, Yamashita E, Yamamoto M, Kumasaka T, Ueki T, Nanba H, Ikenaka Y, Takahashi S, Sato M, Tsukihara T (2000) Crystal structure of N-carbamyl-D-amino acid amidohydrolase with a novel catalytic framework common to amidohydrolases. Struct Fold Des 8(7):729-737 doi:10.1016/S0969-2126(00)00160-X

Pace HC, Brenner C (2001) The nitrilase superfamily: classification, structure and function. Genome Biol 2(1):REVIEWS0001

Pace HC, Hodawadekar SC, Draganescu A, Huang J, Bieganowski P, Pekarsky Y, Croce CM, Brenner C (2000) Crystal structure of the worm NitFhit Rosetta Stone protein reveals a Nit tetramer binding two Fhit dimers. Curr Biol 10(15):907-917 doi:10.1016/S0960-9822(00)00621-7

Pollak P, Romeder G, Hagedorn F, Gelbke H-P (2000) Nitriles Ullmann's Encyclopedia of Industrial Chemistry. Wiley-VCH Verlag GmbH & Co. KGaA

Poulton JE (1990) Cyanogenesis in plants. Plant Physiol 94(2):401-5

Prasad S, Misra A, Jangir VP, Awasthi A, Raj J, Bhalla TC (2007) A propionitrile-induced nitrilase of *Rhodococcus* sp NDB 1165 and its application in nicotinic

acid synthesis. World J Microbiol Biotechnol 23(3):345-353 doi:10.1007/S11274-006-9230-5

Ramteke PW, Maurice NG, Joseph B, Wadher BJ (2013) Nitrile-converting enzymes: An eco-friendly tool for industrial biocatalysis. Biotechnol Appl Biochem 60(5):459-81 doi:10.1002/bab.1139

Schreiner U, Hecher B, Obrowsky S, Waich K, Klempier N, Steinkellner G, Gruber K, Rozzell JD, Glieder A, Winkler M (2010) Directed evolution of *Alcaligenes faecalis* nitrilase. Enzyme Microb Technol 47(4):140-146 doi:10.1016/J.Enzmictec.2010.05.012

Sewell BT, Berman MN, Meyers PR, Jandhyala D, Benedik MJ (2003) The cyanide degrading nitrilase from *Pseudomonas stutzeri* AK61 Is a two-fold symmetric, 14-subunit spiral. Structure 11(11):1413-1422

Sewell BT, Thuku RN, Zhang X, Benedik MJ (2005) Oligomeric structure of nitrilases: effect of mutating interfacial residues on activity. Ann N Y Acad Sci 1056:153-159

Singh R, Sharma R, Tewari N, Rawat DS (2006) Nitrilase and its application as a 'green' catalyst. Chem Biodivers 3(12):1279-87 doi:10.1002/cbdv.200690131

Sosedov O, Stolz A (2013) Random mutagenesis of the arylacetonitrilase from *Pseudomonas fluorescens* EBC191 and identification of variants, which form increased amounts of mandeloamide from mandelonitrile. Appl Microbiol Biotechnol doi:10.1007/s00253-013-4968-9

Stalker DM, Mcbride KE, Malyj LD (1988) Herbicide resistance in transgenic plants expressing a bacterial detoxification gene. Science 242(4877):419-423 doi:10.1126/Science.242.4877.419

Thimann KV, Mahadevan S (1964) Nitrilase .I. occurrence preparation + general properties of enzyme. Arch Biochem Biophys 105(1):133-& doi:10.1016/0003-9861(64)90244-9

Thuku RN, Brady D, Benedik MJ, Sewell BT (2009) Microbial nitrilases: versatile, spiral forming, industrial enzymes. J Appl Microbiol 106(3):703-27 doi:10.1111/j.1365-2672.2008.03941.x

Thuku RN, Weber BW, Varsani A, Sewell BT (2007) Post-translational cleavage of recombinantly expressed nitrilase from *Rhodococcus rhodochrous* J1 yields a stable, active helical form. FEBS J 274(8):2099-108 doi:10.1111/j.1742-4658.2007.05752.x

Vejvoda V, Kaplan O, Bezouska K, Pompach P, Sulc M, Cantarella M, Benada O, Uhnakova B, Rinagelova A, Lutz-Wahl S, Fischer L, Kren V, Martinkova L (2008) Purification and characterization of a nitrilase from *Fusarium solani* O1. J Mol Catal B: Enzym 50(2-4):99-106 doi:10.1016/J.Molcatb.2007.09.006

Wang L, Watermeyer JM, Mulelu AE, Sewell BT, Benedik MJ (2012) Engineering pH-tolerant mutants of a cyanide dihydratase. Appl Microbiol Biotechnol 94(1):131-40 doi:10.1007/s00253-011-3620-9

Wang WC, Hsu WH, Chien FT, Chen CY (2001) Crystal structure and site-directed mutagenesis studies of N-carbamoyl-D-amino-acid amidohydrolase from *Agrobacterium radiobacter* reveals a homotetramer and insight into a catalytic cleft. J Mol Biol 306(2):251-261 doi:10.1006/Jmbi.2000.4380

Watanabe A, Yano K, Ikebukuro K, Karube I (1998) Cyanide hydrolysis in a cyanide-degrading bacterium, *Pseudomonas stutzeri* AK61, by cyanidase. Microbiology 144 (Pt 6):1677-82

Waterhouse AM, Procter JB, Martin DMA, Clamp M, Barton GJ (2009) Jalview Version 2-a multiple sequence alignment editor and analysis workbench. Bioinformatics 25(9):1189-1191 doi:10.1093/Bioinformatics/Btp033

Williamson DS, Dent KC, Weber BW, Varsani A, Frederick J, Thuku RN, Cameron RA, van Heerden JH, Cowan DA, Sewell BT (2010b) Structural and biochemical characterization of a nitrilase from the thermophilic bacterium, *Geobacillus pallidus* RAPc8. Appl Microbiol Biotechnol 88(1):143-153 doi:10.1007/S00253-010-2734-9

Woodward JD (2011) The relationship between structure and specificity in the plant nitrilases. Doctoral dissertation, University of Cape Town

Woodward JD, Weber BW, Scheffer MP, Benedik MJ, Hoenger A, Sewell BT (2008) Helical structure of unidirectionally shadowed metal replicas of cyanide hydratase from *Gloeocercospora sorghi*. J Struct Biol 161(2):111-119 doi:10.1016/J.Jsb.2007.09.019

Wu SJ, Fogiel AJ, Petrillo KL, Hann EC, Mersinger LJ, DiCosimo R, O'Keefe DP, Ben-Bassat A, Payne MS (2007) Protein engineering of *Acidovorax facilis* 72W nitrilase for bioprocess development. Biotechnol Bioeng 97(4):689-693 doi:10.1002/Bit.21289

Wu SJ, Fogiel AJ, Petrillo KL, Jackson RE, Parker KN, DiCosimo R, Ben-Bassat A, O'Keefe DP, Payne MS (2008) Protein engineering of nitrilase for

chemoenzymatic production of glycolic acid. Biotechnol Bioeng 99(3):717-720 doi:10.1002/Bit.21643

Xue YP, Xu SZ, Liu ZQ, Zheng YG, Shen YC (2011) Enantioselective biocatalytic hydrolysis of (R,S)-mandelonitrile for production of (R)-(-)-mandelic acid by a newly isolated mutant strain. J Ind Microbiol Biotechnol 38(2):337-345 doi:10.1007/S10295-010-0778-6